International Symposium
on
Ligaments & Tendons - VIII

The Atrium, Packard Electrical Engineering Building
Stanford University Campus
Stanford, CA

March 1, 2008

Edited by: ***Savio L-Y. Woo, PhD, DSc*** [1]
Steven D. Abramowitch, PhD [1]
Braden C. Fleming, PhD [2]
Matthew B. Fisher, BS [1]

[1]**Musculoskeletal Research Center**
Department of Bioengineering
University of Pittsburgh

[2]**Bioengineering Laboratory**
Department of Orthopaedics
Warren Alpert Medical School
Brown University

Volume 8

Symposium Sponsors

Orthopaedic Research Society

Asian American Institute for Research and Education

Department of Bioengineering
University of Pittsburgh

Musculoskeletal Research Center

FlexCell International Corporation

Let People Move

Steadman • Hawkins Research Foundation

Orthopaedic Research Laboratory Alumni Council

DonJoy Orthopedics

Wyeth

Division of Biomechanical Engineering
Department of Mechanical Engineering, Stanford University

International Symposium on Ligaments & Tendons-VIII

Saturday, March 1, 2008
Stanford University Campus
Stanford, CA

Welcome!

Welcome to the Stanford University Campus and the Eighth International Symposium on Ligaments and Tendons (ISL&T-VIII)!

Once again, we have reunited with our friends and colleagues for another lively scientific discussion of state-of-the-art research on ligaments and tendons. We are pleased that this meeting continues to be a place where students as well as junior and senior level biologists, engineers and clinicians can get together to exchange ideas, learn from one another, and establish collaborations.

Consistent with that theme, this year's program features multidisciplinary topics starting with an in depth discussion on ACL Reconstruction and the Development of Osteoarthritis followed by a look at Knee Kinematics. Then, the focus will shift to the latest findings in the Mechanobiology of Ligaments and Tendons, followed by exciting results on Tissue Healing and Mechanics. Keeping with the high energy, we will discuss Scaffolds for Functional Tissue Engineering Approaches and Novel In-vitro and In-vivo Techniques to Assess Ligament and Tendon Function. Wrapping up the discussion will be topics on the Biomechanics of the Shoulder and Upper Extremity as well as a Clinical Mini-symposium on Substance P.

We would especially like to thank our sponsors, International Program Committee, and local organizers, Dr. Thomas Andriacchi and his esteemed colleagues, for supporting and maintaining the high quality of this meeting. Finally, we would like to thank you for your enthusiastic participation year after year.

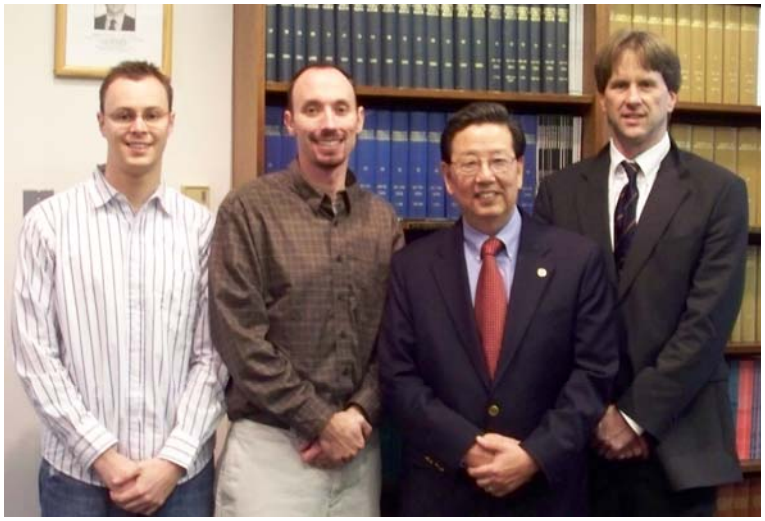

Please enjoy the day!

With our very best wishes.

Sincerely,

Savio L-Y. Woo, PhD, DSc
Steven D. Abramowitch, PhD
Braden C. Fleming, PhD
Matthew B. Fisher, BS
The ISL&T-VIII Planning Committee

General Information

Aims of the Symposium

The *International Symposium on Ligaments & Tendons* provides a forum to discuss state-of-the-art ligament and tendon research. By bringing together some of the best minds in our field, we hope to address challenging problems in ligament and tendon biomechanics and biology, and set new research directions that hold great potential for the future.

Planning Committee

Savio L-Y. Woo, PhD, DSc - Chair
Steven D. Abramowitch, PhD- Program Committee Co-Chair
Braden Fleming, PhD- Program Committee Co-Chair
Matthew B. Fisher, BS
Diann DeCenzo, MS - Treasurer
Anna Goldman, MLS - Administrative Assistant

Local Planning Committee

Tom Andriacchi, PhD **Department of Mechanical Engineering, Stanford University**
Melanie Cole, MLA

International Program Committee

Paul Ackermann, MD (Europe)
Albert Banes, PhD (North America)
Giuliano Cerulli, MD (Europe)
Ajit Chaudhari, PhD (North America)
David Corr, PhD (North America)
Hiromichi Fujie, PhD (Asia)
Helen Lu, PhD (North America)
Martha Murray, MD (North America)
Louis Soslowsky, PhD (North America)
Stavros Thomopoulos, PhD (North America)
Harukazu Tohyama, PhD (Asia)
Kazunori Yasuda, MD (Asia)
Steve Arnoczky, DVM (North America)
Michael Bey, PhD (North America)
K.M. Chan, PhD (Asia)
Chih-Hwa Chen, MD (Asia)
Evan Flatow, MD (North America)
Guoan Li, PhD (North America)
Nicola Maffulli, MD (Europe)
Per Renstrom, MD, PhD (Europe)
Kurt Spindler, MD (North America)
Gail Thornton, PhD (North America)
Michael Torry, PhD (North America)
Vincent Wang, PhD (North America)

Instructions to Presenters

I. Podium Presenters

The time for presentations has been limited, in favor of discussion. Please see the presentation formats listed below. Your moderators have been asked to adhere to the time allotted for your presentation as well as the number of slides.

Important: All speakers are asked to check-in with the session moderators 15 minutes before the session in which they will present to meet the projectionist and the moderator.

Presentation Requirements

- *For 15 minute time slots*
  - ◊ 10 min. presentations each immediately followed by a 5 min. discussion.
  - ◊ Maximum **10 PowerPoint slides** for computer presentation.

- *For 5 minute time slots*
  - ◊ 5 min. presentations followed by a 5-10 min. group discussion of 2-3 papers.
  - ◊ Maximum **5 PowerPoint slides** for computer presentation.

An Important Note on Slides

Kindly note that all speakers must be prepared to present their paper using PowerPoint projection. We ask that you send your PowerPoint presentation file to us by **February 15, 2008** so that we can load all talks into a master computer prior to the symposium. Please make sure that you clearly label your file with the author's name and the title of your presentation.

Note: In view of time and the large number of talks, there will be no opportunity to use your personal computer or load your PowerPoint file during the symposium.

II. Poster Presenters

All posters should be no larger than 45 inches x 45 inches (114.3 cm x 114.3 cm). Poster boards will be available in the lobby. Please set up your poster between 7:30 - 8:00 am and take them down at 5:45 pm.

Note: An opportunity has been provided for you to present your posters orally during different breaks. You will be given 2 minutes to present and this will be coordinated by the poster moderators. Please be sure to attend to your poster at the assigned time.

Symposium Awards

We are proud to continue to recognize our outstanding papers presented at the ISL&T. All these awards are designed to stimulate high quality scientific research by investigators in the study of ligaments and tendons. The awardees will be selected by members of the program committee based on the quality of the abstract and presentation as well as the overall merit of the study.

To acknowledge the work by students, fellows, and residents, we will provide the following two awards:

Best Student Paper Award

Best Research Fellow Paper Award

To be eligible, the presenters must be the first author of the abstract. Each award consists of a certificate and a check for $200 (donated by FlexCell International Corporation).

Best Poster Award

For the second year, the poster award will be presented. This award consists of a certificate as well as a check for $200 (donated by FlexCell International Corporation).

Transportation

Transportation to Stanford University will be provided by 3 buses located at:

Moscone Center– North
747 Howard St.
San Francisco, California 84103
415-974-4000

Buses will leave the Moscone Center– North at 6:30 am. Please board the buses as designated by alphabetical order. After the dinner and award ceremony, the buses will transport attendees back to the Moscone Center (departing at approximately 8:30 pm).

PROGRAM

6:30 am Bus Pick up from Downtown San Francisco

7:30-8:00 am Registration/Check-In and Continental Breakfast

8:00 am Welcome
Savio L-Y. Woo, PhD, DSc

8:10 am Logistics
Braden C. Fleming, PhD

Podium Session 1: ACL Reconstruction & Development of Osteoarthritis
Moderators: Bruce Beynnon, MD & Maury Hull, PhD

8:20 am **Keynote Lecture**
Kinematic Changes Following ACL Injury and Reconstruction: A Pathway to Knee OA **p12**
T Andriacchi*, S Scanlan, S Koo, P Briant, S Bevill*

8:35 am **Keynote Lecture**
Clinical Outcomes Following ACL Reconstruction
K Spindler

8:50 am Even Immediate Normal Anatomic ACL Reimplantation in an Ovine Model Leads to Significant Synovial Inflammation with Potential for Joint Damage **p13**
JWS Chin*, KD Huebner, M Chung, LL Marchuk, JE Beveridge, NG Shrive, DA Hart, CB Frank*

9:05am ACL-Reconstruction & Cartilage Deformation **p14**
SK Van de Velde*, TJ Gill, JT Bingham, LE DeFrate, G Li*

9:20 am Relationship Between the Orientation of the ACL Graft in the Coronal Plane and the Knee Flexion Moment During Walking **p15**
S Scanlan*, K Blazek, A Chaudhari, T Andriacchi*

Podium Session 2: Knee Kinematics & Mechanics
Moderators: Toru Fukubayashi, MD & Michael Torry, PhD

9:35 am ACL-Deficient and –Reconstructed Knees Have Altered Rotational Axes During Daily Activities **p16**
N Zheng*, B Gao, BP Conrad, MW Moser, PA Indelicato*

9:40 am Joint Failure in ACL/MCL Deficiency: The Impact on the Apparent Strain Environment of Healing and Remaining Intact Ligaments **p17**
***JE Tapper**, Y Funakoshi, M Hariu, L Marchuk, GM Thornton, JL Ronsky, RF Zernicke, NG Shrive, CB Frank*

9:45 am **Discussion**

9:50 am Force Sharing in the Three Bundles of the Anterior Cruciate Ligament: Biomechanical Analysis Using a Novel Robotic System **p18**
***H Fujie**, T Hirano, S Fukano, M Imura, D Katakai, H Otsubo, Y Suzuki, K Nakata, K Shino*

9:55 am Biomechanical Comparison of Two Methods of Reconstruction for the Combined Posterior Cruciate Ligament and Posterolateral Corner Injury of the Knee **p19**
***H Ishigooka**, T Sugihara, H Fujiya, T Satoh, M Beppu*

10:00 am **Discussion**

10:05 am Clinical Experience on ACL Reconstruction and Rehabilitation
G Cerulli

10:15 - 10:45 am **Break and Poster Session 1**

Elastic Properties of Achilles Tendon Among Male Soccer Athletes in Grades 3-6 **p20**
***Y Egawa**, S Torii, C Nakamura, T Fukubayashi*

A Comparison of the Low-Load Behavior of Injured and Uninjured Medial Collateral Ligaments in Two Porcine Breeds **p21**
***NM Germscheid**, KA Hildebrand, GM Thornton, DA Hart*

Fatigue-Loaded Healing Ligaments Rupture Earlier and at Greater Strain Than Creep-Loaded Healing Ligaments **p22**
***SJ Bailey**, GM Thornton*

Determination of the Tensile Property of the Ligament and Tendon From the Mouse Using a Novel All-In-One Micro Tensile Test System **p23**
*T Imai, **D Katakai**, M Imura, H Fujie*

Functional Deficiency of CX43 Gap Junctions in Tenocytes From $P2Y_2$ Purinoceptor Knockout Mice **p24**
***M Tsuzaki**, J Qi, ME Wall, JY Thompson, AM Fox, BH Koller, AJ Banes*

Expression of Type II Collagen and Tissue Calcification in Collagenase-Induced Tendon Degeneration **p25**
*SC Fu, **LS Chan**, KM Chan, LK Hung, PY Lui*

Effects of Dynamic Loading and Osteoblast-Fibroblast Interactions on Chondrocyte Response In-Vitro **p26**
***IE Wang**, CT Hung, and HH Lu*

Single Human Tenocytes Respond to Flow in a Novel Microfluidic Device **p27**
***J Wang**, J Qi, ME Wall, R Sumanasinghe, M Tsuzaki, AJ Banes*

Podium Session 3-Mechanobiology & Biochemistry
Moderators: Albert Banes, PhD & Roger Smith, MA Vet MB PhD

10:45 am Cell-Cell Connection is Necessary for Cellular Survival Under Mechanical Loading **p28**
***J Qi**, L Chi, D Bynum, AJ Banes*

11:00 am Synovium-derived Fibroblast Transplantation Possibly Deteriorates Mechanical Properties of the Regenerated Tissue in the Patellar Tendon After the Harvest of Its Central One-Third Portion **p29**
***H Tohyama**, S Okamoto, E Kondo, K Hayashi, K Yasuda*

11:15 am Fibrillar Level Stress Relaxation in Tendon with Subsecond Resolution **p30**
***HRC Screen**, J Seto, S Krauss, P Boesecke, P Fratzl, HS Gupta*

11:30 am Effect of Aggrecan-coated Surfaces on Morphology and Aggrecan Gene Expression in Tendon/Ligament Fibroblasts **p31**
***JJ Lim**, KS Brink, JS Temenoff*

11:35 am In-Vitro Induction of a Tendon Differentiation Marker by rhBMP-12 and rhBMP-13 **p32**
*SP Berasi, U Varadarajan, AJ Dorner, **H Seeherman**, JM, SA Jelinsky*

11:40 am The Regulation of ADAMTS-4 Expression in Human Achilles Tendon And Tendon-Derived Cells **p33**
***GP Riley**, GC Jones, AN Corps, BL Hazleman*

11:45 am **Discussion**

Podium Session 4: Tissue Healing & Mechanics
Moderators: Louis Soslowsky, PhD & Christos Papageorgiou, MD

11:50 am A Novel Elastic Model Indicates Decreased Organization and Mechanics Of Rotator Cuff Repair Due to Exercise Following Immobilization **p34**
***J Sarver**, CD Peltz, L Dourte, GR Williams, J Kadlowec, LJ Soslowsky*

12:05 pm The Effect of Applied Strain on Tendon-Bone Healing in a Rat Model **p35**
RH Brophy, ***D Kovacevic****, CW Imhauser, A Bedi, M Stasiak, K Jackson, XH Deng, SA Rodeo*

12:10 pm Mechanical Properties of Human Regenerated Semitendinosus Tendon **p36**
S Kuribayashi*, Y Shirasaki, S Okinaga, T Sanada, S Li, A Kanamori, K Marumo, M Saito, T Fukubayashi*

12:15 pm **Discussion**

12:20-1:30 pm **Lunch and Poster Viewing**

Podium Session 5, Part I: Functional Tissue Engineering-Bioscaffolds
Moderators: Steven Arnoczky, PhD & Helen Lu, PhD

1:30 pm **Keynote Lecture**
Establishing Measures of Success in Functional Tissue Engineering for Tendon and Ligament Repair and Reconstruction **p37**
DL Butler*, J Lewis, CB Frank*

1:45 pm Collagen-Platelet Rich Plasma Hydrogel Enhances Primary Repair of the Porcine Anterior Cruciate Ligament **p38**
MM Murray*, BC Fleming, E Abreu, E Magarian, A Mastrangelo, M Palmer, KP Spindler*

2:00 pm A Comparison of Mesenchymal Stem Cells and ACL Fibroblasts Responses on Combined Silk Scaffolds **p39**
H Liu, H Fan, SL Toh, ***JCH Goh***

2:15 pm Design of a Novel Stratified Scaffold for ACL-to-Bone Interface Tissue Engineering **p40**
JP Spalazzi*, KL Moffat, HH Lu*

Podium Session 5, Part II: Functional Tissue Engineering-Bioscaffolds
Moderators: Chih-Hwa Chen, MD & Stavros Thomopoulos, PhD

2:30 pm Recapitulating a Tendon Phenotype, RT-PCR Markers *In Vivo* in Comparison to *In Vitro* Culture Systems **p41**
SE Taylor, RKW Smith, PD Clegg

2:35 pm	Scleraxis and Tenomodulin: Mediators of BMP-12-Induced Tenocyte Differentiation *Y Li, HB Sun, **M Ramcharan**, DT Fung, RJ Majeska, MB Schaffler, EL Flatow, Y Li*	**p42**
2:40 pm	Feasibility of Electrochemically Aligned Collagen Bundles for Ligament/Tendon Tissue Engineering ***XG Cheng**, UA Gurkan, JA Uquillas, O Akkus*	**p43**
2:45 pm	**Discussion**	
2:50 pm	*In Vitro* HMBSC Response on Aligned Nanofiber Scaffolds With and Without Hydroxyapetite Nanoparticles ***KL Moffat**, SP Kwei, HH Lu*	**p44**
2:55 pm	Platelets Reduce Post-Operative Knee Laxity and Correlate With Early Graft Properties in a Caprine ACL Reconstruction Model *KP Spindler, MM Murray, JL Carey, **BC Fleming***	**p45**
3:00 pm	**Discussion**	
3:10-3:40 pm	**Break and Poster Session 2**	
	Development of a Silk Cable-Reinforced Gelatin-Silk Fibroin Hybrid Scaffold for Ligament Tissue Engineering *H Fan, H Liu, SL Toh, **JCH Goh***	**p46**
	Effects of Tensile Stress on the Mechanical Properties of a Scaffold-Free Tissue Engineered Construct (TEC) Bio-synthesized From Synovium-Derived Mesenchymal Stem Cells ***K Kumagai**, H Fujie, D Katakai, Y Fujishima, W Ando, N Nakamura*	**p47**
	Effects of 3-D Culture on the Response of ACL-Bone Insertion Fibrochondrocytes and Articular Chondrocytes ***WH Sun**, KL Moffat, YN Kim, HH Lu*	**p48**
	Atomic Force Microscopic Analysis on the Micro Structure of a Synovium-Derived Stem Cells-Based Self-Assembled Tissue (SCAT) ***T Suzuki**, K Kamagai, A Ogawa, H Fujie*	**p49**
	Effect of Anterior Translation on Total Knee Force in a Porcine Model ***DV Boguszewski**, JT Shearn, CT Wagner, DL Butler*	**p50**
	A New Model to Explore the Effects of ACL Graft Tension and Twist on In-Vivo Stifle Biomechanics ***JE Beveridge**, BJ Heard, SP Darcy, L MacDonald, CA Sutherland, NG Shrive, CB Frank*	**p51**

Magnetic Resonance Microscopic Images of Regenerated Semitendinosus Tendon After Harvesting for ACL Reconstruction **p52**
***Y Nomura**, R Kuramochi, N Tawara, A Hirano, T Fukubayashi*

Podium Session 6: Techniques
Moderators: Hiromichi Fujie, MD & Guoan Li, PhD

3:40 pm Second Harmonic Imaging and Fourier Spectral Analysis of Normal and Damaged Tendon Microstructure **p53**
***DT Fung**, J Basta-Pljakic, JB Sereysky, DM Laudier, MH Tseng, MB Schaffler, EL Flatow*

3:55 pm Cell Orientation and Local Strain Distribution in an *In Vitro* Achilles Tendon Tissue Engineering Model **p54**
***RD Sumanasinghe**, J Qi, J Wang, M Tsuzaki, M Wall, W Pfeiler, E Loboa, DA Hart, AJ Banes*

4:00 pm Diffusion Tensor Imaging of Knee Ligaments: A Preliminary *In Vivo* Study **p55**
***VM Wang**, BR Bach, DA Turner, GT Stebbins*

4:05 pm The Effect of *In Vivo* Sensor Implantation in the Sheep Knee **p56**
***ST Herfat**, JT Shearn, D Bailey, ME Mehl, N Perry, MT Galloway, M Griewe, C Gooch, DL Butler*

4:10 pm **Discussion**

Podium Session 7: Shoulder & Upper Extremity
Moderators: Evan Flatow, MD & Thay Lee, PhD

4:15 pm Biomechanical Evaluation of Superior Capsular Reconstruction for Treatment of Irreparable Massive Rotator Cuff Tear **p57**
***T Mihata**, MH McGarry, JM Pirolo, M Kinoshita, TQ Lee*

4:30 pm Are the Mechanical Properties of the Anterior Band of the Inferior Glenohumeral Ligament and the Axillary Pouch Similar? **p58**
*CA Voycheck, AJ Brown, PJ McMahon, **RE Debski***

4:35 pm The Effects of Various Temperatures (-5°C, -25°C, and –80°C) on Biomechanical Properties of Tendon Allografts **p59**
*A Guney, M Oner, M Halici, **S Karaoglu***

4:40 pm **Discussion**

Podium Session 8: Symposium on Substance P
Moderators: Sinan Karaoglu, MD & Jennifer Wayne, PhD

4:45 pm	Substance P Injections Enhance Tendon Healing: A Study in the Rat *O Carlsson, J Dahl,* ***PW Ackermann***	**p60**
5:00 pm	Substance P Expression was Associated With Tendon Pain in a Rat Model of Collagen-Induced Tendon Injuries ***LS Chan****, SC Fu, DTP Fong, KM Chan*	**p61**
5:15 pm	Circulating Substance P Levels and Shoulder Joint Contracture After Arthroscopic Repair of the Rotator Cuff *F Franceschi, UG Longo, L Ruzzini, F Battistoni, G Dicuonzo,* ***N Maffulli****, V Denaro*	**p62**
5:30- **5:40 pm**	Closing Remarks *Savio L-Y. Woo, PhD, DSc*	
5:45 pm	Tour of BioMotion Laboratory, Durand Building	

Dinner and Award Ceremony

5:45- **7:00 pm**	Reception and Cocktail Hour (Cash Bar)
7:00 pm-	Dinner and award ceremony
8:30 pm	Bus Departure

KINEMATIC CHANGES FOLLOWING ACL INJURY AND RECONSTRUCTION: A PATHWAY TO KNEE OA

Tom Andriacchi, Sean Scanlan, Seungbum Koo, Paul Briant, Scott Bevill

Stanford University, Stanford, CA, USA
VA Palo Alto Health Care System, Palo Alto, CA, USA

An analysis of the ambulatory changes following ACL injury in the context of the phenotypic regional variations in articular cartilage provides a unique multi-scale view of a potential pathway to premature osteoarthritis in patients following ACL injury.

Anterior cruciate ligament (ACL) reconstruction (the standard of care) has been a very successful treatment for the initial functional loss (e.g. giving way episodes) following ACL injury. However, there is clinical evidence that ACL reconstruction does not substantially reduce the occurrence of osteoarthritis (OA) [6]. In fact, one 20-year follow-up study of ACL reconstruction patients found that 84% of patients showed radiological signs of OA [7]. Understanding the pathway to premature OA following ACL injury and reconstruction is an important consideration in the addressing new methods for prevention and treatment of OA following ACL injury. .

There is an increasing body of literature suggesting that individual changes in the mechanics of ambulation following ACL injury or reconstruction has a profound influence on the long term cartilage degeneration [1]. In particular, the kinematic rotational and translational changes at the knee during ambulation [1,4,8] following ACL injury have been related to patterns of cartilage thinning [5].

The characteristics of the ambulatory changes combined with an analysis of regional variations in the morphology of tibial plateau cartilage between central and peripheral regions of tibial cartilage suggest a sensitivity of cartilage health to changes in kinematics during walking. In particular, the regional differences in collagen organization, chondrocyte morphology and gene expression for certain structural proteins appear to represent a conditioning to the local mechanical environment specific to either the central or peripheral weight bearing regions [2,3] Taken together these observation suggest that kinematic changes following ACL injury shift the nominal weight bearing regions of the joint to regions that are not conditioned to the new loading conditions (increased or decreased) and cannot adapt, thus initiating a degenerative cascade of events leading to premature osteoarthritis [1].

REFERENCES

1. Andriacchi, TP, Muendermann, A, Smith, RL, Alexander, EJ, Dyrby, CO, Koo, S: A Framework for the in vivo Pathomechanics of Osteoarthritis at the Knee, In: Annals of Biomechanical Engineering, vol. 32, No. 3, 447-457, March 2004.
2. Bevill, SL, Briant, PL, Andriacchi, TP: Central and Peripheral Region Tibial Plateau Chondrocytes Respond Differently to Dynamic Compression, 54th Annual meeting of the Orthopaedic Research Society, San Francisco, CA, March, 2008.
3. Briant, P, Bevill, S, Andriacchi,TP: Topological differences in the cartilage superficial layer of the porcine knee, 52nd Annual meeting of the Orthopaedic Research Society, Chicago, IL, Mar 2006.
4. Georgoulis AD, Papadonikolakis A, Papageorgiou CD, Mitsou A, Stergiou N: Three-dimensional tibiofemoral kinematics of the anterior cruciate ligament-deficient and reconstructed knee during walking. Am J Sports Med 31(1): 75-79,2003
5. Koo S, Dyrby CO, Andriacchi TP: Abnormal ambulation after ACL rupture affects knee articular cartilage spatial thinning pattern, 53rd Annual Meeting of the Orthopaedic Research Society, San Diego, CA, February 2007.
6. Lohmander LS, Ostenberg A, Englund M, Roos H: High prevalence of knee osteoarthritis, pain, and functional limitations in female soccer players twelve years after anterior cruciate ligament injury. Arthritis Rheum 50(10): 3145-3152,2004
7. Maletius W, Messner K: Eighteen- to twenty-four-year follow-up after complete rupture of the anterior cruciate ligament. Am J Sports Med 27(6): 711-717,1999
8. Tashman S, Collon D, Anderson K, Kolowich P, Anderst W: Abnormal rotational knee motion during running after anterior cruciate ligament reconstruction. Am J Sports Med 32(4): 975-983,2004

EVEN IMMEDIATE NORMAL ANATOMIC ACL REIMPLANTATION IN AN OVINE MODEL LEADS TO SIGNIFICANT SYNOVIAL INFLAMMATION WITH POTENTIAL FOR JOINT DAMAGE

J.W.S. Chin, K.D. Huebner, M. Chung, L.L. Marchuk, J.E. Beveridge, N.G. Shrive, D.A. Hart and C.B. Frank
McCaig Institute for Bone & Joint Health, University of Calgary, Calgary, Canada

INTRODUCTION

Injury to the anterior cruciate ligament (ACL) is a major cause of secondary osteoarthritis (OA). ACL reconstruction aims to restore normal joint function after ACL injury; however, this procedure may not retard the progression of OA. At least two possible reasons for OA development have been postulated: normal mechanics may not be restored by ACL reconstruction with tendon grafts and/or the biological environment of the joint may be altered following ACL injury. Increasing evidence suggests that synovial inflammation may play a role in altering the integrity of joint structures, contributing to the development of OA **[1]**. The purpose of this study was to assess whether 'perfect ACL reconstruction' using the normal ACL cored out at only one end and immediately repositioned in its anatomic position versus imperfect reconstruction (a normal ACL placed in an altered position (a normal location but twisted and too tight) would contribute to altered kinematics and to increased synovial inflammation.

METHODS

Skeletally mature female Suffolk Cross sheep underwent reconstructive surgery of their right ACLs (approved by Institutional Animal Care Committee). Six sheep served as normal unoperated controls. Surgeries were performed by removing the femoral insertion of the sheep's own ACL on a bone plug while leaving both the tibial insertion and the ACL intact. Grafts were fixed using Kirschner wires in either an anatomical position (n=3), (ACL reestablished in its original position) or under increased tension and twist (TT) (n=3) with the ACL twist increased by 90° and ligament pulled up by 3 mm. Kinematics were recorded prior to and 4 weeks post grafting by previously reported techniques **[2]** Sheep were sacrificed 4 weeks post-surgery. Synovium was collected, snap frozen in liquid N_2 and stored at -70°C until further analysis. Total RNA was isolated, quantified and RT-PCR carried out for interleukin-1β (IL-1β), tumor necrosis factor-α (TNF-α), matrix metalloproteinase-1 & 13(MMP-1, 13), tissue inhibitor of matrix metalloproteinase-1 (TIMP-1), inducible nitric oxide synthase (iNOS) and cyclooxygenase-2 (COX-2). mRNA levels for each gene were normalized to a housekeeping gene (18S). Statistical analysis for each gene consisted of comparing mRNA levels in the two experimental groups to normal unoperated controls using Student's t-tests ($p<0.05$).

RESULTS

IL-1β, MMP-1, MMP-13, TIMP-1 and iNOS mRNA levels were significantly elevated in anatomical and T.T. groups compared to normals. COX-2 mRNA levels in T.T. group were higher than normals. TNF-α mRNA levels demonstrated no significant differences between the two grafts and normals (Figure 1).

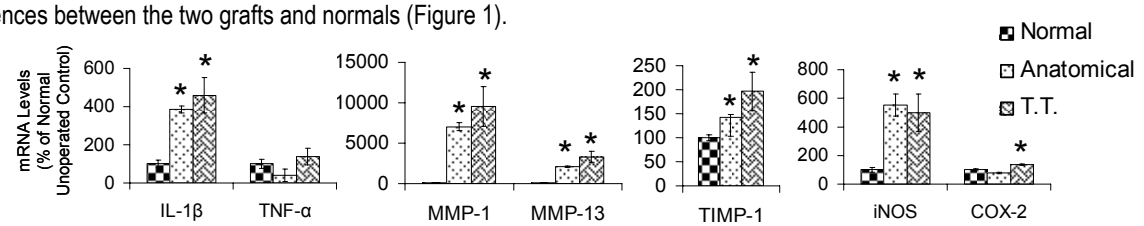

Figure 1: mRNA levels for relevant inflammation and associated molecules in the synovium of sheep with anatomical grafts, T.T. grafts and normal unoperated controls. * denotes statistical significance when compared to normal unoperated controls.

DISCUSSION

As synovium can be used to monitor the inflammatory state of the intra-articular environment **[3],** these results suggest a surprisingly severe synovial inflammation in joints with both graft types at 4 weeks post-op. Even an anatomic ACL graft cored at only one end and replaced immediately appears to cause significantly increased expression of IL-1β which stimulates MMP-1 and -13 synthesis, both of which degrade native collagen in cartilage **[4]**. IL-1β can also induce iNOS and COX-2, further enhancing inflammation **[5]**. While not all inflammatory markers (eg TNF-α) were upregulated (perhaps due to the timing of assessment), and while up-regulation of TIMP-1 suggests the potential for partial inhibition of upregulated MMPs **[6]**, these results collectively suggest the disturbing possibility of early joint damage secondary to surgically induced synovial inflammation, even in 'perfect anatomic grafting'. Abnormally placed but otherwise normal ACL grafts which are cored out, twisted and fixed 'too tight' do alter joint kinematics (shown elsewhere) but this mechanical abnormality did not add significantly to the already upregulated mRNA markers of synovial inflammation. Future studies that include other time points as well as the assessment of other joint tissues will further help to elucidate the role of inflammation and graft tensioning/positioning in contributing to joint damage and in separating biological from biomechanical risks for OA development following ACL reconstruction.

REFERENCES

1. Pearle AD, et al. Osteoarthritis Cartilage 2007 **2**. Tapper JE, et al.J Biomech Eng 2004 **3.** Hellio Le Graverand MP, et al. Matrix Biol. 2000 **4.** Pelletier JP, et al. J Rheumatol Suppl 1989 1999 **5.** Weinberg JB, et al. Subcell Biochem 2007
6. Ishiguro N, et al. Arthritis Rheum

ACL-RECONSTRUCTION & CARTILAGE DEFORMATION

Van de Velde, S K; Gill, T J; Bingham, J T; DeFrate, L E; and Li, G
Bioengineering Laboratory, Massachusetts General Hospital/Harvard Medical School, Boston, MA

INTRODUCTION

It is poorly understood why patients after anterior cruciate ligament (ACL) reconstruction develop osteoarthritis, even though the anteroposterior (AP) stability is successfully restored. In this study, we hypothesize that ACL deficiency causes an increased structural deformation of the tibiofemoral cartilage. More importantly, we hypothesize that ACL reconstruction with a BPTB autograft does not restore the normal cartilage deformation.

METHODS

Eight patients (6 male and 2 female; 19-38 years old) with an acute ACL injury in one knee and the contralateral side intact participated in the study. Both knees were imaged using a specific MR sequence to create 3-D knee models. These models were digitally manipulated until their projections matched the outlines of two orthogonally placed fluoroscopic images [1], as the patient performed a single-leg lunge. Data was collected pre-operatively, and at 6 months following ACL reconstruction. The anterior laxity of the reconstructed knee as measured with the KT-1000 arthrometer was similar to that of the intact contralateral knee. Cartilage deformation was defined as the amount of penetration divided by the sum of the tibial and femoral cartilage thicknesses (Figure 1). A repeated measures ANOVA was used to compare the magnitude of cartilage deformation of the intact, ACL-deficient, and ACL-reconstructed knees. Significance was set at $p<0.05$.

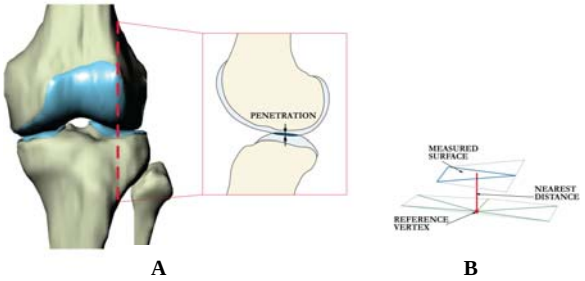

Figure 1: (A) Sagittal section of a left knee showing the definition of cartilage penetration. (B) Method of measuring cartilage thickness and penetration depth from meshed surfaces.

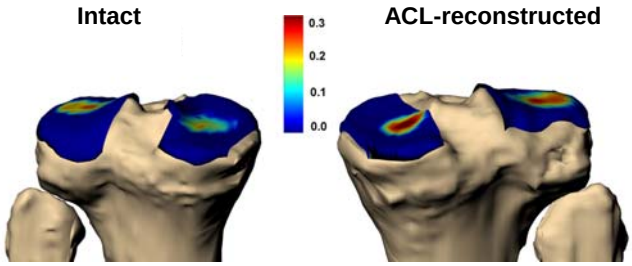

Figure 2: Color map of the cartilage deformation for the intact and ACL-reconstructed tibia at 15° of flexion.

RESULTS

ACL deficiency significantly increased the deformation of cartilage from 0° to 60° of flexion in the medial compartment, and from 0° to 30° in the lateral compartment. The maximum increase in cartilage deformation after ACL rupture occurred at 0° of flexion (18 ± 6% intact knee, 30 ± 8% ACL-deficient knee) in the medial compartment.

ACL reconstruction improved the cartilage deformation throughout the range of motion. However, at 0° and 15° of flexion, a significant increase in cartilage deformation persisted in both compartments following reconstruction. The maximum increase in cartilage deformation after ACL reconstruction occurred at 0° of flexion in the lateral compartment (25 ± 8% intact knee, 34 ± 6% ACL-deficient knee, 36 ± 5% ACL-reconstructed knee).

DISCUSSION

The articular cartilage of ACL-deficient knees undergoes an increased cartilage deformation. Even though ACL reconstruction improved the cartilage deformation, a persistent significant increase in cartilage deformation was observed at 0° and 15° of flexion. These findings emphasize the difficulty of restoring normal cartilage biomechanics under physiological loading using current surgical techniques, even though the joint stability could be restored satisfactorily.

REFERENCES

1. Li G et al. *J Bone Joint Surg Am.* 2006, 88(8):1826-34.

RELATIONSHIP BETWEEN THE ORIENTATION OF THE ACL GRAFT IN THE CORONAL PLANE AND THE KNEE FLEXION MOMENT DURING WALKING

Sean Scanlan[1], Katerina Blazek[1], Ajit Chaudhari[2], and Tom Andriacchi [1,3]

[1] Stanford University, Stanford, CA, USA
[2] The Ohio State University, Columbus, OH, USA
[3] VA Palo Alto Health Care System, Palo Alto, CA, USA

INTRODUCTION

The reduced knee flexion moment (balanced by a net quadriceps moment) commonly observed in ACL deficient subjects during walking [2] has been interpreted as a compensatory strategy to avoid anterior tibial translation due to quadriceps contraction at the knee in the absence of the restraint of the ACL. However, it's been shown that reduced net quadriceps moments still persist in some patients even after ACL reconstruction [5]. The relationship between the placement of the ACL graft and ambulatory function remains an open question, particularly with regard to the placement of the femoral tunnel in the coronal plane. The purpose of this study was to test the hypothesis that the peak external knee flexion moment during walking is correlated with the coronal plane orientation of the ACL graft.

METHODS

Seventeen subjects with clinically successful unilateral ACL reconstructions and no other history of serious lower limb injury (avg 34 yrs, 1.7 m, 70 kg, 7 male, 9.2 mo injury to reconstruction, 24 mo past reconstruction) were recruited for the study after providing IRB-approved informed consent. Sagittal-plane MR images (3D-SPGR, 1.5T) were obtained for the ACL reconstructed knee of each of the subjects lying in a supine, extended position. The images were reconstructed in the axial plane and the ACL graft and proximal tibia were manually segmented. Principal component analysis was then used to determine the principal longitudinal axis of the ACL and to fit a plane to the tibial plateau. The orientation of the ACL graft was measured relative to the tibial plateau in the coronal plane. Subjects also underwent a gait test at three self-selected walking speeds (fast, normal, slow). A force-plate and a previously-described link model were used to estimate the net external forces and moments acting at the joints [1]. Linear regression was used to obtain an interpolated value of the peak knee flexion moment at a 1.0m/s walking speed for each subject. Linear regression analysis was also performed on the pooled subject data to determine the correlation between the peak external knee flexion moment during walking and the coronal ACL graft angle.

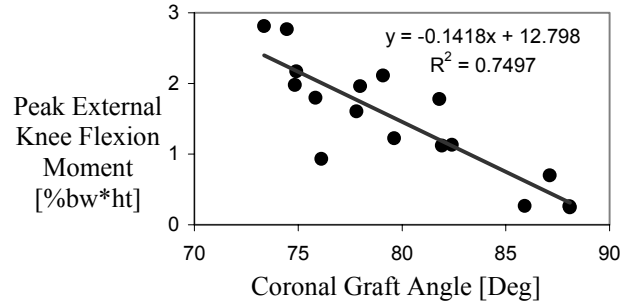

Figure. 1 Relationship between the peak knee flexion moment during walking and coronal ACL graft angle.

RESULTS

The peak knee flexion (net quadriceps) moment during walking was correlated (R^2=0.75, $p<0.001$) with the orientation of the ACL graft in the coronal plane (Fig. 1). A more vertically oriented graft correlated with a reduced peak flexion moment.

DISCUSSION

The results of this study support the hypothesis that the intra-articular placement of the ACL graft influences the *in vivo* mechanics of the ACL reconstructed knee. In subjects where the graft was placed in a nonanatomic vertical orientation (the coronal angle of the native ACL is approximately 67º [3]), their flexion moments during walking approached the "quadriceps avoidance" pattern observed in the ACL deficient knee [2]. These findings can potentially be explained by cadaveric studies that have shown that a more vertically oriented ACL graft provides less tibiofemoral translational and rotational stability [4]. Thus it appears that as the graft is placed in a more vertical orientation and consequently its capacity to replicate the function of the native ACL is diminished, the patient subconsciously adapts their gait to avoid the possible instability of a large quadriceps contraction similar to a patient with complete ACL deficiency.

REFERENCES

[1]Andriacchi TP, et al. 1997 *Basic Orthopaedic Biomechanics,* 37-68. [2]Berchuck M, et al. 1990 *J Bone Joint Surg* 72(6):871-7. [3] Fugimoto E, et al. 2004 *Magn Reson Imaging* 22(8):1125-9. [4] Loh et al, 2003 *Arthroscopy* 19(3):297-304. [5]Webster KE, et al. 2005. *Am J Sports Med* 33(2):247-54.

ACL-DEFICIT AND -RECONSTRUCTED KNEES HAVE ALTERED ROTATIONAL AXES DURING DAILY ACTIVITIES

+Zheng, N, Gao, B., Conrad, B.P., Moser, M.W., Indelicato, P.A.
University of Florida, Gainesville, FL nigelz@ufl.edu

INTRODUCTION

The anterior cruciate ligament (ACL) plays an important role in controlling knee joint stability [1]. ACL injury and changes in knee joint motion have been associated with cartilage thinning and progressive development of knee osteoarthritis [2]. The rotational axes of the ACL-deficient (ACL-D) knee during non-ambulation activities like seated flexion/extension had substantially higher variance in kinematic patterns than those of normal knees [3-4]. We hypothesized that ACL-D and ACL-reconstructed (ACL-R) knees have less stability compared with bilateral ACL-intact (H) knees during daily activities. The purpose of this work was to compare the 3D joint stability of unilateral ACL-D and ACL-R knees with that of H knees during level walking (LW), stair ascending (SA) and stair descending (SD).

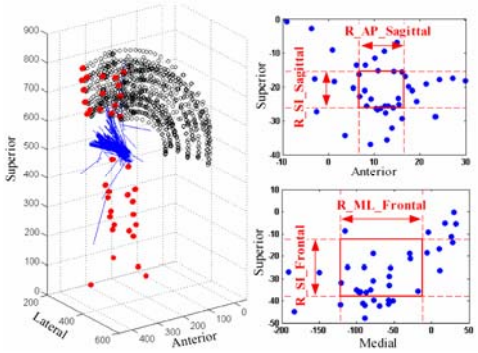

Fig.1 Rotation axes of a healthy knee during stair descending (left) and their intersection points with sagittal and frontal planes (right). All units are mm.

METHODS

Forty-eight subjects (23 H, 15 ACL-D and 10 ACL-R) were recruited and tested using an IRB approved protocol. ACL-D and ACL-R subjects were 2 months to 2 years post injury or surgery when tested. Eighty-nine retro-reflective markers and an 11-camera motion analysis system (MAC, CA) were used to collect the motion during LW, SA and SD [5]. Instantaneous helical axis of the knee joint in each gait cycle was calculated every 1/15 second [6] and expressed as femur relative to the tibial anatomical coordinates [7]. The helical axes of the knee joint were analyzed by examining their intersection points with the sagittal plane and the frontal plane (Fig.1). The interquartile range (IQR) was calculated to evaluate the stability of knee rotation axes. The differences of IQR were tested using one-way analysis of variables for each activity.

RESULTS

IQRs of ACL-D and ACL-R knees during all three daily activities were significantly different than those of H knees (Fig.2). No significant differences between ACL-R and ACL-D were found except the medial-lateral (ML) frontal IQR during SD. During LW, AP sagittal IQR and both frontal IQRs of ACL-R knees were significantly greater than those of H knees. Both sagittal IQRs of ACL-D knees were significantly greater than those of H knees. During SA, the superior-inferior (SI) sagittal and ML frontal IQR of ACL-R knees were significantly greater than those of H knees. During SD the ML frontal IQR in the ACL-R group were significantly greater than that in both H and ALC-D group. The SI sagittal IQRs of both ACL-D and ACL-R knees were significantly greater than that of H knees during SD.

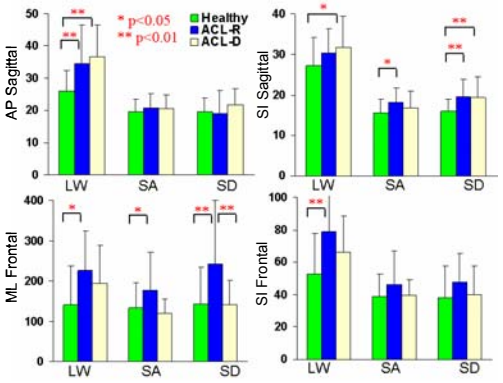

Fig.2 Interquartile ranges (range between the 3rd and 1st quartiles) of intersections of knee axes with the sagittal and frontal planes during level walking (LW), stair ascending (SA), and stair descending (SD). All units are mm.

DISCUSSION

By using the 3D knee kinematics measurement and helical axes analysis, we formulated a quantitative approach to evaluate dynamic stability of knee joint during daily activities. Greater IQRs in the ACL-D and ACL-R group indicated that the ACL-D and ACL-R knees had altered rotational axes during daily activities. This study found that both ACL-D and ACL-R knees had greater spatial variation of rotational axes and less joint stability compared with intact knees. No improvement was found for ACL-R knees when compared with ACL-D knees. Because these activities, especially LW, are repeated thousands of times every day, this abnormality may lead to the progressive cartilage degeneration and knee OA reported clinically.

REFERENCES: 1. Wilson DR et al, *J Biomech*, 2000; 2. Andriacchi TP et al, *Clin Orthop Relat Res*, 2006; 3. Montgomery SC. et al, *Knee* 1998; 4. Dennis DA. et al, *J Biomech*. 2005; 5. Zheng N. et al, *ORS* paper 164 2007; 6. Spoor CW. et al, *J Biomech*, 1980; 7. Gao B and Zheng N *ASB* 2007.

JOINT FAILURE IN ACL/MCL DEFICIENCY: THE IMPACT ON THE APPARENT STRAIN ENVIRONMENT OF HEALING AND REMAINING INTACT LIGAMENTS

JE Tapper, Y Funakoshi, M Hariu, L Marchuk, GM Thornton, JL Ronsky, RF Zernicke, NG Shrive, CB Frank
Joint Injury and Arthritis Research Group, University of Calgary, Calgary, Alberta

INTRODUCTION

The objective of this study was to investigate the impact of combined ACL/MCL transection on the apparent strain environment of the healing ACL and MCL, and the remaining intact LCL and PCL, during dynamic in vivo motion.

METHODS

The dynamic in vivo 3D kinematics of the stifle joint during walking were measured in eight sheep using a 4-camera motion analysis system (0.4±0.4mm) with surgically implanted bone markers. Kinematics were measured for 30 strides with the joints intact and at 2, 4, 8, 12, 16, and 20 wk after either combined transection of the ACL and MCL (n=5) or sham surgery without ligament transection (n=3). All animal surgeries and testing were approved by the University of Calgary Animal Care Committee and complied with the guidelines of the Canadian Council on Animal Care. At sacrifice (20 wks), a 3D digitizer (±0.05mm) was used to define tibial and femoral coordinate systems. The bone markers positions, articular surface geometry, and centroids of the insertions of the stifle joint ligaments [ACL_{AM}, ACL_{PL}, MCL, LCL, PCL] were then digitized within these coordinate systems. The transformation matrices between anatomical and global coordinate systems, and the 3D positions and linear and angular velocities of the tibia and femur were calculated from marker data, so that the 3D distance between ligament insertions and the velocities at the insertions sites could be determined. The relative velocity of the two insertion sites along the axis of each ligament was calculated to determine the apparent strain rate throughout the gait cycle. The distance between ligament insertions (DBI), the ligament apparent strain ($DBI/minDBI_0$), the maximal apparent strain rate, and the apparent strain at which the maximal apparent strain rate occurred were determined. The within subject changes from the intact kinematics were assessed using cross-sectional time series regression.

RESULTS

At 2 wk after transection, the maximal apparent strain rate was increased, relative to sham controls, in the intact PCL alone (Table 1). At 20 wk after transection, the maximal apparent strain rate was increased in both bands of the healing ACL and the intact PCL, but was unchanged in the healing MCL and the intact LCL. The apparent strain at which the maximal apparent strain rate occurred was increased at 2 wk in both bands of the ACL and the MCL. For the ACL, that strain (2 wk: 15.7%, 20 wk: 21.2%) was greater than the maximal apparent strain observed in the intact joint (11.3%). These changes persisted at 20 wk in the ACL but normalized in the MCL. The apparent strain at which the maximal apparent strain rate occurred was decreased in the intact LCL and PCL at both 2 and 20 wk.

DISCUSSION

Combined ACL/MCL transection had a significant impact on the in vivo apparent strain environment of not only the healing ACL and MCL, but also the remaining intact LCL and PCL. Changes in strain rate affect the structural properties of normal ligaments[1,2]. The impact of strain rate on the properties of healing ligaments is not known. Increased apparent strain rates, that occurred at high levels of apparent strain, may explain the lack of healing of the transected ACL[3]. Decreases in the apparent strain at which the maximal apparent strain rate occurred may have played a role in the tissue remodelling observed in the intact LCL and PCL[3,4].

1. Woo SL et al. 1990. JOR 8:712-721. 2. Noyes FR et al. 1974. JBJS A. 56:236-253. 3. Zachos TA et al. 2002. Vet Surg 31:596-603. 4. Funakoshi Y et al. 2007. JOR 25:997-1006

Table 1. The rate of change of apparent strain rate in the ovine stifle joint during walking in the intact joint and at 2 and 20 wk after ACL/MCL transection. The Δ indicates a significant difference from the intact joint and the * indicates a significant difference from the sham group.

	INTACT			2 WEEKS				20 WEEKS			
	mm / s	se	% / s	mm / s	se	% / s		mm / s	se	% / s	
ACL_{AM}	32.9	2.7	145	52.0	7.8	226	Δ	65.2	12.4	275	Δ*
ACL_{PL}	33.3	2.0	170	49.1	6.7	244	Δ	62.5	12.1	304	Δ*
MCL	32.5	3.6	87	34.7	3.2	93		30.5	4.4	83	
LCL	29.3	2.0	97	34.4	1.6	113		23.9	2.1	76	
PCL	38.7	3.9	160	52.3	5.1	219	Δ*	53.7	5.2	225	Δ*

FORCE SHARING IN THE THREE BUNDLES OF THE ANTERIOR CRUCIATE LIGAMENT: BIOMECHANICAL ANALYSIS USING A NOVEL ROBOTIC SYSTEM

Hiromichi Fujie[1], Takashi Hirano[1], Shoji Fukano[1], Machiko Imura[1], Daisuke Katakai[1]
Hidenori Otsubo[2], Yoshiyuki Suzuki[3], Ken Nakata[3], and Konsei Shino[3]

[1] Biomechanics Laboratory, Department of Mechanical Engineering, Kogakuin University, Tokyo, Japan
[2] Sapporo Medical University, Sapporo, Japan
[3] Osaka University Medical School, Osaka, Japan

INTRODUCTION:

The restoration of knee function after the injury in the anterior cruciate ligament (ACL) relies on surgical reconstruction procedure. However, current reconstruction techniques neither reproduce normal knee kinematics nor fully restore the functions of the ACL. For more successful clinical results, it is required to know the detailed function of the normal ACL and to assess reconstruction techniques. For these purposes, a novel robotic system, developed in our laboratory for mechanical testing of human knee joint in multi-degrees of freedom (DOF), was applied to the determination of the forces in the anteromedial, intermediate, and posterolateral bundles in response to anterior force, proximal force (joint compression force), valgus moment, and internal moment to the knee, as well as a combined load to simulate pivot-shift test.

METHODS:

A novel robotic system[1)], consisted of a 6-DOF manipulator, servo motor controllers, control computer, and a universal force-moment sensor (UFS) was utilized in the present study. Preliminary tests revealed that the clamp-to-clamp stiffness of the system is better than 312 N/mm. The system is controlled by a custom-made PID-hybrid position/force control software on the LabView (version 8.0, National Instruments). It is possible to simultaneously control the both displacement of, and force/moment applied to, the human knee joint in 6-DOF.

Using a laser digitization system, the knee joint coordinate system[2)] was fixed to the knee. Three-dimensional paths of the intact knee in response to the anterior force (up to 100 N), proximal force (up to 100 N), valgus moment (up to 10 Nm), and internal moment (up to 5 Nm) to the knee, as well as a combined load (flexion with a combined loading of 50 N of proximal force, 5 Nm of valgus moment, and 3 Nm of internal moment) to simulate pivot shift test were recorded. Then the ACL was separated to anterioromedial (AM), intermediate (IM), and posterolateral (PL) bundles following a previous study [3)]. The cross-sectional area of the IM bundle was similar to that of the AM bundle and approximately 1/4 to the area of the entire ACL. After the AM bundle was transected the 3-D paths of intact knee motion were reproduced. The intact paths were reproduced after the transection of the IM bundle and then the PL bundle. Force data measured with the UFS were used to determine the in-situ forces in the bundles in response to the above-mentioned force/moment applications[4)].

RESULTS & DISCUSSION:

At 30 degree of flexion, the share of the PL bundle force in the all bundle forces was approximately 40% in response to the application of the anterior force or valgus moment. The share was decreased to less than 20% in response to the application of the proximal force or internal moment. In the simulation of the pivot shift test, the share was increased to approximately 40%, which was slightly higher than that reported by Gabriel, et al [5)]. Analysis of joint motion data suggested that the force share of the PL bundle was high when the rotational center was medially shifted and/or medial joint opening was caused. With the increase of flexion angle, the force in the PL bundle was decreased while the forces in the AM and IM bundles were increased in all the conditions except the internal moment application. The force in the IM bundle was approximately same level or slightly larger as compared with that in the AM bundle in all the conditions. These results imply that the 3 ACL bundles differently play important roles in various loading situations.

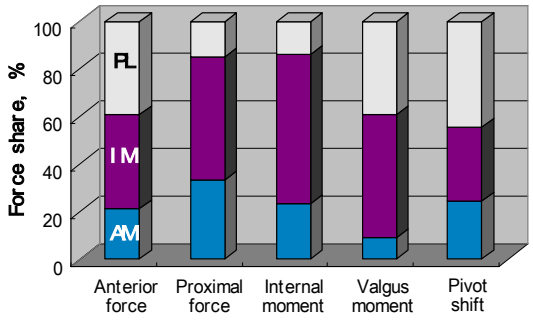

Fig.1: ACL bundle forces at 30 degree of flexion in response to anterior force, proximal force, internal moment, and valgus moment as well as a simulated pivot shift loading.

REFERENCES:

1) Fujie et al., *JBME* 2004, 2) Grood & Suntay, *JBME* 1983, 3) Norwood and Cross, *AJSM* 1979, 4) Fujie et al., *JBME* 1995, 5) Gabriel et al., *JOR* 2004.

ACKNOWLEDGMENT:

This study was financially supported by the Grant-In-Aid for Scientific Research (C) (#18591643) from MEXT, and by Kogakuin University Project Research (2006-).

Biomechanical Comparison of two methods of reconstruction for the Combined Posterior Cruciate Ligament and Posterolateral Corner injury of the Knee

H. Ishigooka[1], T. Sugihara[1], H. Fujiya[2], T. Satoh, M Beppu[1]

[1]Department of orthopedic surgery, St. Marianna University School of Medicine, Kanagawa, Japan

[2]Department of Sports Medicine St. Marianna University School of Medicine, Kanagawa, Japan

INTRODUCTION

A gold standard technique has not yet been established for the reconstruction of combined ligament injury of the posterior cruciate ligament (PCL) and the posterolateral corner (PLC) of the knee. The purpose of this study was to compare biomechanically our new reconstruction which fixed the popliteal tendon (PLT) to the fibula head as fibula fixation (FF) method (Fig. 2) and the Laplades reconstruction which fixed the PLT to the posterior of the tibia as the tibia fixation (TF) method (Fig.5).

MATERIALS AND METHODS

Ten fresh porcine knees using an Instron force analysis system were examined with six degrees of freedom movement (Fig. 1). By applying a posterior load of 50 N, varus rotation load of 2 N-m, and an external rotation load of 2 N-m to the tibia at 30, 60, and 90 degree knee flexions, the normal distance of the joint translation and the rotational angles were recorded. Then, the same measurements were performed after cutting the PLC, cutting the PCL, and reconstructing all ligaments. Two intersecting tunnels were made in the fibular head for LCL and PLT as FF method to five knees, and single tunnel was made from the posterior to anterior of the tibia as a TF method to the other five knees and tibialis posterior tendon graft were fixed using endo-buttons. The femur side of the PLT and LCL were fixed using a screw and a washer.

Fig. 1

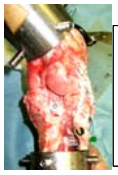

Fig.2 FF method

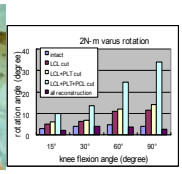

Fig.3 varus r.

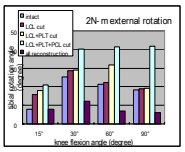

Fig.4 external r.

Fig.5 TF method

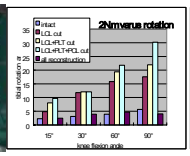

Fig.6 varus r.

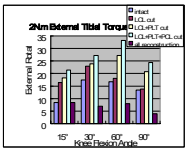

Fig.7 external r.

RESULTS

The stability of the knee joint before cutting the ligaments was as follows: the posterior displacement distance of the tibia, the varus rotation angle and the external rotation angle of the tibia were an average of 7.3mm, 4.2 degrees and 21.6 degrees respectively. After cutting all ligaments, instability increased to 23.9mm, 24.0 degrees and 41.1 degrees respectively. After the PCL, PLT, and LCL were reconstructed stability recovered by the FF method 5.3 mm, 3.3 degrees (Fig. 3) and 8.4 degrees (Fig. 4) respectively and by the TF method 4.3 mm, 3.8 degrees (Fig. 6) and 6.8 degrees (Fig. 7) respectively. The stability was obtained by both methods, but FF method was more stable for varus rotation, and TF method was more stable for external rotation.

DISCUSSION

Recently, several methods have been reported in reconstruction of PCL-PLC combined knee ligament injury. It was revealed through our experiment using two fresh human cadaveric knees (ISAKOS 2005) that the ligament from lateral condyle of the femur to the head of the fibula became tense and nearly straight during tibia external rotation. Therefore, we decided to use these two points as the reconstruction route for FF method. The angle of the PLT decreased from tibial axis in the FF method and it decreased stability of the external rotation than TF method. However, the insertion of the PFL was located to more posterolaterally than TF method and that made ridged stability for the varus rotation. We reduced the risk of a cutout of the fibula head and reduced the ligamentous killer turn by making two tunnels which intersected in the fibula. Surgical approach of the FF method is easier than TF method because the posterior of the fibula is shallower than the posterior of the tibia. This method provides a stable anatomical procedure for treating this injury.

REFERENCE 1) Ishigooka. H, Sugihara. T et al. Anatomical study of the popliteofibular ligament and surrounding structures. J Orthop Sci 2004;9(1):51-8.

Elastic properties of Achilles tendon among male soccer athletes in grades 3 – 6

Yosuke Egawa PhD, Suguru Torii MD, Chiaki Nakamura, Toru Fukubayashi MD PhD
Faculty of Sport Sciences, Waseda University, Saitama, Japan

[INTRODUCTION]

Extreme repetitive stress on the apophysis without considering the physical characteristics of children induces a disorders of the growing skeleton[2]. However, only a few studies have evaluated indexes of the muscle-tendon complex as a risk factor for apophysitis. The present study investigates the relationship between the elastic properties of the Achilles tendon, physical characteristics, muscle tightness (MT), and tenderness associated with typical apophysitis (calcaneal tubercle, tibial tuberosity and iliac spine) in Japanese elementary school athletes.

[METHODS]

We examined boys ranging in age from 8 to 12 years (elementary grades 3 - 6 in Japan) with normal physical appearance, and no history or locomotor complaints who regularly played soccer. Muscle tightness was determined as angle of the ankle at maximal dorsiflexion. Elongation of the tendon and aponeurosis of the medial gastrocnemius muscle (MG) during isometric plantar flexion, respectively, were determined using a real-time ultrasonic apparatus (ALOKA-SSD1000 JAPAN) in vivo while torque gradually increased from zero to maximal effort (MVC) within 5 s. The relationship between the estimated muscle force and tendon elongation (L) was fitted to a linear regression, the slope of which was defined as the elastic index of the tendon structures. Kawakami et al. have confirmed the precision and linearity of the image[1].

[RESULTS]

The sizes of the body and lower leg increased with age. The elastic index of the Achilles tendon and the standard deviations were greater in 5th and 6th, than in 3rd and 4th graders (Fig. 1). Point tenderness was greatest in 4th graders (9 - 10 years). When the boys were categorized into groups with and without point tenderness, MT did not significantly differ. However, the elastic index was higher among boys with point tenderness ($p = 0.07$; Fig. 2).

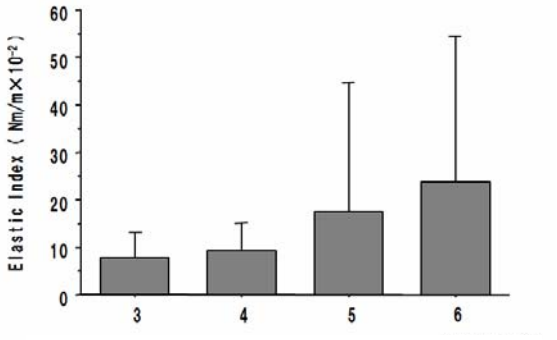

Fig. 1 Elastic properties of Achilles tendon in grades 3-6.

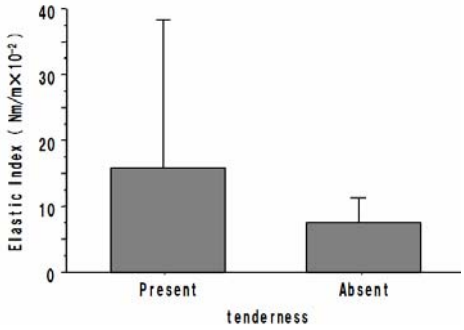

Fig. 2 Comparison of elastic indexes among male soccer athletes in grades 3 – 6 with and without tenderness.

[DISCUSSION AND CONCLUSION]

Repetitive traction of the apophysis caused by a stiffer muscle-tendon unit leads to injury of the apophysis and growth plate, and our method appears sufficiently sensitive to determine the pathomechanics of apophysitis.

[REFERENCES]

1. Kawakami, Y., Y. Ichinose, and T. Fukunaga. Architectural and functional features of human triceps surae muscles during contraction. J Appl Physiol. 85:398-404, 1998.
2. Volpon, J. B. and G. de Carvalho Filho. Calcaneal apophysitis: a quantitative radiographic evaluation of the secondary ossification center. Arch Orthop Trauma Surg. 122:338-341, 2002.

A COMPARISON OF THE LOW-LOAD BEHAVIOR OF INJURED AND UNINJURED MEDIAL COLLATERAL LIGAMENTS IN TWO PORCINE BREEDS

Germscheid NM; Hildebrand KA; Thornton GM; Hart DA
McCaig Centre, University of Calgary, Calgary, AB

INTRODUCTION

A porcine model of dermal wound healing has a genetic basis.[1] The red Duroc (RD) pig developed a unique healing phenotype characterized by hypercontracted, hyperpigmented scars whereas, the Yorkshire (YK) pig did not.[2] Healing of other connective tissues, such as the medial collateral ligament (MCL), may be genetically mediated within this animal model. The objective was to investigate whether porcine ligament low-load behavior exhibits a differential healing response within two pig breeds. We hypothesized that a differential healing response would exist within the low-load behavior of two porcine breeds; the RD pig would exhibit a greater healing response than the YK breed.

METHODS

Gap injuries were created in the right knee MCLs of 6 YK and 6 RD female pigs. The animals resumed activity for 10-weeks. Institutional animal care committee approval was granted. Contralateral (contra) limbs served as unoperated controls and normal knees were obtained from 12 gender and breed matched pigs. All animals were skeletally immature throughout the study. The knee joints were mounted to the MTS system where the whole joint underwent 2 cycles of 20N of compression to 8N of tension at 1mm/min. The femur-MCL-tibia complex was created. Two additional cycles were performed. Digital calipers were used to measure the MCL length and cross-sectional area. The MCL was loaded for 30 cycles at 1Hz to 100N (cyclic creep). Subsequently, it was loaded to 100N and held for 20 min. (static creep). Total creep was measured from the peak of cycle 1 in cyclic creep to the end of the 20 min period of static creep. A multiple random effects regression model with repeated measures was used to compare MCL scars to contra and normal MCLs. Factors such as weight, leg-sidedness, breed, and group were evaluated. T-tests were used to compare the healing differential between porcine breeds. Results were significant when $p \leq 0.05$.

RESULTS

Porcine MCL scars crept approximately 2-fold greater than contralateral and normal MCLs (Table 1). Breed differences were only observed within static and total creep strain estimates. Static and total creep strains were significantly greater in RD MCL scars compared to YK MCL scars (Table 1). An identical relationship occurred in contralateral and normal groups (Table 1). Breed differences were observed in static and total creep strains for both injured and uninjured MCLs. Therefore, mean percentage increases in scar creep strain (static and total) were compared between breeds to determine whether a healing response differential existed between breeds. This was found to be non-significant (Table 2).

Table 1 – Creep Strain Data (* indicates greater than YK ($p<0.05$); ‡ indicates greater than contra and normal ($p<0.01$)).

Group	Breed	Creep Strain (mean ± SD (%))		
		Cyclic	Static	Total
Scar	YK	0.49 ± 0.04‡	1.99 ± 0.22‡	2.48 ± 0.22‡
	RD	0.49 ± 0.05‡	2.25 ± 0.31*‡	2.74 ± 0.36*‡
Contra	YK	0.22 ± 0.03	1.18 ± 0.11	1.40 ± 0.11
	RD	0.24 ± 0.04	1.33 ± 0.17*	1.58 ± 0.20*
Normal	YK	0.25 ± 0.02	1.25 ± 0.05	1.35 ± 0.04
	RD	0.25 ± 0.00	1.50 ± 0.06*	1.60 ± 0.04*

Table 2 – Healing Differential Data

Comparison	Breed	Mean Percent Increase in Creep Strain (%)	
		Static	Total
Scar vs contra	YK	69	77
	RD	69	73
Scar vs normal right leg	YK	69	74
	RD	70	76

DISCUSSION

The results reveal that the low-load behavior of injured tissue is inferior to uninjured tissue. These findings are similar to previous work conducted on rabbits.[3] Despite breed differences within static and total creep strains of injured and uninjured MCLs, a differential healing response was not observed between YK and RD MCLs. This suggests that the difference between breeds is a result of the uninjured tissue, concluding that uninjured RD MCL creeps significantly more than YK MCL. This is contrary to the hypercontracted healing response observed within RD porcine skin. Future studies are needed to further validate these findings by determining if and what differences are occurring at the molecular level in uninjured YK and RD MCL.

REFERENCES

1.Gallant-Behm et al: *Wound Rep Regen* 14(1): 46-54, 2006. 2. Gallant et al: *Wound Rep Regen* 12: 305-319, 2004. 3. Thornton et al: *J Orthop Res* 18: 238-246, 2000.

FATIGUE-LOADED HEALING LIGAMENTS RUPTURE EARLIER AND AT GREATER STRAIN THAN CREEP-LOADED HEALING LIGAMENTS

S.J. Bailey and G.M. Thornton
McCaig Institute for Bone and Joint Health, University of Calgary, Calgary, Alberta, Canada

INTRODUCTION

Ligaments in vivo experience a complex combination of repetitive and sustained loading [1]. In normal ligaments, repetitive (fatigue) loading was found to be more damaging than sustained (creep) loading [2]. Ligaments healing from an injury have decreased failure properties compared to normal ligaments [3], which may correspondingly affect the ability of healing ligaments to function under physiologic loads. The range of these physiologic loads is around 5 to 10% of normal failure strength [4]. Our purpose was to investigate the effect of long term fatigue and creep loading on healing medial collateral ligaments (MCLs). Our hypothesis was that healing ligaments subjected to fatigue loading would rupture earlier than those subjected to creep loading at the same stress.

METHODS

In this study approved by the institutional animal care committee, 6 one-year-old female New Zealand White rabbits had bilateral MCL gap injuries created surgically. After 14 weeks of healing, one knee from each animal was allocated to fatigue loading and the other knee to creep loading. One fatigue MCL scar was not included due to an error in the test and one creep MCL scar was not included because of a large hole in the scar. After standardized preparation, mounting in an MTS system, and dissection to isolate the MCL scar, the knee underwent two compression-tension cycles, from -5N to +2N, stopping at +1N to establish "ligament zero". After measuring MCL scar geometry, an environment chamber (37°C and 99% RH) was installed and allowed to equilibrate. Then, all MCL scars underwent 30 preconditioning cycles from +1N to a force corresponding to 5% of the ultimate tensile strength (UTS) of 14-week scars [5]. *Fatigue*: MCL scars were cycled until rupture, using a sine wave at 1Hz from +1N to a load corresponding to 60%UTS (within normal physiologic range ~10% normal UTS). *Creep*: MCL scars were loaded from +1N to a load corresponding to 60%UTS using a half sine wave at 1Hz, and were then held at that load until rupture or for a maximum of 24 hours. Rupture time (T_R) was defined as the last time the scar supported 99% of the test load. For two creep tests, the scars did not rupture within 24 hours. For one fatigue test, the test was stopped prematurely at 8.5 hours. Initial strain (ε_i) was the peak strain of the first loading cycle. Strains at the rupture time (ε_R) and at 50% of the rupture time ($\varepsilon_{50\%R}$) were determined. Increase in strain at rupture ($\Delta\varepsilon_R$) was the difference between ε_i and ε_R. Fatigue and creep were compared using Student's t-test with significance set at $p<0.05$.

RESULTS

Healing ligaments subjected to fatigue loading ruptured earlier than those subjected to creep loading (Table 1). The initial strain and the strain at 50% of the rupture time were not different comparing fatigue and creep; however, the rupture strain and the increase in strain at rupture were greater comparing fatigue to creep.

Table 1: Fatigue and Creep of 14-week MCL scars. *excluded (stopped test) [a]fatigue different than creep ($p<0.05$)

	FATIGUE					CREEP				
Pair	T_R (hrs)	ε_i	$\varepsilon_{50\%R}$	ε_R	$\Delta\varepsilon_R$	T_R (hrs)	ε_i	$\varepsilon_{50\%R}$	ε_R	$\Delta\varepsilon_R$
1	8.5*	0.0418	0.0669	0.0693*	0.0274*	8.2	0.0557	0.0826	0.0949	0.0198
2	4.7	0.0554	0.0846	0.1309	0.0755	24	0.0372	0.0550	0.0570*	0.0339*
3	0.6	0.0636	0.0978	0.1236	0.0599	24	0.0594	0.0906	0.0933*	0.0393*
4	14.2	0.0437	0.0925	0.1280	0.0844	17.1	0.0733	0.1076	0.1134	0.0401
5	13.9	0.0537	0.0665	0.1279	0.0741	--	--	--	--	--
6	--	--	--	--	--	19.3	0.0491	0.0772	0.1123	0.0631
Mean	8.3[a]	0.0541	0.0854	0.1276[a]	0.0735[a]	18.5	0.0549	0.0826	0.1069	0.0410
Std dev	6.8	0.0082	0.0137	0.0030	0.0101	6.5	0.0133	0.0192	0.0103	0.0217
n	4	4	4	4	4	5	5	5	3	3

DISCUSSION

Fatigue-loaded healing ligaments had shorter rupture time than creep-loaded healing ligaments by a factor of 2.2, when loaded to 60%UTS of healing ligaments. The shorter rupture time during fatigue loading is consistent with the relationship observed for normal ligaments [2]; however, fatigue-loaded normal ligaments ruptured earlier than creep-loaded normal ligaments by a factor of 22, when loaded to 60%UTS of normal ligaments. The results of this study suggest that, while rehabilitating a ligament injury, repeated exercises which cause loading of the healing ligament even at physiologic levels may require more careful monitoring than sustained exercises.

REFERENCES [1] Holden JP et al. J Biomech 27:517, 1994 [2] Thornton GM et al. Clin Biomech 22:932-40, 2007 [3] Frank C et al. Am J Sports Med 11:379, 1983 [4] Butler DL et al. Chapter 16 In: Functional Tissue Engineering Eds: Guilak et al. pp. 213-226, 2003 [5] Bailey SJ and Thornton GM, 54th ORS, 2008 accepted

DETERMINATION OF THE TENSILE PROPERTY OF THE LIGAMENT AND TENDON FROM THE MOUSE USING A NOVEL ALL-IN-ONE MICRO TENSILE TEST SYSTEM

Toshifumi Imai[1], Daisuke Katakai[1], Machiko Imura[1], and Hiromichi Fujie[1]
[1] Biomechanics Laboratory, Department of Mechanical Engineering, Kogakuin University, Tokyo, Japan

INTRODUCTION:

The normal and knockout mice were used in a previous study to determine the effects of proteoglycans (PGs) on the mechanical properties of intact tendons and ligaments[1]. In our laboratory, the effect of one of PGs, biglycan, on the mechanical property of healing patellar tendons (PTs) was determined using biglycan-knockout mice with a custom-made tensile tester[2]. However, with the tester, it was required to remove the specimen from a clamp after the measurement of cross section and then to fix the specimen to another clamp for the tensile test. This procedure might have altered the mechanical condition of the specimen since the mouse PT was so small and weak. To avoid the problem, a novel all-in-one micro tensile test system was developed for ligaments and tendons from the intact and knockout mice in the present study. The accuracy of the cross-sectional measurement was assessed and then the system was successfully applied to the tensile test of the normal PTs from the intact mouse.

METHODS:

The tensile test system was consisted of a linear actuator (LAH-46-3002, Hormonic Drive Systems, Japan) having the maximum load of 390 N with the position repeatability less than 0.5 μm, a load transducer (LUR-A-50NSA1, Kyowa, Japan) having the maximum load of 50 N with the rated output of 0.5% , upper and lower custom-made clamps, a bath immersed with saline solution, a dimension analyzer system with a CCD camera (CV-3500, Keyence, Japan) with 2 million pixels, and a windows PC (Fig.1). The actuator, load transducer and two clamps were aligned vertically and connected by aluminum alloy plates. The clamps were allowed to rotate about a vertical axis in a range of 180 degrees using a ball bearing connected between the plates. This mechanism allowed to reconstruct the cross-sectional shape of the specimen by a series of transverse width measurement with the dimension analyzer during the rotation of a tested specimen. After the cross-sectional shape measurement the tensile test was performed without changing the fixation of the specimen to the clamps. While translational displacement was produced with the linear actuator, the tensile load applied to the specimen was measured with the load transducer and transformed to tensile stress The non-contact measurement of the length between two gauge markers fixed to the specimen was performed with the dimension analyzer, and the strain was calculated from the length change. Finally, the stress-strain relationship of the specimen was obtained. A program was developed on LabView (version 8.0, National Instrument) for both system control and data acquisition in the cross-sectional shape measurement and tensile test.

To assess the accuracy of the cross sectional area measurement , a metal wire having a round cross section with 0.7 mm of diameter was fixed to the clamps. The width of the wire was measured at every 10 degree of rotation, and the cross-sectional shape and area were determined. Then, the intact patella-PT-tibial bone block complex was harvested from the normal mouse (C3H/HeN) at the age of 12 weeks. After both the medial and lateral 1/3 of the PT were removed the complex was subjected to the cross-sectional shape measurement followed by the tensile test at a rate of 0.01 mm/s. The maximum stress and tangent modulus at 10 % strain were finally obtained.

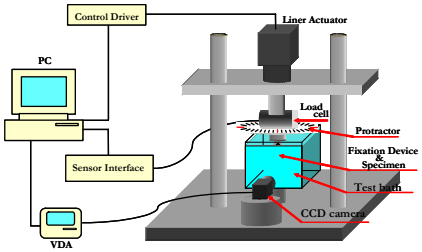

Fig.1: All-in-one tensile test system for the mouse ligaments and tendons

RESULTS&DISCUSSION:

The cross-sectional shape of the wire was determined to be a slightly warped round with the area of 0.37 mm^2 which indicated 2% measurement error. It was suggested that it was possible to accurately determine the cross-sectional area with the developed tensile test system. The tangent modulus and tensile strength of the PT were approximately 80 MPa and 8.9 MPa, respectively. The strain at failure was less than 20 %, similar to those of PTs of other animals determined in the previous studies[3]. In future, the developed all-in-one tensile test system will be applied to the determination of the effects of PGs on the mechanical properties of intact and healing ligaments and tendons using knockout mice.

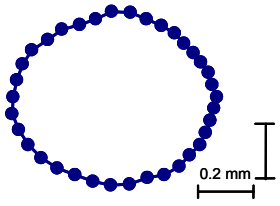

Fig.2: Cross-sectional shape measurement of a metal cylinder with the diameter of 0.7 mm

REFERENCES

[1] Robinson PS, et al. J Biomech Eng (ASME) (2005), [2] Fujie H, et al. ORS (2006). [3] Yamamoto E, et al. J Biomech Eng (ASME) (2005).

FUNCTIONAL DEFICIENCY OF CX43 GAP JUNCTIONS IN TENOCYTES FROM $P2Y_2$ PURINOCEPTOR KNOCKOUT MICE

Tsuzaki, M.[1]; Qi, J.[1]; Wall M.E.[1]; Thompson, J.Y.[2]; Fox, A.M.[2]; Koller B.H.[3]; Banes, A.J.[1,2]
[1]Flexcell International Corporation, Hillsborough, [2]Biomedical Engineering, NCSU/UNC, Raleigh/Chapel Hill, [3]Genetics, UNC, Chapel Hill, NC.

INTRODUCTION

Gap junctions (GJs) are specialized intercellular junctions through which ions and second messengers passively move, thus modulating various biological processes. Connexin 43 (Cx43), the major Cx found in tendon GJs,(1) plays an essential part in the signaling response of tenocytes to chemical and mechanical stimuli. Purinoceptors are also essential to tendon mechanotransduction. Achilles tendon cells lacking the $P2Y_2$ receptor ($P2Y_2$-/-), the primary ATP/UTP responsive purinoceptor, do not transmit a localized mechanical stimulus (membrane indentation with a micropipette) to adjacent cells. It was hypothesized that the mechanism underlying this lack of mechanosensitivity in $P2Y_2$(-/-) cells was deficiency in functional Cx43 GJ coupling and the nucleotide receptors.

METHODS

Tenocytes from Achilles tendons were isolated from 6 week-old wild type (*wt*) and $P2Y_2$ knockout ($P2Y_2$-/-) male mice,(2a,b) grown in DMEM-H, 20% FBS and antibiotics, and each used between passages 3-4. Cells were seeded as micromass, spot cultures on glass cover slips, grown to quiescence by reducing the serum content to 2.5% over 5 days, and used on day 6. Cells were immunostained for Cx43 with anti-Cx43 antibody and Alexa Fluor 488-conjugated secondary antibody. Cells were also stained with DAPI for nuclei and rhodamine phalloidin for actin, and viewed with a fluorescent microscope. Western blotting was performed for Cx43 in the cellular protein, and the immunoreactive Cx43 bands were detected with enhanced chemiluminescence. Levels of statistical significance ($p<0.05$) were determined with a Student's *t*-test or one-way ANOVA with a Dunnett's post-hoc test.

RESULTS

Wt and $P2Y_2$(-/-) tenocytes displayed robust Cx43 staining, but differed in cellular localization. Wt cells had positive Cx43 immunohistochemical reactivity in the Golgi, within the cytoplasm and at the plasma membrane, indicative of mature, functional GJs. Despite intracellular abundance, $P2Y_2$(-/-) cells had fewer Cx43 puncta at the plasma membrane and more perinuclear/nuclear localizations. Results of the Western blot confirmed Cx43 bands in phosphorylated and nonphosphorylated forms in both cell types, but Cx43 expression was down-regulated in $P2Y_2$(-/-) cells.

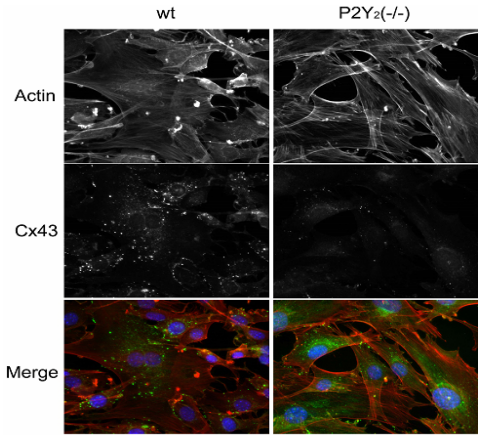

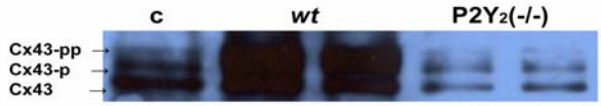

Fig. 1. Immunofluorescent localization of Cx43 (green) in *wt* and $P2Y_2$(-/-) tenocytes with actin (red) and nuclei (blue).

Fig. 2. Western blot for Cx43 in *wt* and $P2Y_2$(-/-) tenocytes. C: control (MC3T3-E1 cellular protein)

DISCUSSION

This is the first report in tendon that purinoceptors may modulate Cx43 expression, assembly/disassembly and GJ function. $P2Y_2$(-/-) tenocytes do not respond to the cell-cell communication challenge of membrane indentation via Ca^{2+} wave propagation, likely due to a lack of functional Cx43 GJs. While $P2Y_2$(-/-) cells displayed abundant Cx43 protein, they had reduced punctate staining at the plasma membrane, indicating that Cx43 trafficking was deficient. Furthermore, Cx43 expression as 43 kDa bands was down-regulated in $P2Y_2$(-/-) cells. Taken together, these data suggest an interplay between nucleotide receptors and Cx43 GJs that may modulate responsiveness to mechanical stimuli and thus modulate mechanotransduction pathways in tenocytes.(3)

References: 1. McNeilly CM et al. Anatomy 189: 593-600, 1996. 2a.b. Banes AJ et al. J Orthop Res 6: 73-82, 83-94, 1988. 3. Banes AJ et al. Curr Opin Orthop 12: 389-396, 2001.

EXPRESSION OF TYPE II COLLAGEN AND TISSUE CALCIFICATION IN COLLAGENASE-INDUCED TENDON DEGENERATION

Fu SC, Chan LS, Chan, KM, Hung LK, Lui PY

1. Department of Orthopaedics and Traumatology, Faculty of Medicine, The Chinese University of Hong Kong, Hong Kong SAR, China
2. The Hong Kong Jockey Club Sports Medicine and Health Sciences Centre, Faculty of Medicine, The Chinese University of Hong Kong, Hong Kong SAR, China

kaimingchan@cuhk.edu.hk

INTRODUCTION

Tendon degeneration is involved in various kinds of chronic tendon pain such as insertion tendinopathy, calcified tendinopathy. Failed cell differentiation into tenocytes was implicated with the detection of chondrocyte markers in clinical samples of Achilles tendinopathy (1). It was speculated that a process similar to endochondral ossification may account for the calcification in calcified tendinopathy (2). However, it is not known if tendon healing to degenerative injuries would lead to erroneous differentiation into chondrocyte and even ectopic bone formation. In the present study, we used a rat model of collagenase-induced tendon degeneration to study if acquisition of chondrocyte phenotype and tissue calcification were associated with the failed healing to tendon degeneration.

METHODOLOGY

A total of 36 male Sprague Dawley rats (6-8 weeks old) were used in the present study. A 20 µl aliquot of 0.015 mg/ul collagenase was injected intratendinously into the left patellar tendon of 30 rats. Equal volume of saline was injected in the remaining 6 rats as control. The rats receiving collagenase injection were euthanized at 2, 4, 8, 12 and 16 weeks post injection (n=6), and the saline control were euthanized at 16 weeks post-injection. Patellar tendon samples were harvested, formalin-fixed and paraffin-embedded for preparations of 5 um thick sections. Hematoxylin and Eosin staining was performed and the extent of degenerative injuries was evaluated by polarization microscopy as loss of collagen birefringence. Expression of Type II collagen, sox 9, osteocalcin and MMP13 was determined by Immunohistochemistry. Tissue calcification was detected by von Kossa staining.

RESULT

The results showed that collagenase-induced degenerative tendon injuries were not healed up to 16 weeks post injury, with persistent loss of collagen birefringence and progressive tissue calcification. Expression of Type II collagen became evident at 4 weeks post injury, while tissue calcification was obvious from 12 weeks post injury (Figure 1). Expression of Type II collagen was localized in the regions of disturbed matrix (loss of birefringence) in 4 weeks post injury and it was mainly detected around the sites of calcification from 8 to 16 weeks post injury (Figure 2). Von Kossa staining revealed focal sites of intratendinous calcification and chondrocyte–like cells were observed at the edges of the calcification sites (Figure 3). Immunoreactivity of sox 9 was only found in chondrocyte-like cells in the degenerative tendons. All tendon samples were negative for immunostaining of MMP13 and osteocalcin.

Figure 1

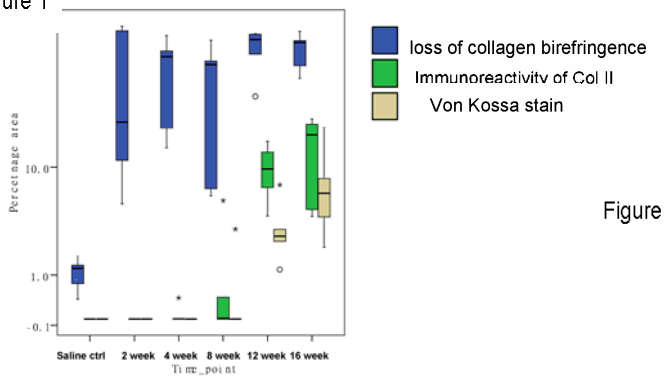

Figure 2

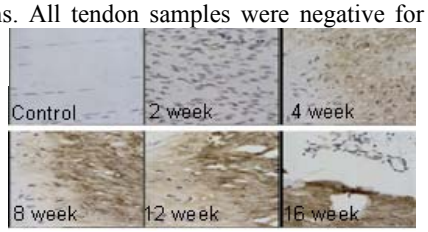

Figure 3

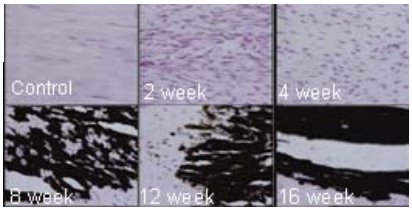

DISCUSSION

We observed failed healing of degenerative tendon injuries, which was associated with the acquisition of chondrocyte phenotype and tissue calcification in tendons. It is possible that degenerative injuries could not be healed properly and erroneous cell differentiation was resulted. The temporal and spatial relationship of degenerative injuries, chondrogenesis and tissue calcification may suggest a sequence of events that involve altered cellular responses in damaged extracellular matrix which favour ectopic calcification. However, the lack of MMP13 and osteocalcin expression did not support the occurrence of endochondral ossification, suggesting that failed healing to tendon degeneration can not fully explain the clinical observation of calcified tendinopathy.

References:

1. Corps AN et al. Rheumatology. 45(3):291-4, 2006.
2. Fenwick S et al. Rheumatology. 41(4):474-6, 2002.

EFFECTS OF DYNAMIC LOADING AND OSTEOBLAST-FIBROBLAST INTERACTIONS ON CHONDROCYTE RESPONSE *IN VITRO*

I.E. Wang, C.T. Hung and H.H. Lu
Department of Biomedical Engineering, Columbia University, New York, NY, USA

INTRODUCTION: The anterior cruciate ligament (ACL) inserts into bone through a fibrocartilage interface, which acts to minimize stress concentrations across soft and hard tissues. A significant limitation of soft tissue-based ACL reconstruction graft is its inability to integrate with subchondral bone. Our long term goal is to promote biological fixation of these grafts through interface regeneration. As such, the mechanism of interface regeneration is not known. Vogel *et al.* reported that compressive loading promoted fibrocartilage formation in flexor tendons[1]. Additionally, our published results suggest that osteoblast-fibroblast interactions play a role in initiating interface regeneration[2], likely by promoting fibrochondrogenic differentiation during tendon-bone healing. As chondrocytes are often found at the tendon-bone junction[3], the **objective of this study** is to evaluate the effects of dynamic compressive loading as well as osteoblast-fibroblast interactions on chondrocyte response. It is hypothesized that cellular interactions combined with compression will induce significant changes in chondrocyte phenotype.

METHODS: Cells and Cell Culture: Bovine osteoblasts (Ob), ACL fibroblasts (Fb), articular chondrocytes (Ch) and ACL-to-bone insertion fibrochondrocytes (fCh) were isolated from neonatal calves, and cultured in optimized fully supplemented DMEM[2]. Triculture Model: Fb and Ob were seeded on treated coverslips ($5x10^4$ cells/type). Ch embedded in 2% agarose discs (4x2mm, 10M cells/ml) were tricultured with Fb and Ob (*Fig.1*). Parallel cultures of fCh served as positive controls. Dynamic Loading: Two groups of Ch discs (alone or in triculture) were dynamically loaded (DL) using a custom device for 5 days/week, 3 hrs/day with 10% strain at 1Hz[4]. Two free-swelling (FS) groups: Ch alone and in triculture were also established. Cell Response: Analyses were performed at 1, 14, 28 days. Cell growth, alkaline phosphatase (ALP) activity, glycosaminoglycan (GAG) production and aggregate modulus were determined following published methods[2, 4].

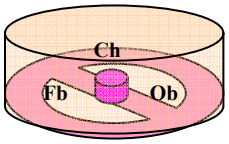

Fig. 1: Triculture Model.

RESULTS: Cell Proliferation: No significant change in chondrocyte number was found over time due to triculture or dynamic loading. In contrast, triculture, dynamic loading and triculture+loading suppressed the proliferation of insertion fibrochondrocytes (*Fig. D*). GAG Production and Mechanical Properties: Triculture with osteoblasts and fibroblasts significantly lowered GAG production by chondrocytes (*Fig. A*), and this decrease was reflected in a significantly lower aggregate modulus for the chondrocyte-laden matrix (*Fig. B*). While dynamic loading has no adverse effect on GAG production, it could not rescue the suppressive effects of tri-culture (*Figs. A, B*). ALP Activity: Tri-culture and dynamic loading independently suppressed chondrocyte ALP activity (*Fig. C*). In contrast, triculture coupled with compression significantly increased the ALP activity of chondrocytes at day 14.

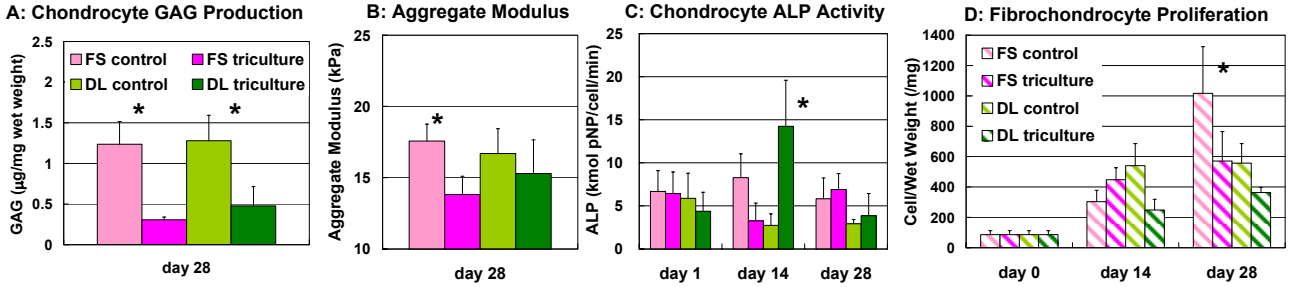

Fig. 2. Chondrocyte Response: A) GAG Production. B) Aggregate Modulus. C) ALP Activity. D) Fibrochondrocyte Proliferation.

DISCUSSION: Our results suggest that dynamic loading have a significant effect on chondrocyte response, especially when these cells are under the influence of osteoblast-fibroblast interactions. Shan *et al.* reported that the effects of osteoblast-fibroblasts co-culture are mediated by paracrine factors[5], thus dynamic loading will likely facilitate these interactions. With dynamic loading and triculture, chondrocytes produce less GAG and measured higher ALP activity, which is suggestive of cell trans-differentiation considering the results of Sun *et al.*, which reported lower GAG production and higher ALP activity in fibrochondrocytes than articular chondrocytes[6]. Moreover, chondrocyte response in triculture and under dynamic loading differs significantly from those of insertion fibrochondrocytes, this may be due to changes in the osteoblast-fibroblast interaction response when cultured with each cell type (*i.e.* injury vs. healthy conditions). These effects and their relevance in interface regeneration will be evaluated in future studies. **REFERENCE-**1).Malaviya et al., 2000. 2).Wang et al., 2007. 3).Rodeo et al., 1993. 4).Mauck et al., 2002. 5).Shan et al., 2007. 6).Sun et al., 2007. This study was supported by NIH-NIAMS.

SINGLE HUMAN TENOCYTES RESPOND TO FLOW IN A NOVEL MICROFLUIDIC DEVICE

J. Wang[1], J. Qi[1,2], M.E. Wall[1], R. Sumanasinghe[1], M. Tsuzaki[1], A.J. Banes[1,2]
[1]Flexcell International Corp., Hillsborough, North Carolina, [2] Joint Department of Biomedical Engineering, NCSU/UNC, Raleigh and Chapel Hill, North Carolina, USA

INTRODUCTION

Tenocytes are constantly subjected to mechanical stimuli from the surrounding matrix, which is necessary for normal function and development. However, overloading tendon tissue with high strains, shears, or repetitive motion often leads to matrix damage. Understanding the cellular and molecular mechanisms involved in tenocyte responses to mechanical load under normal and pathologic conditions will improve knowledge of tendon repair and healing. Microfabrication, or lab-on-a-chip technology, provides scientists with unique tools for analyzing cellular responses to mechanical stimulation. The purpose of this study was to develop a microfluidic device for on-chip shear stress application and analysis of single cell reactions with fluorescence markers under a controlled mechanical microenvironment.

METHODS

The microfluidic device (Fig. 1) is a multi-layered polydimethylsiloxane (PDMS) structure built using soft lithography and replica molding techniques. The typical transport microchannels were 80 μm wide by 150 μm high by 2 mm long, generating a channel volume of 24 nl. The cell culture chamber widths were 45, 100, 150 and 200 μm, and the height was the same as the transport channels. Fluid and cell delivery were facilitated by a syringe pump at flow rates between 20 – 40 μl/min. Human tenocytes were utilized in this study and maintained in Medium 199 with 20% FBS. Ten μl of the cell suspension at 4×10^5 cells/ml were loaded into the cell culture chamber. After culturing for 3 - 7 days, cells were perfused with Earles' balanced salt solution for 4 hours at a shear stress of 2 dynes/cm^2. Cells were then fixed with 3.7 % formaldehyde in the chip and stained with DAPI and rhodamine phalloidin to label nuclei and actin, respectively.

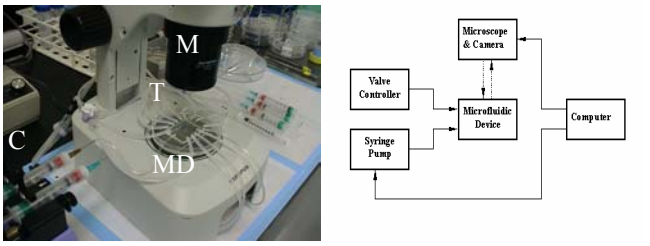

Figure 1. Microfluidic device (MD) system setup consisting of a stereo microscope (M), controller (C), and tubing (T).

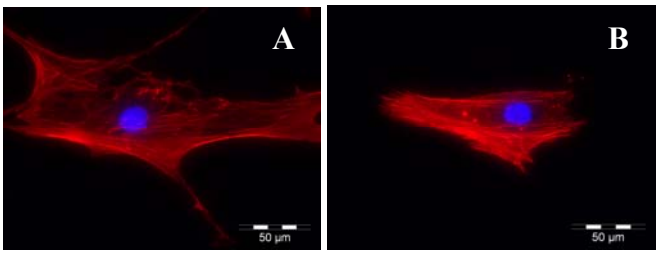

Figure 2. Human tenocytes in a microchannel under static culture conditions (A) and after exposure to 2 dynes/cm^2 shear stress for 4 hrs (B). Cells were labeled with DAPI (blue) and rhodamine phalloidin (red).

RESULTS

Single or low number groups of human tenocytes adhered and spread in the microchannels. Cells cultured in a microchannel up to 7 days showed normal fibroblast morphology (Fig. 2A). A selected shear stress could be precisely applied to the cell surface in the microchannel. After 4 hours of fluid shear stress at 2 dynes/cm^2, the cytoskeleton was reorganized (Fig. 2B). Lamellipodia retracted, and organized, robustly stained actin fibers were apparent at the cell periphery, especially facing the fluid flow direction (Fig. 2B).

DISCUSSION

We have demonstrated the design and development of a microfluidic device in which single tenocytes can be cultured and subjected to fluid shear stress. Additionally, the device allowed for optical analysis of the tenocytes during and after mechanical loading. The cells were fluorescently labeled and visualized without interference from background fluorescence. Staining of the cells within the culture chamber indicated that tenocytes responded to the fluid shear stress by rearranging their actin cytoskeleton. This device could be used to apply various shear stress regimens in the presence and/or absence of chemical mediators to analyze the responses of a single cell to changes in its microenvironment. As a research tool, this single cell based-microfluidic device may be useful in understanding cellular responses to mechanical load and the pathways involved in mechanotransduction.

CELL-CELL CONECTION IS NESSASARY FOR CELLULAR SURVIVAL UNDER MECHANICAL LOADING

Jie Qi[1,2], Liqun Chi[1], Donald Bynum[3] and Albert J. Banes[1,2]
[1]Flexcell International Corp., 437 Dimmock's Mill Rd. suite 28, Hillsborough, NC, [2]Joint Department of Biomedical Engineering, University of North Carolina at Chapel Hill, NC and North Carolina State University in Raleigh, NC, [3]Orthopaedics, University of North Carolina at Chapel Hill, NC.

Introduction - Interleukin-1β (IL-1β) is a proinflammatory cytokine that is up-regulated by mechanical loading. Human tenocytes grown in three-dimensional (3D) type I collagen gels at low, but not high cell density, succumbed to death after mechanical loading. However, IL-1β treatment increased cell survival in mechanically loaded human tenocytes. We have reported that IL-1β up-regulated the expression of connexin 43 (Cx43), therefore we hypothesized that cell-cell communication via gap junctions formed by connexins, may play a key role in cell survival and mechanosensitivity and may be regulated by biochemical signals, such as cytokines (e.g., IL-1β). In this study, the role of cell-cell connection in cell survival post-mechanical loading was investigated by using the gap junction inhibitor, heptanol.

Method - Human tenocytes from passages 2-4 were grown in 3D type I collagen gels in the presence of 2% fetal bovine serum with or without 100 pM IL-1β. The 3D cultures were subjected to 3.5% elongation at 1 Hz for 1 h per day for up to five days using a TissueTrain™ system and Flexercell® Strain Unit. Cells were then fixed for staining.

Results - IL-1β increased the expression of Cx43, and the elongated cellular processes had increased punctuate staining for Cx43 (Figure 1). Over 90% of tenocytes were killed by 3.5% cyclic strain at high cell density in the presence of heptanol (Figure 2).

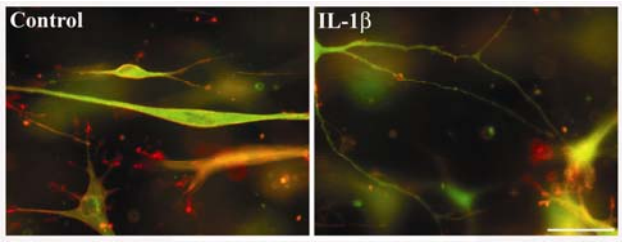

Figure 1. Human tenocytes grown in 3D type I collagen gels were fixed and double stained with rhodamine phalloidin (red) and an anti-Cx43 antibody (green). Scale bar, 50 microns.

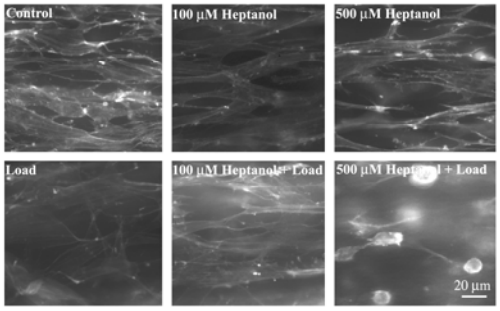

Figure 2. Human tenocytes grown in 3D type I collagen gels were fixed with 3.7% formaldehyde and stained with rhodamine phalloidin. Scale bar, 20 microns.

Conclusion - These results indicate that cell-cell connections via Cx43 gap junction linked pathways play an important role in determining cellular mechanosensitivity and survival.

SYNOVIUM-DERIVED FIBROBLAST TRANSPLANTATION POSSIBLY DETERIORATES MECHANICAL PROPERTIES OF THE REGENERATED TISSUE IN THE PATELLAR TENDON AFTER THE HARVEST OF ITS CENTRAL ONE-THIRD PORTION

H. Tohyama[1], S. Okamoto[1], E. Kondo[1], K. Hayashi[2], K. Yasuda[1]
[1]**Department of Sports Medicine, Hokkaido University School of Medicine, Sapporo, Japan**
[2]**Department of Biomedical Engineering, Okayama University of Science, Okayama, Japan**

INTRODUCTION

The central one-third portion of the patellar tendon is a common substitute for ligament reconstruction of the knee. Several clinical reports indicate that some complications are associated with the harvest from the patellar tendon. To explain these complications from biomechanical changes in the patellar tendon after the harvest of its central one-third portion, we previously investigated the changes in mechanical properties of the regenerated tissue in a patellar tendon defect after the removal of its central one-third portion and found that the tangent modulus of the regenerated tissue in a patellar tendon defect were only 38% of the normal tendon even 12 weeks after the removal of its central one-third portion. Recently, cell-based therapies on the basis of tissue engineering techniques have attracted notice as potential treatments for tendon injuries. Therefore, we hypothesized that transplantation of autologous synovium-derived fibroblasts would significantly improve mechanical properties of the tissue regenerated in the patellar tendon defect. The purpose of the present study is to test this hypothesis.

MATERIALS AND METHODS

Twenty-eight mature female Japanese white rabbits weighing of 3.2±0.6 kg (mean ± SD) were used in this study. In all animals, synovial tissues were harvested from the left knee to obtain synovium-derived fibroblasts. Two weeks after the harvest, a full thickness defect was made at the central portion in the right patellar tendon. Then, the animals were divided into the following two groups of 14 rabbits each. In the control group, we applied PBS of 0.1ml to the defect created in the patellar tendon. In the transplantation group, we transplanted autologous fibroblasts (approximately 1.5×10^6 cells/ml), which had been cultured in the standard medium, into the tendon defect. For biomechanical and histological evaluations of the tissue regenerated in the patellar tendon defect, Animals were sacrificed at 6 and 12 weeks after the surgical treatment.

RESULTS AND DISCUSSION

Concerning mechanical properties of the tissue regenerated in the patellar tendon defect, the tangent modulus and the tensile strength of the transplantation group were significantly lower than those of the control (the tangent modulus: p=0.027, the tensile strength: p=0.001), while these mechanical parameters at 12 weeks were significantly higher than those at 6 weeks (the tangent modulus: p=0.018, the tensile strength: p=0.009) (Fig. 1). There were no significant differences in the strain at failure between two groups (p=0.339) or between two periods (p=0.697). At 6 weeks, vascular formation was abundantly found in the regenerated tissue of the transplantation group, compared to that of the control group (Fig. 2). Histological findings of the present study suggested that transplantation of autologous synovium-derived fibroblasts can enhance vascularization of the tissue regenerated in the patellar tendon defect. However, the present study throws out the caveat that the transplantation of autologous fibroblasts possibly deteriorates mechanical properties of the regenerated tissue in the patellar tendon defect under certain conditions.

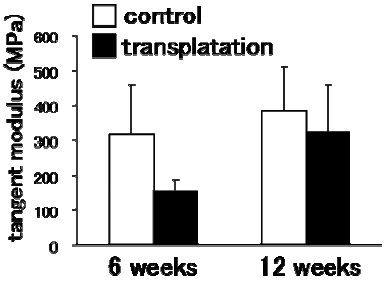

Fig. 1 Tangent modulus of the regenerated tissues.

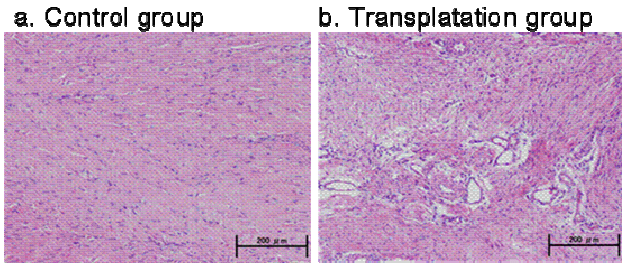

Fig. 2 Histology of the regenerated tissues (6 weeks).

FIBRILLAR LEVEL STRESS RELAXATION IN TENDON WITH SUBSECOND RESOLUTION

H. R. C. Screen[1], J. Seto[2], S. Krauss[2], P. Boesecke[3], P. Fratzl[2] and H. S. Gupta[2]

1. Dept of Engineering, Queen Mary University of London, UK. **2**. Dept of Biomaterials, Max Planck Institute of Colloids & Interfaces, Germany. **3**. Beamline ID2, European Synchrotron Radiation Facility, France

INTRODUCTION:

Tendon is composed of nanoscale cross-linked collagen fibrils and glycosaminoglycans, assembled hierarchically, to form fibre bundles and macroscopically visible fascicles. Under tensile strain, this architecture is likely to induce deformation throughout the tissue hierarchy, yet there are very few methods able to probe the real-time dynamics of the microscopic and submicroscopic structural changes. In conjunction with tensile loading, *in situ* synchrotron small angle X-ray scattering (SAXS) [1] and confocal microscopy [2] are able to measure deformation at the fibril (50 – 200 nm) and fiber bundle (10 – 50 μm) levels, respectively. Initial studies of fibril extension during tensile loading have demonstrated that fibril strain is only a fraction of the total tissue strain, implying that tendon extension involves interfibrillar shearing [3,4]. This study utilizes *in-situ* synchrotron SAXS to investigate stress relaxation, using a special X-ray detector readout method to rapidly acquire scattering frames with sub-second time resolution. Structural dynamics at the fibrillar level were correlated with the macroscopic stress during relaxation.

METHODS:

Fascicles were dissected from 5 month male Wistar rat tails, and stored in medium (DMEM + 10% FCS) for up to 15 hours prior to use. SAXS experiments were carried out concurrently with micromechanical stress relaxation experiments, using a specially designed loading rig with video extensometry for strain detection [1]. A FRELON CCD detector was used to acquire SAXS frames (wavelength 1 angstrom, sample to detector distance 10 m), with a special readout system, enabling 2D SAXS frames with extremely short exposure times (< 0.1 s) to be acquired consecutively, and fibrillar dynamics thus measured from the start of each stress relaxation increment. Lateral shifts in meridional peak positions in the SAXS spectra were used as measures of fibril strain ε_F.

RESULTS:

Macroscopic stress relaxation always showed a double exponential decay (rapid relaxation time constant $\tau_1 \sim 10$ s followed by a much slower relaxation $\tau_2 \sim 100$ s) and was fitted to $\sigma(t) = \sigma_0 + \sigma_1 e^{-t/\tau 1} + \sigma_2 e^{-t/\tau 2}$ (fig. 1a). However, fibril strain (ε_F) was far less predictable. In some samples fibril strain did follow stress (fig 1a), yet a total of four different responses were recorded, shown schematically in fig 1b. These could all be written in the general form $\varepsilon_F(t) = \varepsilon_{F0} + \varepsilon_{F1} e^{-t/\tau 1} + \varepsilon_{F2} e^{-t/\tau 2}$. Each behaviour could be described by changing the signs of the pre-factors ε_{F1} and ε_{F2}. Notably, the time constants obtained from macroscopic stress relaxation described precisely fibril strain behaviour.

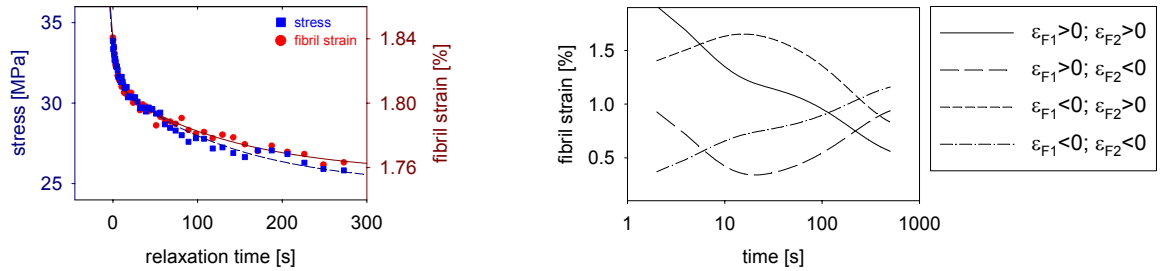

Figure 1:(a)Typical stress and strain relaxation experiment.(b)Variable behaviour of fibril strain (model plots).

DISCUSSION:

A simple structural model of two viscoelastic elements in series was used to model the deformation behaviour at the nanoscale. It consisted of a Voigt element (the cross-linked collagen fibril) in series with a Maxwell element (the amorphous, anionic, hydrated proteoglycans surrounding fibrils), with tensile stress transmitted in a series manner. The system reproduced the double exponential time behaviour, and the four different fibril strains. Experimentally, fibril strains did not always relax along with the sample strains, and in some instances actually increased as the sample relaxed. The model can explain these data by assuming local nonzero strain rates. These may occur with sliding between fiber bundles at higher hierarchical levels, indicating the importance of non-collagenous matrix in influencing viscoelastic behaviour. In order to understand physiological tendon loading, it is first essential to determine its micro-mechanics, including viscoelastic behaviour. This model could be used to extract experimentally the molecular level viscous and elastic constants for the collagen and proteoglycan phases of tendons, to predict the dependence of macroscopic mechanical behaviour on changes in the interfibrillar matrix and interfibrillar structure.

REFERENCES:

[1] Gupta HS et al., (2006) *PNAS* 103:17741-6. [2] Screen HRC et al., (2003) *Biorheol.* 40:361-8. [3] Sasaki N et al., (1996) *J. Biomech.* 29: 1131-6. [4] Puxkandl R et al., (2002) *Philo. Trans. Roy. Soc. Lond. B.* 357: 191-7.

EFFECT OF AGGRECAN-COATED SURFACES ON MORPHOLOGY AND AGGRECAN GENE EXPRESSION IN TENDON/LIGAMENT FIBROBLASTS

J.J. Lim, K.S. Brink, J.S. Temenoff
Coulter Department of Biomedical Engineering, Georgia Tech and Emory University, Atlanta, GA, USA

INTRODUCTION

Ligament tissue is largely acellular and poorly vascularized, resulting in a poor capacity for healing, and current treatments are unable to restore tissue to pre-injury strengths. For ligament reconstruction, a secure interface between the ligament graft and bone is essential for proper function. Native ligament-bone insertion points contain a region of fibrocartilage with a gradual transition of mechanical properties. Aggrecan, an extracellular matrix (ECM) proteoglycan found in cartilage and ligament-bone insertion points, has been shown to promote the production of cartilaginous ECM by dermal fibroblasts (French, MM. Ann Biomed Eng. 2004;32:50-6). As a first step in investigating the role of aggrecan in cell differentiation down the (fibro)chondrocytic lineage, we explored the effect of culture on aggrecan-coated surfaces on the morphology of tendon and ligament fibroblasts and marrow stromal cells (MSCs) and gene expression in tendon and ligament fibroblasts *in vitro*.

METHODS

Wells of a 24-well plate were treated with 5 μg of bovine aggrecan by suspending aggrecan in phosphate-buffered saline (PBS) and allowing it to evaporate in a sterile environment. Bovine tendon/ligament fibroblasts (P1) and MSCs (P2) were plated at $4.4x10^4$ (low density), $8.8x10^4$ (medium), and $2.0x10^5$ (high) cells per well on aggrecan-coated and tissue culture-treated polystyrene (TCPS) control surfaces in fetal bovine serum-supplemented media. Morphology was observed over 5 days by light microscopy. To investigate the nature of the cellular interaction with aggrecan, medial collateral ligament (MCL) fibroblasts (P1) and MSCs (P2) (medium density) were also cultured in serum-free media on aggrecan-coated and control surfaces. Additionally, 5 μg of aggrecan was added to the media of MCL fibroblasts (P1) and MSCs (P2) cultured on control surfaces (medium density, serum-containing media) at the time of seeding or 24 hrs after seeding. Gene expression of mixed tendon/ligament (P2) and MCL fibroblasts (P1) cultured on aggrecan-coated and control surfaces for 3 days (medium density, serum-containing media) was analyzed by reverse transcription-polymerase chain reaction (RT-PCR) for collagen type I, collagen type II, aggrecan, and PPAR-γ2. In both mixed and MCL fibroblasts, all cells in a well were analyzed for gene expression; however, aggregates of MCL fibroblasts were also separated from non-aggregating cells and analyzed for comparison.

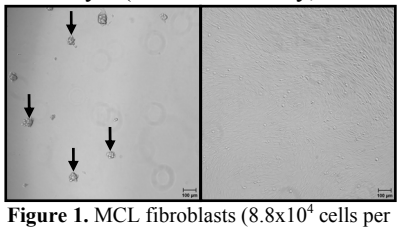

Figure 1. MCL fibroblasts ($8.8x10^4$ cells per well) on aggrecan-coated (left) and control (right) surfaces in serum-containing media. Fibroblasts formed dense cellular aggregates (arrows) in the presence of aggrecan (n=3).

RESULTS

Aggrecan-coated surfaces induced formation of dense cellular aggregates within 24 hrs of cell seeding, independent of cell type and seeding density (Fig. 1). Aggregate formation also was not dependent on the presence of serum proteins, with aggregates forming in serum-free media. When aggrecan was suspended in culture media, the adhered cells appeared morphologically similar to cells on control surfaces, indicating that aggrecan must be adsorbed to the surface prior to cell seeding to induce aggregation. RT-PCR results suggest that cells on aggrecan-coated surfaces upregulate expression of aggrecan. Tendon/ligament fibroblasts experienced a 2.01±0.42 fold (p=0.053) upregulation of aggrecan over controls (Fig. 2), and MCL fibroblasts experienced a 3.16±0.37 fold (p=0.003) upregulation. Aggregate-only MCL fibroblast samples experienced a 6.42±0.60 fold (p=0.004) upregulation of aggrecan over controls (Fig. 3).

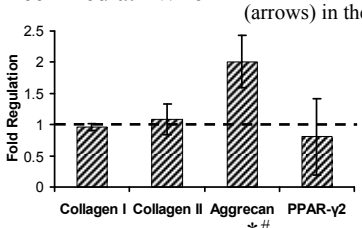

Figure 2. Gene expression of tendon/ligament fibroblasts cultured on aggrecan-coated surfaces after 3 days normalized to cells on TCPS.

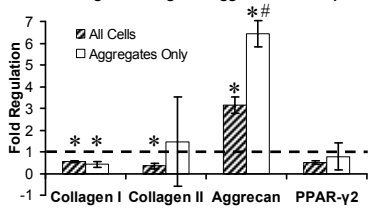

Figure 3. Gene expression of MCL fibroblasts cultured on aggrecan-coated surfaces after 3 days normalized to cells on TCPS. Cells were collected as either all cells in a well (n=3) or only the aggregates (n=3). * indicates significantly different from controls ($p<0.05$). # indicates significantly different from all-cell samples.

DISCUSSION

These results indicate that adsorbed aggrecan has a marked effect on fibroblast and MSC morphology and upregulates gene expression of a key cartilaginous ECM protein, aggrecan, in fibroblasts after 3 days, particularly in the aggregating cells. In the future, similar aggrecan-treatments may be utilized on 2D surfaces, as well in 3D scaffolds, to promote chondrogenic/fibrochondrogenic differentiation at the ligament-bone insertion point.

ACKNOLEDGEMENTS: Arthritis Foundation Investigator Award, NSF Graduate Fellowship to KSB

THE REGULATION OF ADAMTS-4 EXPRESSION IN HUMAN ACHILLES TENDON AND TENDON-DERIVED CELLS

G.P. Riley[1,2], G.C. Jones[1,2], A.N. Corps[2] and B.L. Hazleman[2]

[1] School of Biosciences, University of East Anglia, Norwich, UK
[2] Rheumatology Research Unit, Addenbrooke's Hospital, Cambridge, UK

INTRODUCTION

Tendons such as the Achilles are susceptible to both chronic painful tendinopathy and 'spontaneous' ruptures. There is a normal balance between the synthesis and degradation of tendon matrix components, which is altered in tendon disease. We recently showed that ADAMTS-4 (A Disintegrin And Metalloproteinase with ThromboSpondin motifs) mRNA increased 8-fold in ruptured Achilles compared to normal tendons. In this study we tested various factors for the regulation of ADAMTS-4 mRNA expression and examined the expression of ADAMTS-4 protein in human tendon tissues and cells.

METHODS

All procedures were conducted with local ethical committee approval and patient consent. Normal Achilles specimens were obtained from cadavers or amputees. Tissue from patients with tendinopathy or tendon rupture was taken from (or adjacent to) the site of the lesion. Early passage tendon cells were cultured in monolayers or in 3D collagen gels, with and without the addition of various cytokines. Total RNA was isolated from cells or tissue samples by a modified Tri-Spin protocol. ADAMTS-4 mRNA was assayed by qRT-PCR and normalized to 18S rRNA. Protein extracted from cells or tissue samples was subjected to SDS-PAGE and immunoblotting.

RESULTS

In tendon tissue extracts probed by Western blotting, mature ADAMTS-4 (68 kDa) was detected only in ruptured tendons, while processed ADAMTS-4 (53 kDa) was detected in both chronic painful tendinopathy and in normal tendon (See Figure). In cultured Achilles tendon cells, transforming growth factor-β (TGF-β) stimulated ADAMTS-4 mRNA expression (typically 20-fold after 24 hours), while interleukin-1 induced a smaller, shorter-term stimulation which synergised markedly with that induced by TGF-β. Increased levels of immunoreactive proteins consistent with mature and processed forms of ADAMTS-4 were detected in TGF-β-stimulated cells, and a smaller form (40-45 kDa) was secreted into the supernatant medium. ADAMTS-4 mRNA was expressed at higher levels by tendon cells in collagen gels than in monolayer cultures. In contrast, the expression of ADAMTS-1 and -5 mRNA was lower in collagen gels compared with monolayers, and these mRNA showed smaller or opposite responses to growth factors and cytokines compared with that of ADAMTS-4 mRNA.

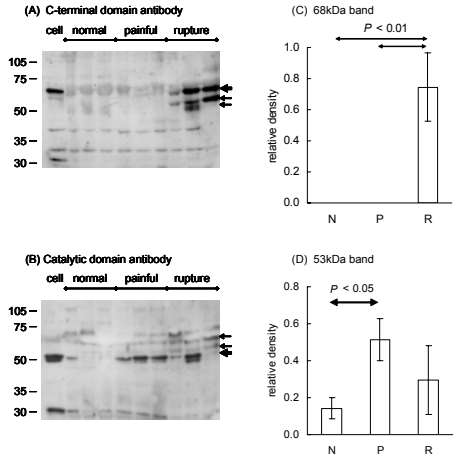

ADAMTS-4 immunoreactivity in human tendon tissue.
Western blots of protein extracts (10 μg/lane) from 3 samples each of normal, painful and ruptured tendon tissue were probed using the ADAMTS-4-specific antibodies (A) C-terminal domain antibody (AHP821GA) and (B) Catalytic domain antibody (PA1-1749). The lane marked *cell* contained extract from a TGF-β-treated tendon cell culture. The bold *arrows* indicate the mature (68 kDa) and processed (53 kDa) forms of the ADAMTS proteins discussed in the text. (C,D) Image analysis of the 68 kDa and 53 kDa bands in each sample, normalized to the *cell* band on the same blot. Mean ± sem from 6 samples per group.

CONCLUSIONS

This is the first report of active forms of ADAMTS-4 in human tendon, with different forms of the enzyme expressed in diseased tendon compared with normal tendon. We also report that regulation of ADAMTS-4 expression in tenocytes is different compared to two other 'aggrecanase' enzymes (ADAMTS-1, -5). ADAMTS-4 is therefore thought to be implicated in tendon matrix proteoglycan turnover, and changes in its expression and processing are consistent with some role for ADAMTS-4 in chronic tendon disease. Further studies will be required to determine the contribution of ADAMTS-4 to the observed changes in proteoglycan in tendinopathy.

A NOVEL ELASTIC MODEL INDICATES DECREASED ORGANIZATION AND MECHANICS OF ROTATOR CUFF REPAIR DUE TO EXERCISE FOLLOWING IMMOBILIZATION

Joseph J. Sarver, Cathryn D. Peltz, LeAnn Dourte, Gerald R.Williams, Jennifer Kadlowec[1], Louis J. Soslowsky
McKay Orthopaedic Research Laboratory, University of Pennsylvania, Philadelphia PA, USA
1 Department of Mechanical Engineering, Rowan University, Glassboro NJ, USA

INTRODUCTION:

Between 30% and 70% of the 35,000 rotator cuff repairs performed in the US this year [1] will fail [2]. While many factors that contribute to this high failure rate are beyond the surgeon's control, the level of post-operative activity can be adjusted. Recent animal studies in our lab have shown that shoulder immobilization improved repaired insertion site tissue organization and mechanical properties [3], while only temporarily increasing joint stiffness [4]. Whether exercise following immobilization would improve tissue mechanics and organization is unknown. We hypothesized that exercise following a short-period of immobilization would result in improved repaired insertion site organization and mechanics.

METHODS:

A total of 17 Sprague-Dawley rats were used in this study which is described in more detail in an Orthopaedic Research Society abstract to be presented [5]. Briefly, all animals underwent uni-lateral acute detachment and repair of the surpraspinatus tendon followed by 2 weeks of continuous immobilization of the repaired shoulder [5]. Following immobilization, animals were randomly assigned to either caged (n=8) or exercised (n=9) activity groups and sacrificed 12 weeks later for tensile testing of the repaired tendon-bone complex. The ramp to failure data were analyzed using a novel structurally based elastic function, in which tensile mechanical behavior is modeled as a population of elastic elements with normally distributed slack lengths. According to this model, elastic elements are recruited as tendon displacement increases past each element's slack length. Thus, soft tissue non-linear mechanical behavior is explained by the distribution of these slack lengths, and previous studies have shown this distribution to correlate with tissue organization and crimp [6]. Stress-strain data were then fit using this model and the resulting slack distribution parameters (mean and standard deviation) as well as modulus were compared across groups.

RESULTS:

The average slack strain distribution parameters of the exercised (EX) group were significantly larger than the caged-activity (CA) group (distribution mean: 8.1 ± 3.1% EX vs 5.6 ± 2.1% CA, p = 0.03 and standard-deviation: 5.5 ± 2.2% EX versus 3.6 ± 1.6 % CA p = 0.04) as illustrated in Figure 1. In addition, the grip-to-grip apparent modulus (slope from 10 – 15% strain in figure 2) of the exercised group was less than the caged-activity, although this difference was only a trend (18.0 ± 12.4 MPa EX vs 27.5 ± 11.9 MPa CA, p = 0.06).

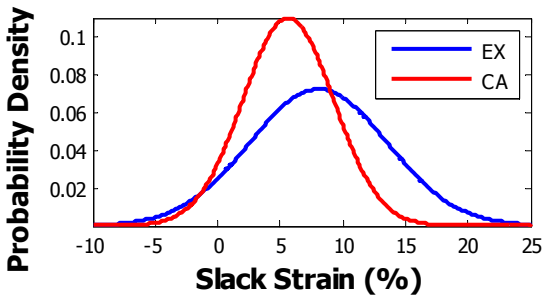

Figure 1: Larger and more variable slack strain distribution for the exercised (EX) versus caged activity (CA) groups.

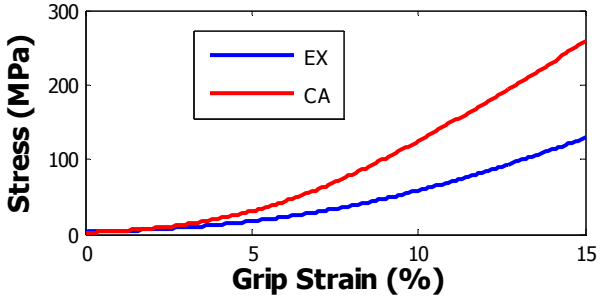

Figure 2: Larger and more variable slack distribution leads to larger exercised (EX) vs caged activity (CA) toe-region.

DISCUSSION:

Contrary to our hypothesis, the exercised group had a significantly larger variability in slack strain compared to the caged activity group, suggesting that exercise following 2 weeks of immobilization reduced tissue organization. This is further supported by the trend of decreased grip-to-grip modulus for the exercised group. These results are consistent with our previous work which showed that exercise immediately following repair decreased tissue organization and mechanical properties compared to continuous immobilization [3], and suggests that 2 weeks of immobilization is insufficient to allow for the beneficial effects of exercise on tissue organization and mechanics to be realized. Future work will use polarized light to corroborate the structural distribution parameters as well as include this novel elastic function into the quasi-linear viscoelastic (QLV) model to analyze stress-relaxation data.

REFERENCES:

[1] AAOS.org ,[2] Bishop J, JSES 2006 p290; [3] Gimbel JA, JBiomechEng 2007 p400; [4] Sarver JJ, JSES 2008; [5] Peltz CP, TORS 2008; [6] Hurschler C, JBiomechEng 1997 p392.

THE EFFECT OF APPLIED STRAIN ON TENDON-TO-BONE HEALING IN A RAT MODEL

Brophy RH, Kovacevic D, Imhauser CW, Bedi A, Stasiak M, Jackson K, Deng XH, Rodeo SA.
Tissue Engineering, Regeneration, and Repair Program, Hospital for Special Surgery, New York, NY

INTRODUCTION

Anterior cruciate ligament (ACL) reconstruction requires healing between a tendon graft and bone, which results from bone ingrowth into the tendon. Little is known about the effect of mechanical load on tendon-to-bone healing, which may have important implications for post-operative rehabilitation following ligament reconstruction. The purpose of this study was to compare the effect of cyclic strain to prolonged immobilization on tendon-to-bone healing using a novel approach to apply repetitive controlled strain to a healing tendon graft in an in vivo rat model to test the test the following hypotheses: (1) early graft motion causes inflammation that delays initial healing; (2) prolonged immobilization initiates the healing process but fails to progress to a mature tendon-bone interface.

METHODS

72 male Sprague Dawley rats weighing about 250 to 350 grams underwent ACL reconstruction using a flexor digitorum longus autograft. A custom-designed jig was used to drill co-linear tunnels in the femur and tibia, permitting placement of an external fixator across the knee that was parallel to the ACL graft. All other ligaments and tendon crossing the knee were sectioned to ensure that the ACL graft was loaded.

The rats were randomly assigned to immobilization or daily loading for either 2 weeks or 4 weeks. Rats were able to ambulate in their cages with the external fixation bar locked to immobilize the knee. Each day, rats assigned to daily loading were secured to a novel in-vivo joint distraction device under anesthesia such that displacement of the femur and tibia was constrained to axial translation parallel to the graft tunnels, placing axial strain on the graft. The joint was distracted at 0.24 mm/sec for a total distance of about 14 to 16 mm and then returned to neutral for a total of 50 cycles, and the resulting load-displacement curve was recorded. Preliminary cadaveric experiments verified that the ACL graft was loaded using our protocol.

At the end of the study period, the animals were sacrificed for micro-CT and histologic analysis. Biomechanical testing is ongoing. Statistical analysis was performed using 2-way ANOVA with appropriate post-hoc testing, and significance was set at $p < 0.05$.

RESULTS

Micro CT: In the tibial aperture, the micro-CT demonstrated significantly lower bone volume ($p=0.03$) and total mineral content ($p=0.05$) in the strained rats at 4 weeks compared to 2 weeks. There was a strong trend towards thicker trabeculae in the immobilized rats compared to the strained rats at 2 weeks ($p=0.08$) and 4 weeks ($p=0.06$). At 4 weeks, the strained rats also demonstrated a trend towards greater trabecular spacing compared to the immobilized rats ($p=0.08$). In the tibial exit, there was also a strong trend towards less bone volume in the strained rats at 4 weeks compared to 2 weeks ($p=0.06$).

Histology: Concentrations of "catabolic" $ED1^+$ macrophages at the tibial aperture trended lower in strained rats at 4 weeks (1.44 ± 1.15) compared to 2 weeks (3.5 ± 0.35) ($p=0.07$). Concentrations of "anabolic" $ED2^+$ macrophages demonstrated no significant findings. At the tibial tunnel exit after two weeks, daily straining resulted in more positively stained cells for Factor VIII (1.53 ± 0.14) compared to immobilization (0.48 ± 0.21) ($p=0.06$). However in the entire tibial tunnel, there was a trend towards less staining for Factor VIII among strained rats at 4 weeks (0.62 ± 0.49) compared to 2 weeks (1.54 ± 0.22) ($p=0.06$). In the tibial tunnel, tartrate-resistant acid phosphatase (TRAP) levels (expressed by osteoclasts) were significantly higher in the immobilized rats compared to the strained rats at 2 weeks ($p=0.02$) but by 4 weeks there was a significant decrease in TRAP in the immobilized rats ($p=0.002$), resulting in significantly higher levels of TRAP in the strained rats compared to the immobilized rats at 28 days ($p=0.01$).

DISCUSSION

This study successfully used a novel approach to apply repetitive controlled strain to a healing ACL tendon graft in an in vivo rat model to compare the effect of cyclic loading versus immobilization on tendon-to-bone healing. Over time, daily loading lead to a significant decrease in new bone formation and total mineral content at the tendon-bone interface of the tibial aperture. Additionally, daily loading negatively impacted trabecular architecture, with thinner trabeculae and increased trabecular spacing compared to immobilization. Early graft motion may promote inflammation that initially slows graft healing whereas immobilization may promote early healing but may limit maturation of the healing tendon-bone interface. Applying strain to the tendon-bone interface appears may be associated with greater angiogenesis, based on the higher levels of Factor VIII, and increasing numbers of osteoclasts over time. On-going studies using this system will provide further insight into the effect of mechanical loading on the strength of the healing tendon-bone interface.

Mechanical Properties of Human Regenerated Semitendinosus Tendon

S Kuribayashi[1], Y Shirasaki[2], S Okinaga[1], T Sanada[1], S Li[3], A Kanamori[3], K Marumo[4], M Saito[4], T Fukubayashi[5]

[1]Tokyo Teishin Hospital, Tokyo, [2] Advanced Industrial Science and Technology, Ibaraki, [3] Tsukuba University School of Medicine, Ibaraki, [4] Jikei University School of Medicine, Tokyo, [5] Waseda University, Saitama, Japan

INTRODUCTION

Recently, it has been shown that the semitendinosus (ST) tendon can regenerate after being harvested in its entire length and thickness to be used for anterior cruciate ligament (ACL) reconstruction. Although studies of clinical and functional outcome, as well as imaging analyses have demonstrated recovery of muscle function and apparent anatomic regeneration of the ST tendon, the mechanical properties of the tissue remain unknown. The purpose of this study is to assess the mechanical, anatomical, and histological features of the human regenerated ST tendon, and to propose the possibility of reusing the regenerated tendon as a replacement graft in revision cases.

METHODS

From November 2006 to September 2007, five patients with a mean age of 22 (18-31) years old gave their informed consent to participate in this study. All patients had undergone ACL reconstruction (13 mos-8 yrs prior) using a ST tendon autograft with an Endobutton® and were to undergo revision ACL reconstruction with their regenerated ST tendon. During revision surgery, a 2-3 cm specimen was taken from the proximal or distal end of the regenerated ST tendon for analysis of its mechanical and morphological properties. The cross sectional area of each specimen was measured at the midsection using a micrometer. A grip system with sinusoidal-shaped teeth was used to hold the specimens while a load to failure test was performed at a rate of 10mm per minute. The force-displacement relationship was measured using a TENSILON UTM-10 (A&D Co. Ltd. Tokyo, Japan) loading apparatus. Specimens that were thick were divided into two pieces. The mechanical properties of three normal gracilis (G) tendon were also measured and used for comparison.

RESULTS

Table 1 shows the results from the mechanical test. The maximum load of the regenerated ST tendon was 250 - 500 N, when a midsubstance rupture occurred.

Tissue	Grip to grip Length (mm)	Area (mm^2)	Maturation Time (Month)	Failure mode	Maximum Load (N)	Stiffness (N/mm)
ST 1	11	11.4	96	Slip	180*	60
ST 2a	10	11	23	Slip	140*	39
ST 2b	13	11		Rupture	288	52
ST 3a	13	6.6	13	Rupture	290	108
ST 3b	7.2	7.1		Rupture	229	80
ST 4a	5.2	6.1	13	Rupture	138	47
ST 4b	6	7		Slip	66*	14
ST 5a	20	10.9	48	Rupture	248	25
G	15.2±4.9	3.8±1.3	-	Rupture	184±39	87±22

Table 1. Tissue dimensions & mechanical properties. (ST tendon split into two fragments, i.e., a & b) *pro forma amount

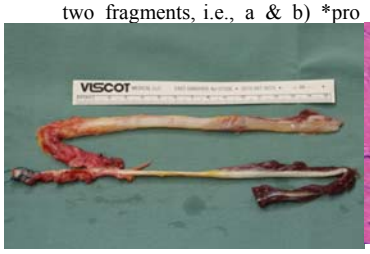

Fig 1. The regenerated ST tendon and normal G tendon.

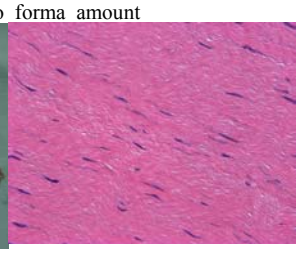

Fig 2. Histological appearance of the regenerated ST tendon. (from ST4, HE ×400)

Macroscopically, the regenerated ST tendon was significantly greater in cross-sectional area than the normal ST tendon (Fig 1). Regarding the histological findings, bundles of collagen fibers oriented along the longitudinal axis were clearly identifiable, together with uniformly distributed scattered rows of spindle-shaped cells that closely resembled tenocytes (Fig 2).

DISCUSSION

This study presents the mechanical properties of human regenerated ST tendon. The regenerated ST tendon can nearly double the strength of the normal G tendon which would make it an excellent substitute for various reconstructive surgeries.

REFERENCES

1) Noyes, et al, JBJS, 66:344-352, 1984. 2) Cross, et al, AJSM, 20:221-223,1992. 3) Yoshiya, et al, Arthroscopy,

ESTABLISHING MEASURES OF SUCCESS IN FUNCTIONAL TISSUE ENGINEERING FOR TENDON AND LIGAMENT REPAIR AND RECONSTRUCTION

DL Butler[1], J Lewis[2], CB Frank[3]
[1]Department of Biomedical Engineering, University of Cincinnati, Cincinnati, OH; [2]Department of Orthopaedic Surgery, University of Minnesota; [3]Division of Orthopaedic Surgery, University of Calgary

INTRODUCTION. We recently conducted a Functional Tissue Engineering Design Evaluation Conference in Hilton Head, South Carolina, sponsored by NIH, foundations, and companies [1]. Bioengineers, surgeons, biologists and material scientists from academia, industry and government were invited to develop general and tissue-specific criteria for evaluating musculoskeletal tissue engineered concepts and constructs and to determine threshold values of success where available. In this process, participants were asked to be sensitive to academic concerns, industry needs and agency constraints on funding from government agencies. We all recognized that bioengineers and surgeons understand the clinical problems that motivate our research, that pre-clinical studies must be performed to study promising treatments in vivo, but that the gap between clinical and pre-clinical studies can be large. However, experts still do not agree on the evaluation criteria, parameters and their threshold values used to judge a proposed treatment as safe and efficacious.

METHODS. One NIH representative first emphasized the differences in objectives between NIH, who focuses on basic research with less emphasis on translation and direct clinical application, vs. industry whose focus is application with much less emphasis on basic research. Industry representatives echoed these concerns and re-emphasized the need for profitability, the need for ease in manufacturing and the need to get approval for biologics through the FDA. Participants were then assigned to four breakout groups, including: ligament and tendon [2]; articular cartilage; bone and intervertebral disc; and meniscus and TMJ. Group members were encouraged to start by defining only one or two important clinical problems for each tissue application (based on the rationale that if successful, other problems could then be tackled using the same approach). Each group then attempted, for each clinical problem, to develop tissue engineering evaluation parameters and corresponding values. Once these problems were carefully defined, each breakout group was asked to tackle pre-clinical problems that would arise in attempting to simulate these clinical problems in animals. The meeting concluded with discussions about how these clinical/pre-clinical constraints might influence in vitro tissue engineering studies conducted in the future.

RESULTS. All groups wrestled with the question, “should we compare results in an animal model to the gold standard of care (a position supported by surgeons and industry) or to “normal tissue properties” (a position more popular with bioengineers, biologists and material scientists). Some even questioned whether animal repair results should ever be compared to normal since this may be unrealistic and may certainly appear to be worse than the current clinical gold standard. Another question raised was whether the parameters that are identified should mimic subfailure functional properties and limits or actually match the failure properties of the controls.

The ligament and tendon breakout group agreed to focus on the clinical problems of ACL injury and reconstruction and on rotator cuff tendon injury. Current standards of clinical treatment (ACL autografts and allografts and rotator cuff repairs) were identified as well as the potential advantages and constraints of a TE application. The group agreed on a set of normal tissue characteristics for both applications (function, biomechanical properties, histology and biochemistry) and then identified pre-clinical models, measures and values that they felt would best assess tissue engineered constructs. The group concluded by briefly discussing the challenges in tissue engineering these structures in the laboratory. The specifics of these selections will be presented.

CONCLUSIONS. It was concluded that the multi-stakeholder consensus strategy used in this conference could not only help establish new criteria, but provide a real benefit to researchers and product development people in academia and industry and help to set guidelines for the FDA and ASTM. Participants also agreed that this approach could be repeated for other tissue applications in more effective and efficient ways. A white paper is currently in review at *Tissue Engineering* [3].

REFERENCES. 1. NIAMS, NIBIB and NIDCR at NIH, ORS, OREF, Bose, Flexcell, Johnson & Johnson, LifeCell, Smith & Nephew, Stryker and Synthasome. 2. L&T Breakout Group included David Butler, Braden Fleming, Martha Murray, Scott Tashman, Chris Wagner and Sandy Williams. 3. Functional Tissue Engineering Conference Group, “Evaluation Criteria for Musculoskeletal and Craniofacial Tissue Engineering Constructs: A Conference Report,” *Tissue Engineering* (in review)

COLLAGEN-PLATELET RICH PLASMA HYDROGEL ENHANCES PRIMARY REPAIR OF THE PORCINE ANTERIOR CRUCIATE LIGAMENT

Martha M. Murray[1], Braden C. Fleming[2], Eduardo Abreu[1], Elise Magarian[1], Ashley Mastrangelo[1], Matthew Palmer[1] and Kurt P. Spindler[3]

[1]Dept of Orthopaedic Surgery, Harvard Medical School, Boston MA

[2]Dept of Orthopaedic Research, Alpert Brown Medical School, Providence RI

[3]Dept of Orthopaedic Surgery, Vanderbilt University, Nashville TN

INTRODUCTION: The anterior cruciate ligament (ACL) fails to heal after suture repair. One hypothesis for this failure is the premature loss of the fibrin clot, or provisional scaffolding, between the two ligament ends in the joint environment. To test this hypothesis, a substitute provisional scaffold of collagen-PRP hydrogel was used to fill the ACL wound site at the time of suture repair (Figure 1) and the structural properties of the healing ACLs evaluated from 4-14 weeks after surgery.

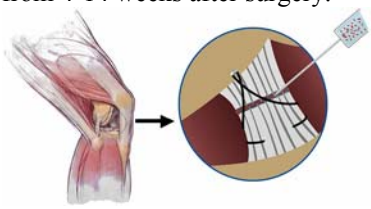

Figure 1. Schematic of the enhanced suture repair technique. In 1A, the location of the ACL is illustrated. 1B represents a schematic of a transected ACL treated with suture repair. For enhanced suture repair, the collagen-PRP hydrogel is introduced into the wound site to fill in the remaining gap.

METHODS: Bilateral ACL transections were performed in nineteen 30 kg Yorkshire pigs and treated with suture repair. In each animal, one of the repairs was augmented with placement of a collagen-platelet rich plasma (PRP) hydrogel at the ACL transection site, while the contralateral knee had suture repair alone. In addition, six control knees with intact ACLs from three additional animals were used as a control group. Five animals were euthanized at four weeks, three at 6 weeks, three at 9 weeks and three at 14 weeks. No post-operative immobilization was used. At the designated time points, the animals underwent biomechanical testing to determine tensile properties.

RESULTS: The use of a collagen-PRP hydrogel to enhance suture repair resulted in significant increases in stiffness, yield load and maximum load of the healing ligaments compared to suture repair alone at the four week time point; however, both groups remained significantly inferior to the intact ligament group. When suture repairs were supplemented with a collagen-PRP hydrogel, the maximum load was approximately 2-fold greater ($t = 4.15$, $p = 0.014$) than the suture repair alone, a difference that was also present at the six week time point (28 +/- 20 N max load for suture repair alone vs 52 +/- 44 N for suture repair + hydrogel). At fourteen weeks, the supplemented suture repair yield load increased to 126 +/- 24N, while the suture repair alone increased to 72 +/- 18N. At fourteen weeks, the supplemented suture repair was still lower than the intact ACL yield load (202.5 +/- 43N), but this difference was not found to be statistically significant ($p=0.08$).

POST-TESTING HISTOLOGY: Sagittal large sections of the entire knee through the ACL scar mass were made for the four week specimens and representative sections stained with hematoxylin and eosin. Histologic examination of the sections suggests that the scar mass between the ends of the transected ligaments in the collagen-PRP hydrogel group is hypercellular and hypervascular at four weeks. The vast majority of the cells seen within the scar mass were fibroblastic, with only rare inflammatory cells seen within the repair tissue. The distal tibial remnant of the transected ACL appeared to be covered anteriorly with a hypertrophic tissue that was continuous with the anterior fat pad and the ACL wound site. In addition, the ACL remnants themselves (both proximal and distal) contained areas of hypertrophic epiligamentous tissue between fascicles.

CONCLUSION: We conclude that use of a stabilized provisional scaffold, such as a collagen-PRP hydrogel, to supplement primary repair of the ACL can result in improved biomechanical properties over suture repair at four to fourteen weeks with increasing strength over time; however, even after 14 weeks in vivo, normal ligament strength is not completely restored. Further studies to determine the longer-term effect of primary repair enhancement are needed.

ACKNOWLEGEMENTS

This study was supported by CIMIT through DoD funding under cooperative agreement no. DAMD17-02-2-0006, as well as support from the National Football League Medical Charities program. Salary support was provided by NIH grant K02 AR049346 (MMM).

A COMPARISON OF MESENCHYMAL STEM CELLS AND ACL FIBROBLASTS RESPONSES ON COMBINED SILK SCAFFOLDS

Haifeng Liu[1], Hongbin Fan[1], Siew Lok Toh[2, 3], James C.H. Goh[1, 2] *

1 Department of Orthopedic Surgery, National University of Singapore, Singapore
2. Division of Bioengineering, National University of Singapore, Singapore
3. Department of Mechanical Engineering, National University of Singapore, Singapore

INTRODUCTION

The aim of this study was to compare the cellular responses of bone marrow-derived mesenchymal stem cells (BMSCs) and anterior cruciate ligament fibroblasts (ACLFs) on combined silk scaffolds for ligament tissue engineering application.

METHODS

Rabbit BMSCs and ACLFs were isolated and cultured *in vitro* for two weeks after seeding on the silk scaffolds. Samples were evaluated and compared for their cellular morphology, proliferation, gene and protein expression of tenascin-C, type I and type III collagen. In addition, the two cell types were transfected with green fluorescent protein (GFP) to trace their fate in the knee joints.

RESULTS

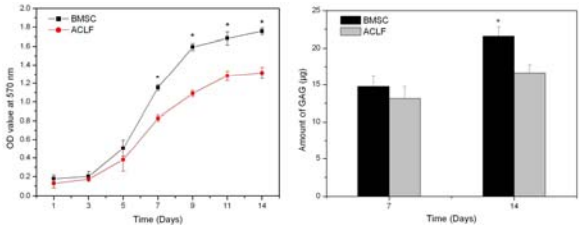

Figure 1. The cellular proliferation and GAG production of BMSCs and ACLFs cultured on the combined silk scaffolds. * Significant difference between two groups at $p<0.05$.

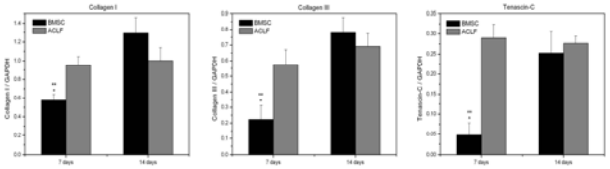

Figure 2. Expression of ligament-related ECM genes by BMSCs and ACLFs cultured on the combined silk scaffolds for 7 and 14 days. Levels, quantified using real-time RT-PCR, are normalized to the housekeeping gene, GAPDH. * Significant difference between two groups at each time point ($p<0.05$) and ** Significant difference of one group between two time points ($p<0.05$).

*Corresponding author.
E-mail address: dosgohj@nus.edu.sg (James C. H. Goh)

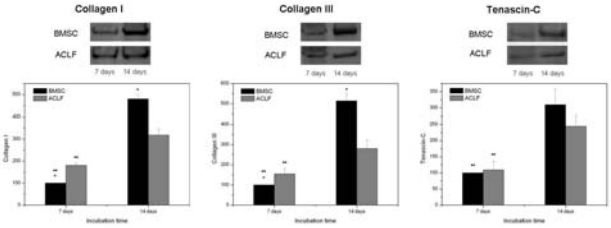

Figure 3. Western blot analysis of ligament-related ECM proteins by BMSCs and ACLFs cultured on the combined silk scaffolds for 7 and 14 days. To compare results from different samples, the responses of BMSCs cultured on the scaffolds for 7 days were standardized to 100. * Significant difference between two groups at each time point ($p<0.05$) and ** Significant difference of one group between two time points ($p<0.05$).

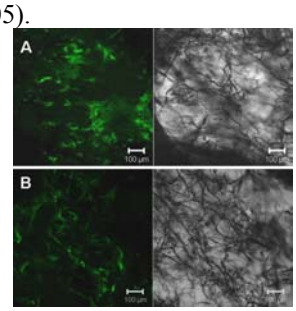

Figure 4. Fluorescence images of implants with GFP-transfected BMSCs (A) and ACLFs (B) at 4 weeks postimplantation. Scale bars = 100 μm.

DISCUSSION

These preliminary results demonstrate that BMSCs have much clearer and distinct advantages over ACLFs, with respect to cell proliferation, GAG excretion, gene and protein expression for ligament-related ECM markers, and *in vivo* survivablity. Based on the present data, BMSCs are more suitable than ACLFs for healing environment and development of a tissue-engineered ligament.

REFERENCES

Liu HF, Fan HB, Wang Y, Toh SL, Goh JCH. The interaction between a combined knitted silk scaffold and microporous silk sponge with human mesenchymal stem cells for ligament tissue engineering. Biomaterials (2007), doi:10.1016/ j.biomaterials.2007.10.035.

DESIGN OF A NOVEL STRATIFIED SCAFFOLD FOR ACL-TO-BONE INTERFACE TISSUE ENGINEERING

J.P. Spalazzi, K.L. Moffat, and H.H. Lu
Department of Biomedical Engineering, Columbia University, New York, NY

INTRODUCTION: Soft tissue-based ACL reconstruction grafts are limited by their inability to reestablish a functional interface with bone tissue[1]. The native ACL-bone interface consists of three regions: ligament, fibrocartilage, and bone[2-4]. Graft integration is a critical factor governing its clinical success, and the regeneration of an anatomic interface on ACL grafts will improve graft outcome. Our interface tissue engineering effort has focused on biomimetic scaffold design and the optimization of interactions among interface relevant cell types. We have designed a triphasic scaffold comprised of three distinct yet continuous phases, each designed for the formation of a specific tissue type found at the ACL-bone interface: Phase A for ligament, Phase B for interface, and Phase C for bone. This study describes the optimization of this novel scaffold for interface tissue engineering, focusing on exercising spatial control in the phase-specific distribution of interface relevant cell populations such as fibroblasts, chondrocytes and osteoblasts. Moreover, the distribution of these three cell populations on the optimized scaffold was tracked *in vitro*, and the formation of phase-specific cellular regions on the scaffolds was determined.

MATERIALS AND METHODS: *Fabrication*- Phases A, B, and C consist of poly(lactide-*co*-glycolide) (PLGA, 10:90) knitted mesh, PLGA (85:15) microspheres, and PLGA(85:15)/Bioactive Glass (45S5, BG) composite microspheres, respectively. The microspheres were formed via an emulsion method[5]. Randomly oriented PLGA (85:15) nanofiber meshes were formed by electrospinning and inserted between adjacent phases. Continuous scaffolds were formed by sintering above the T_g. *Nanofiber Mesh Characterization*- Porosity and pore diameter were determined using mercury porosimetry, and fiber diameter by image analysis. Permeability to cells was determined by seeding bovine fibroblasts on one side of the mesh and staining with hematoxylin after 7 days of culture. *Cell Tracking*- Bovine fibroblasts (Fb), chondrocytes (Ch), and osteoblasts (Ob) were fluorescently labeled with DiO, DiD, and DiI, respectively. Fb and Ob were seeded on Phases A and C, while Ch were loaded into Phase B in 0.5% agarose ($5x10^5$ cells/phase). At days 1, 4, and 14, cross-sections were imaged using confocal microscopy.

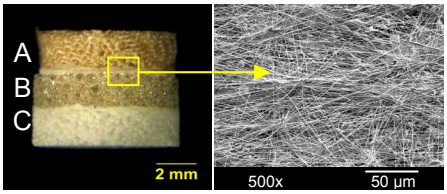

Fig 1. Modified triphasic scaffold (left) with electrospun nanofiber mesh dividers between the scaffold phases. Scanning electron micrograph of nanofiber mesh (right)

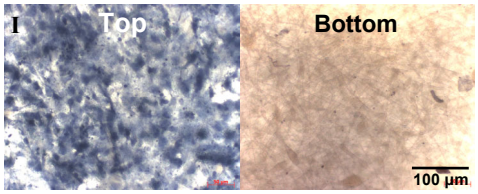

II	Unaligned Mesh
Porosity	82 ± 4 %
Pore Diameter	4.9 ± 0.8 µm
Permeability	(5.7±0.6)E-12 $m^4/N \cdot s$
Fiber Diameter	570 ±150 nm

Fig 2. I) Fibroblasts seeded on top of mesh (left) were not able to penetrate through to the bottom (right) after 7 days of culture (Hematoxylin stain, 20x). II) Nanofiber mesh exhibits a high porosity and surface area with a small pore diameter to limit cell migration

RESULTS: Structural characterization of the nanofiber mesh revealed that it exhibits high porosity and permeability which is suitable for cell culture (*Fig 2*). Moreover, the mesh pore diameter averaged 5 µm, and evaluation of cell migration revealed that the nanofiber mesh served as an effective barrier, as no cells were found on the bottom of the mesh at day 7 (*Fig 2*). Cell tracking results revealed that at day 1, Fb, Ch, and Ob were localized on Phases A, B, and C of the scaffold, respectively. More importantly, after 14 days of culture, all cell types were found to remain in their intended phases (*Fig 3*).

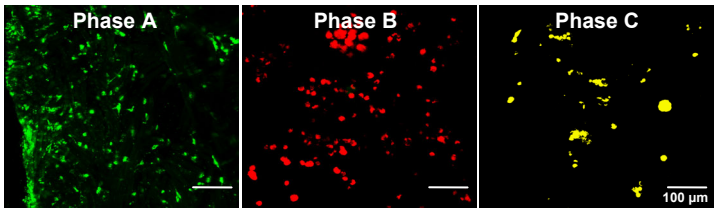

Fig 3. Fb (green), Ch (red), and Ob (yellow) were localized primarily to Phases A, B, and C, respectively, at day 14 (bar = 100 µm).

DISCUSSION: The results of this study demonstrate that phase-specific and cell type-specific distribution of interface relevant cell types can be achieved through novel scaffold design. This controlled distribution is expected to promote the formation of distinct yet continuous matrix regions mimicking those observed at the native ACL-bone insertion site, with ligamentous matrix in Phase A, fibrocartilaginous matrix in Phase B, and mineralized tissue in Phase C. Future studies will evaluate the maintenance of this controlled matrix heterogeneity on the stratified scaffold *in vivo*.

REFERENCES: 1) Rodeo, *Am J Sports Med,* 27(4):476, 1999; 2) Weiler, *Arthroscopy*, 18(2):124,2002; 3) Gao, *J Anat,* 188:367, 1996; 4) Visconti CS, *Arch Biochem Biophys* 328(1):135, 1996; 5) Lu, *J Biomed.Mater Res.,*1:64A(3):465,2003.
ACKNOWLEDGEMENTS: The Wallace H. Coulter Foundation (HHL), NIH-NIAMS (R21 AR052402, HHL), and NSF GK-12 Fellowship (GK-12 0338329, JPS).

RECAPITULATING A TENDON PHENOTYPE, RT-PCR MARKERS *IN VIVO* IN COMPARISON TO *IN VITRO CULTURE* SYSTEMS

S.E. Taylor[1], R.K.W. Smith[2] and P.D.Clegg[1]
[1]Veterinary Clinical Sciences, University of Liverpool, South Wirral.UK
[2]Royal Veterinary College, University of London, Hawkshead, Hertfordshire.UK

INTRODUCTION

Tendon has a poor intrinsic repair capacity therefore tissue engineering approaches are being studied to improve the functional repair of this tissue. In the horse, clinical treatment with bone marrow derived mesenchymal stromal cells (BM-MSCs) is being increasingly used. However, scientific evidence is currently lacking regarding the cellular differentiation and fate of these cells. The objectives of these experiments were to determine if quantitative real-time polymerase chain reaction (RT-PCR) could identify key genes capable of identifying cells with a tendon phenotype, and furthermore, identify if this phenotype remained when the tendon derived cells were cultured in monolayer or three dimensional collagen matrices with and without BM-MSCs.

MATERIALS & METHODS

Three matched tissue samples of tendon, cartilage and bone were retrieved from skeletally mature horses subjected to euthanasia for non-orthopaedic disease. Tendon samples were also collected from a 100days foetus, a 200days foetus, a skeletally immature horse and three horses with acute superficial digital flexor tendonitis. Samples were stored in RNAlater at -80ºC prior to RNA extraction and reverse transcription. RT-PCR using exon spanning primers was carried out to identify a panel of putative tendon marker genes. Tenocytes were digested from the superficial digital flexor tendon (SDFT), and common digital extensor tendon (CDET) of 4 skeletally mature horses and cultured for 5 passages in monolayer. Additionally passage one tenocytes were seeded into collagen gels, with or without an equal proportion of BM-MSCs, and subjected to tensile strain for 5days using the Flexcell™ Tissue Train culture system. RNAs were extracted at each passage in monolayer and following 5 days of tensile strain. A panel of putative marker genes identified from the matched tissue samples were quantified using RT-PCR. Statistical analysis of matched samples was carried out using a mixed effects model using S-plus software. Unmatched data was compared using a student's t test.

RESULTS

The matched adult tissue samples did not identify a specific gene that was highly expressed in tendon but not in the other mesenchymal tissues. Scleraxis expression was higher in tendon than bone but this was not statistically significant (P=0.06). Tenascin-C expression was significantly lower in tendon than in bone and cartilage (P=0.02 and P=0.04 respectively). Foetal and immature tendon showed high expression of tenomodulin, tenascin and scleraxis compared with adult tendon. Progressive passaging of monolayer tenocytes showed significantly reduced expression of collagen type I, decorin and fibromodulin and Six1 with increasing passage number (P=0.003, P=0.0001, P=0.04, P=0.04 respectively). At passage one in monolayer cultures both COMP and Decorin showed higher expression in tenocytes than BM-MSCs while tenascin expression was higher in BM-MSCs. Horses with clinical tendonitis of the SDFT showed increased expression of collagen type I, tenomodulin and tenascin compared with normal adult horses (P=0.008, P=0.02, and P=0.01 respectively). Culture of tenocytes and BM-MSCs within collagen gels subjected to tensile strain reduced the levels of expression of collagen type I and tenascin. Tensile strain had minimal influence of tenocytes, but BM-MSCs showed reduced expressions of Collagen-I, -V & tenascin C. Equal proportions of tenocytes and BM-MSCs resulted in a gene expression profile that was similar to culture of tenocytes alone.

DISCUSSION AND CONCLUSIONS

Unlike cartilage that can be identified by high expression of collagen type II we have failed to identify one single gene that can distinguish tendon from other mesenchymal tissues. Whilst it would appear scleraxis is able to differentiate between tendon and bone, it is not able to distinguish between cartilage and tendon. From these experiments the following panel of genes are the most discriminating in defining a tendon phenotype: collagen types I, II, and X, scleraxis and tenascin. These experiments identify that tenocytes and BM-MSCs have distinct phenotypes when cultured under different culture conditions. The similar gene expression with co-culture suggests that there is cellular interactions leading to BM-MSC differentiation.. This work supports the use of BM-MSCs may for clinical treatment of tendinopathy.

Acknowledgements Funded by Horserace Betting Levy Board.

SCLERAXIS AND TENOMODULIN: MEDIATORS OF BMP-12-INDUCED TENOCYTE DIFFERENTIATION

Y. Li[1], H.B. Sun[1], M. Ramcharan[2], D.T. Fung[1], R.J. Majeska[1], M.B. Schaffler[1], E.L. Flatow[1] and Y. Li[3]
[1]Leni and Peter W. May Department of Orthopaedics, Mount Sinai School of Medicine, NY, [2]Biomedical Engineering, CCNY, NY, [3]Key State Pathobiology Laboratory, Jilin University, Changchun, China
Email: herb.sun@mssm.edu

INTRODUCTION: Engineering of tendon tissue from mesenchymal stem cells (MSCs) will require precise, selective methods to control tenocyte differentiation [1]. BMP-12, a cytokine of the TGFβ family [2], appears to stimulate tenocyte differentiation, since MSCs transfected with BMP-12 formed tendon-like tissues *in vivo* [2, 3] and *in vitro* [4, 5]. To date, however, the signaling pathways mediating tenocyte differentiation in response to BMP-12 are unclear. Therefore, we characterized BMP-12-induced changes in MSC expression of scleraxis (Scx) [6] and tenomodulin (Tnmd) [7], which are two transcriptional regulators related to tenocyte differentiation.

METHODS: Human MSCs were assayed for tenocyte differentiation in monolayer culture and colony forming assays. Monolayer cultures were grown to 80% confluency and treated with 0 - 25ng/ml BMP-12 (R&D) at various time points, and then analyzed after 7 days using real-time PCR. In colony assays, MSCs were plated at $2.5x10^4/cm^2$ and treated with BMP-12 for 3 – 24 hr prior to analysis at 7 days by *in situ* hybridization. For specific gene knockdown experiments, MSCs plated for colony forming assays were transfected with si-Scx or si-Tnmd RNAs prior to BMP-12 treatment. Real-time PCR (using total RNA with GAPDH control) and colony formation/*in situ* hybridization analyses were performed in separate experiments. *In situ* hybridization utilized antisense oligonucleotide probes. Experiments were repeated at least three times. Differences from control ($p<0.05$, t-test) are indicated by *.

RESULTS: In MSC monolayers, BMP-12 induced Scx and Tnmd expression and increased Scx (+) and Tnmd (+) cell numbers, dependent onBMP-12 concentration (2.5 – 25ng/ml) and time (3 – 12 hr). Colony formation assays corroborated these results; seven days after a 24 hr BMP-12 treatment, ca. 40% of colonies were Scx (+) and/or Tnmd (+). Both Scx and Tnmd expression and Scx (+)/Tnmd (+) colony number were inversely correlated with the MSC marker Nucleostemin (Nst), indicating that tenocyte differentiation was linked to reduced stem cell numbers. Finally, Scx suppression with siRNA blocked BMP-12-induced Tnmd expression and Tnmd (+) colony formation; however, Tnmd knockdown had no effect on induction of Scx expression and Scx (+) colony formation (Figure 1).

Fig 1. Knockdown of Scx in MSCs abolishes BMP-12 induction of Tnmd expression (A) and Tnmd (+) colony formation (B)

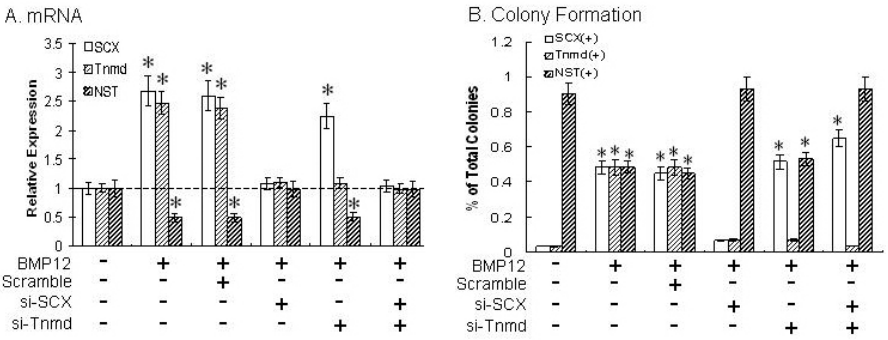

DISCUSSION: In this study we demonstrated that BMP-12 induces MSCs to differentiate into tendon-forming cells expressing both Scx and Tnmd, associated with a reduction, but not total abolition, of stem cell capacity. The induction was both dose- and time-dependent, suggesting a causal relationship and confirming the utility of this approach to selectively modulate tenocyte differentiation. Furthermore, the siRNA knockdown experiments established that Scx may serve as a required upstream mediator of Tnmd expression within the BMP-12 induced tenocyte differentiation pathway.

REFERENCES: [1] Herzog et al (2003). *Blood* 102:3483. [2] Wolfman et al (1997). *J Clin Invest* 100: 321. [3] Lou et al (2001). *J Orthop Res* 19:1199. [4] Lou et al (1999). *Clin Orthop Rel Res* 369:333. [5] Wang et al (2005). *J Biosci Bioengineer* 100:418. [6] Schweitzer et al (2001). *Development* 128:3855. [7] Shukunami et al (2006). *Dev Biol* 298:234-47. [9] Kafienah et al (2006). *Stem Cells* 24:1113.

ACKNOWLEDGEMENTS: Aircast Foundation and NIH Grants AR52743 (ELF), AR41210 (MBS) and AR050968 (HBS).

FEASIBILITY OF ELECTROCHEMICALLY ALIGNED COLLAGEN BUNDLES FOR LIGAMENT/TENDON TISSUE ENGINEERING

X.G. CHENG, U. A. GURKAN, J. A. UQUILLAS, O. AKKUS*

Orthopedic Bioengineering Lab, Weldon School of Biomedical Engineering, Purdue University, West Lafayette, IN

INTRODUCTION

Collagen, as a biomaterial, is limited in application for tissue repair due to lack of practical approach to induce orientational anisotropy and packing order. We recently invented an electrochemical process to form highly oriented and densely packed collagen bundles with improved mechanical properties [1]. Here we report the morphology and migration of tendon-derived fibroblasts on such aligned collagen bundles individually as well as three-dimensional constructs formed by grouping several bundles. Our preliminary results demonstrate that fibroblasts can be oriented and populated on such highly oriented collagen constructs. Mechanical competence, biocompatibility and optimal biodegradability of the collagen constructs show great promise for ligament/tendon tissue engineering applications.

METHODS

Extraction and seeding of tendon-derived fibroblast on collagen bundles: Each collagen bundle was prepared electrochemically as described earlier [1]. Aligned collagen bundles were 0.1 mm in diameter and 30 mm in length and they were crosslinked by genipin. Collagen bundles were immersed in 70% EtOH and fully rinsed before cell migration and proliferation. Fibroblasts were extracted from Achilles tendons of a 50 days old male Long-Evans rat. The growth medium was composed of α-MEM (Sigma, M4526) supplemented with 10% FBS (Sigma, F6178), 2 mM L-Glutamine (Sigma, G7513), 100 U/ml Penicillin and 100 µg/ml Streptomycin (Invitrogen, 15140-122), 1.5 µg/ml Fungizone (Gibco, 15290-018). The cells were passed 3 to 5 times before being used for cell migration and proliferation [2]. The constructs were stained with Alexa Fluor 488 Phalloidin (Molecular Probes) on the 7th day and imaged under the confocal microscope (Olympus FV1000).

RESULTS

SEM image (Fig 1a) shows that aligned-CX collagen is densely packed with uniform anisotropic order. The method allows for continuous bundles as long as 6 cms (Fig 1b). Four aligned-collagen bundles (Fig 1b) were woven together to form a construct (Fig 1c) and allowed for fibroblast migration at a rate of 1.2 mm/day. Cells eventually covered the entire surface of the construct and their cytoskeletal filaments were stretched along the orientation of the aligned collagen as demonstrated by the confocal image of actin filaments in cell cytoskeleton. (Fig. 1d)

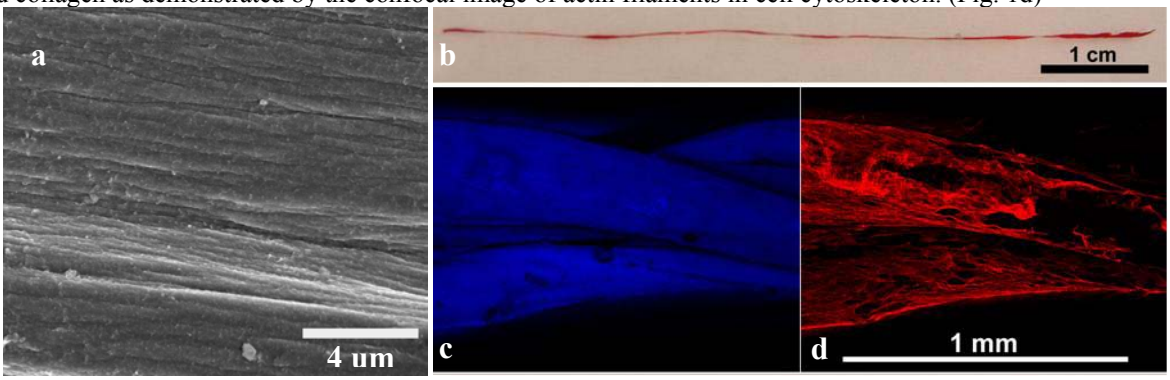

Fig 1. A) SEM image of an aligned collagen bundle. B) Image of Sirius red stained individual aligned collagen bundle. C) Confocal image of collagen construct woven from 4 individual bundles C) Confocal image of cytoskeletons of cells migrated onto the construct.

DISCUSSIONS

Our study demonstrated that aligned-CX collagen construct formed via the electrochemical process had great potential for dense connective tissue engineering such as tendon/ligament replacement. The biocompatibility and tissue repair and regeneration ability of aligned-CX collagen construct will be evaluated by in animal model in the future.

REFRENCES [1] X. Cheng, N. Wasserman, O. Akkus, Proceedings of ASME Summer Bioengineering Conference, Keystone, Colorado, 2007.
[2] K.G. Cornwell, P. Lei, S.T. Andreadis, G.D. Pins, Journal of Biomedical Materials Research Part A 80A (2) (2007) 362-371.

IN VITRO HMBSC RESPONSE ON ALIGNED NANOFIBER SCAFFOLDS WITH AND WITHOUT HYDROXYAPATITE NANOPARTICLES

K. L. Moffat, S. P. Kwei, and H. H. Lu
Department of Biomedical Engineering, Columbia University, New York, NY, USA

Introduction: Rotator cuff tears represent one of the most common shoulder injuries, with 75,000 repairs performed annually in the U.S[1]. Full-thickness tears result largely from avulsion of the cuff tendon, which often occurs at the supraspinatus tendon-to-bone insertion[2]. The tendon inserts into bone through a fibrocartilagenous interface, with aligned non-calcified collagen fibers traversing the interface and calcified collagen fibers penetrating into subchondral bone[3-5]. **Our long term goal** is to develop a biomimetic scaffold which will promote the biological fixation of rotator cuff tendon to bone by facilitating the regeneration of the tendon-bone insertion. To this end, we have designed nanofiber-based poly(lactide-*co*-glycolide) (PLGA) scaffolds with and without a mineral phase[6]. **The objective of this study** is to evaluate the fibrochondrogenic differentiation of human bone marrow stromal cells (hBMSCs) on PLGA nanofiber scaffolds with or without hydroxyapatite (HA) nanoparticles. It is anticipated that hBMSC response will differ on PLGA and PLGA-HA nanofiber scaffolds.

Materials and Methods: *Scaffold Fabrication*–Aligned nanofibrous scaffolds of PLGA (85:15, Lakeshore) and HA nanoparticles (100-150nm, Nanocerox) were produced via electrospinning[6], and a rotating target was used to form aligned fibers[7]. PLGA nanofiber scaffolds with 0% and 5% HA were formed. *Cells & Cell Culture*–hBMSCs (Cambrex) were seeded on the scaffolds ($3.14x10^4$ cells/cm^2) and cultured in ITS+ media containing 40 µg/mL L-proline, 100 µg/mL sodium pyruvate, 0.1 µM dexamethasone, and 50 µg/mL ascorbic acid[8,9]. For fibrochondrogenic differentiation, 10 ng/mL of TGF-β3 was added. End-Point Analyses–Cell viability and morphology were examined by confocal microscopy (Live/Dead assay, n=3), proliferation by PicoGreen assay (n=5), ALP activity was determined by colorimetric assay (n=5). GAG deposition was determined by Alcian blue stain (n=2). Gene expression for collagen type I was evaluated by RT-PCR (n=3) and normalized to GAPDH.

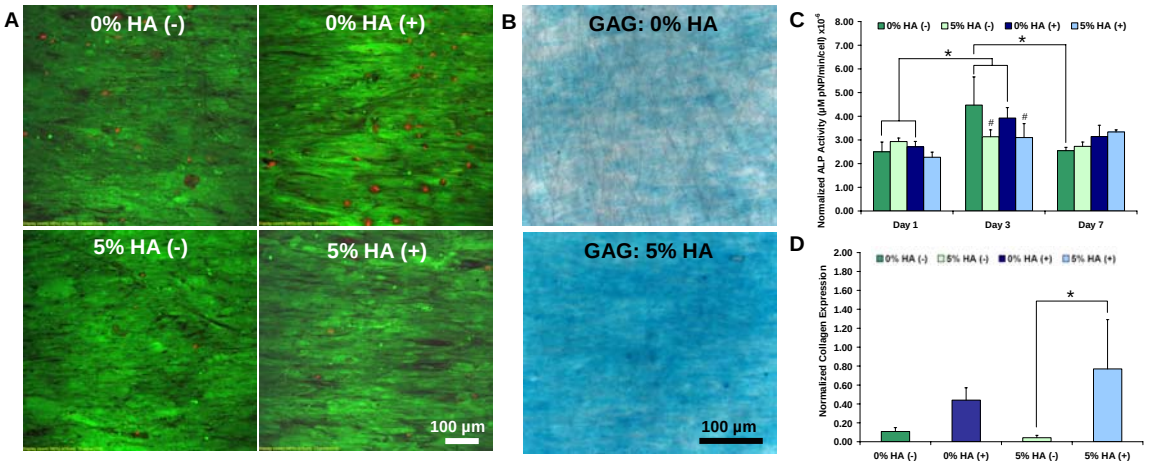

***Figure 1**: **A)** hBMSCs remain viable on the nanofiber scaffolds (Day 7, 20x). **B)** Proteoglycan deposition was greater on the 5% HA scaffolds (Day 7, Alcian Blue, 20x). **C)** ALP activity was higher on 0% HA substrates (*,# $p<0.05$). **D)** Type I collagen expression increased significantly under TGF-β3 stimulation (Day 3, normalized to GAPDH, * $p<0.05$).*

Results and Discussion: The hBMSCs remained viable (*Fig. 1A*) and proliferated on all substrates. Nanofiber scaffolds with 5% HA stained strongly for proteoglycans (*Fig. 1B*), followed by those stimulated with TGF-β3. ALP activity increased over time on scaffolds without HA, and this difference was significant at day 3 (*Fig. 1C*). Both 0% HA (+) and 5% HA (+) scaffolds exhibited higher type I collagen expression than the groups with TGF-β3, with a significant increase observed for the 5% HA scaffolds at day 3 (*Fig. 1D*). These observations suggest that the presence of HA nanoparticles in the nanofiber scaffold reduces hBMSC mineralization potential and increases proteoglycan deposition by these cells. Moreover, when stimulated by TGF-β3, the expression of fibrochondrocyte-related markers, such as type I collagen, was significantly up-regulated on the nanofiber scaffolds. These results demonstrate the potential of the nanofiber scaffolds for tendon-bone interface tissue engineering. Future studies will focus on optimizing these scaffolds for fibrochondrogenic differentiation of hBMSCs for tendon-bone healing.

References: [1]Vitale *et al*., 2007; [2]Iannotti *et al*., 1994; [3]Woo *et al*., 1987; [4]Benjamin and Evans, 1990; [5]Cooper and Misol, 1970; [6]Moffat *et al*., 2007; [7]Matthews *et al*., 2002; [8]Li *et al*., 2005; [9]Baker and Mauck, 2007.

PLATELETS REDUCE POST-OPERATIVE KNEE LAXITY AND CORRELATE WITH EARLY GRAFT PROPERTIES IN A CAPRINE ACL RECONSTRUCTION MODEL

KP Spindler[1], MM Murray[2], JL Carey[1], BC Fleming[3]
[1]Dept of Orthopaedic Surgery, Vanderbilt University, Nashville TN
[2]Dept of Orthopaedic Surgery, Harvard Medical School, Boston MA
[3]Dept of Orthopaedic Research, Alpert Brown Medical School, Providence RI

INTRODUCTION

Although ACL reconstruction (ACLR) is a common procedure for approximating normal anteroposterior (AP) laxity of the ACL injured knee, normal kinematics are not restored and joint laxity increases with healing in many patients. Recent work has shown improved ACL strength when defects have been treated with a collagen-platelet gel [1]. The collagen-platelet hydrogel could potentially be used to enhance graft healing in ACLR. We hypothesized that: 1) placement of a platelet gel around the graft at the time of surgery would enhance the structural properties of the healing graft, and decrease postoperative knee laxity, and 2) the structural properties of the graft would be directly proportional to the platelet concentration.

METHODS

Twelve goats underwent unilateral ACL reconstruction with autologous bone-patellar tendon-bone graft. In six goats, a collagen-platelet hydrogel (experimental) was placed around the graft. In the remaining six goats, the collagen carrier alone (sham) was used. After six weeks in vivo, the AP laxity at 30° and 60° of flexion and the tensile properties of the ACL reconstructed knee were measured. T-tests were then performed to determine differences between treatments (Hypothesis 1). Regression analyses between systemic platelet count and the graft tensile properties were performed (Hypothesis 2).

RESULTS

At 30° of flexion, the average (±standard deviation) AP laxity in the collagen-platelet group was 8.3±4.2 mm greater than the intact control, which was significantly reduced ($p<0.05$) from the collagen only group which was 15.0±3.9 mm greater. A decrease in AP laxity was also observed at a knee flexion angle of 60°; however, this difference approached but did not reach statistical significance (Collagen-platelet group: 12.0±3.9 mm vs Collagen only group: 17.4±3.9 mm; $p=0.08$). Higher platelet concentrations correlated with less abnormal AP laxity at both 60° ($R^2=0.56$) and 30° ($R^2=0.62$). There was no difference in the maximum load or stiffness of the ACL graft between groups. However, there was a strong direct correlation between maximum load at failure ($R^2=0.68$) as well as ACL graft stiffness ($R^2=0.82$; Fig. 1) with the platelet concentration for both groups combined.

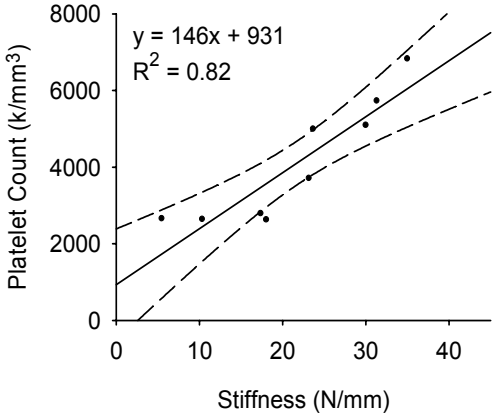

Fig. 1 Correlation of systemic platelet concentration versus ACL graft failure stiffness for both groups. The solid line represents the correlation equation with the 95% confidence level indicated by the dashed line.

DISCUSSION

The application of platelets to a collagen-hydrogel at the time of ACLR reduced early AP laxity. The AP laxity values of our collagen only group were consistent with those previously reported for the ACLR goat knee after 6 weeks of healing [2]. Although no significant differences in the structural properties were found between groups, the systemic platelet count was highly predictive of ACL reconstruction graft strength and stiffness at six weeks. In the caprine model we were unable to significantly concentrate the platelets; therefore, improvements in the healing response may be possible by concentrating the platelets as we have shown in other animal models [1]. These findings demonstrate the importance of further research on delineating the role of these important cells in intra-articular healing especially their potential in treatment of ACL injuries.

ACKNOWLEDGEMENTS

Funding by Vanderbilt Kenneth Schmerehorn Endowed Professorship, RIH Orthopaedic Foundation and the NIH (AR049199 & AR054099).

REFERENCES

1. Murray et al: JOR, 2006, 2. Abramowitch et al: J Orthop Res, 2003.

DEVELOPMENT OF A SILK CABLE-REINFORCED GELATIN-SILK FIBROIN HYBRID SCAFFOLD FOR LIGAMENT TISSUE ENGINEERING

Hongbin Fan[1], Haifeng Liu[1], Siew Lok Toh[2, 3], James C.H. Goh[1, 2] *

1 Department of Orthopedic Surgery, National University of Singapore, Singapore
2 Division of Bioengineering, National University of Singapore, Singapore
3 Department of Mechanical Engineering, National University of Singapore, Singapore

INTRODUCTION

The aim of this study was to develop a novel silk cable-reinforced porous gelatin-silk fibroin (G/SF) hybrid scaffold for ligament tissue engineering. It can combine the advantages of braided scaffold and porous scaffold.

METHODS

The scaffold was fabricated by lyophilizing the cross-linked gelatin and SF mixture with braided silk cables. It showed a honey-combed micro-porous sponge around silk cables which mimicked the structure of extracellular matrix (ECM) of native ligament. The silk cables could significantly increase the tensile strength of porous scaffold to match the mechanical requirements for ligament. The scaffolds were loaded with rabbit MSCs and cultured *in vitro* for two weeks. Samples were evaluated for their cellular morphology, proliferation, gene and protein expression of tenascin-C, type I and type III collagen.

RESULTS

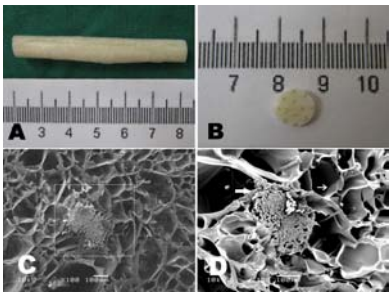

Figure1. Observation of scaffold. (A) gross observation of scaffold; (B) cross section of scaffold; (C) porous structure observed by SEM (×100); (D) Magnified view of the white rectangle frame from (C), demonstrating the hybrid G/SF microsponge around the silk cables (SEM ×150), the arrows point to the silk cable and micro pores.

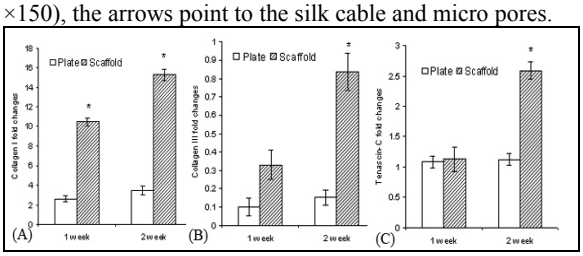

Figure 2. Collagen I, collagen III, and tenascin-C mRNA transcription of MSCs seeded on plate and scaffold at 1 week and 2 weeks. (Data in mean ± SD, n=4, *p< 0.05).

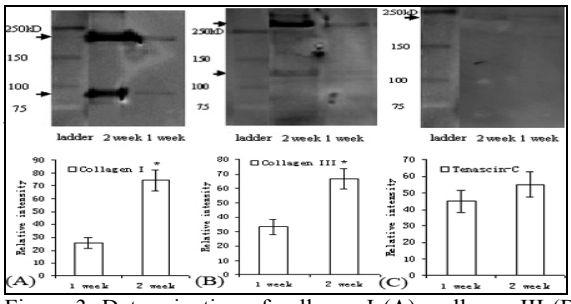

Figure 3. Determination of collagen I (A), collagen III (B), and tenascin-C (C) protein expression in MSCs on scaffold at 1 week and 2 weeks with western blot assay. The arrows indicated the positive bands. (Data in mean ± SD, n=4, *p< 0.05).

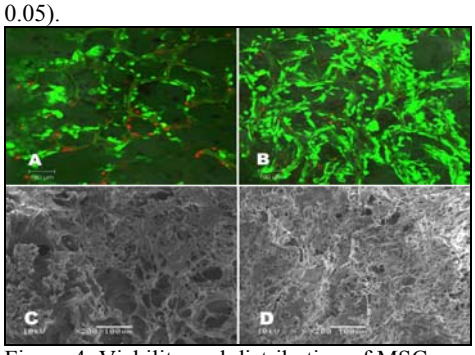

Figure 4. Viability and distribution of MSCs on scaffold. (A) MSCs on scaffold evaluated by confocal microscope at 1 week (FDA/PI staining; green: live cells; red: dead cells); (B) MSCs on scaffold evaluated by confocal microscope at 2 weeks (FDA/PI staining); (C) MSCs on scaffold observed by SEM (×200) at 1 week; (D) MSCs on scaffold observed by SEM at 2 weeks (×200).

DISCUSSION

The results implied that the scaffold, apart from providing proper mechanical strength and enlarged surface area, also supported the proliferation and differentiation of MSCs for ligament tissue engineering.

REFERENCES

Fan HB, Liu HF, Toh SL, Goh JCH. Enhanced differentiation of mesenchymal stem cells co-cultured with ligament fibroblasts on gelatin/silk fibroin hybrid scaffold. Biomaterials (2007), doi: 10.1016/ j.biomaterials.2007.10.048.

*Corresponding author.
E-mail address: dosgohj@nus.edu.sg (James C. H. Goh)

EFFECTS OF TENSILE STRESS ON THE MECHANICAL PROPERTIES OF A SCAFFOLD-FREE TISSUE ENGINEERED CONSTRUCT (TEC) BIO-SYNTHESIZED FROM SYNOVIUM-DERIVED MESENCHYMAL STEM CELLS

K. Kumagai, H. Fujie, D. Katakai, Y. Fujishima, W. Ando*, N. Nakamura*
Biomechanics Lab, Kogakuin University, 2665-1 Nakanomachi, Hachiouji, Tokyo, 192-0015, Japan
*Department of Orthopaedic Surgery, Osaka University Medical School

INTRODUCTION

Ligaments and tendons have limited healing capacities and therefore, feasibility of cell- based therapies has been investigated. For effective cell delivery, synthetic or animal-derived scaffolds are frequently used; however, the long-term safety and efficiency of scaffolds still remain unclear. To avoid the problem, we have been developing a novel tissue-engineering technique for the repair of ligaments and tendons which involves a scaffold-free tissue engineered construct (TEC) bio-synthesized from synovium-derived mesenchymal stem cell [1, 2]. As the TES is composed of cells with their native extracellular matrix, it is free from concern regarding long-term immunological effects. Our previous studies indicated that the tensile property of the TEC is dependent on cell density, culture period, and amount of ascorbic acid*).However, we have a hypothesis that the TEC changes its mechanical property and structure in response to externally applied tensile stress, in the same way as remodeling phenomena occurred in normal ligaments and tendons. The detailed information regarding the remodeling of the TEC may improve the tissue engineering for ligament and tendon repair. Therefore, the effect of tensile stress on the mechanical property of the TEC was determined in the present study.

METHODS

Specimen preparation: MSCs obtained from the synovial membranes of human knee joints were cultured in DMEM in monolayer. After the cells density reached to 4.0 x 10^5 cells/cm^2 (6-cm dish), 0.2 mM of ascorbic acid 2-phosphate was injected to promote the bio-synthesis of extracellular matrix. One month after the injection, synthesized matrices were detached from culture plate and allowed to undergo active contraction for 1 hour to develop TECs[1, 2]. Cyclic tensile stimulation: We developed a cyclic tensile stimulation apparatus for the TEC. A custom-made stainless steel chucks were fixed to the linear actuator and load transducer. The specimen was subjected to a cyclic tensile load with the range of 2.5-5.0 mN at 37 °C in an incubator for 1 hour in DMEM followed by an unloaded condition for 23 hours (loaded group). For comparison, the TEC were set unloaded for 24 hours in the incubator (control group). Tensile test and histological observation: The TEC was then subjected to a tensile testing at a rate of 0.05 mm/s in saline solution at 37 °C using a custom-made micro tensile tester developed in our laboratory [3]. Histological observation of surface structure of the TEC was determined using a differential interference contrast microscopy.

RESULTS AND DISCUSSION

In the tensile test, the strain was smaller in the loaded group than in the control group. The tangent modulus at the strain between 5 and 15% was significantly higher in the loaded group as compared with the control group (fig.1). Histological observation indicated that the fibrous structure was aligned to the direction of cyclic force application in the loaded group. However, no fibrous structure was observed in the control group. These results suggest that the TEC changes its mechanical property and structure in response to externally applied cyclic tensile stress.

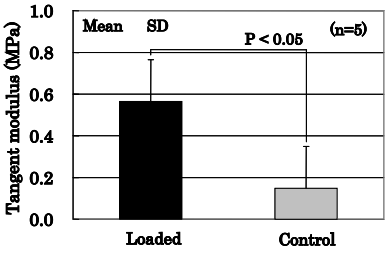

Fig.1. Tangent modulus of the TEC in the loaded and control groups in tensile test.

REFERENCES

1) Ando W. et al. Proceedings of the 51st ORS. 2005. 2) Ando W. et al. Proceedings of the 52st ORS, 2006. 3) Fujie H. et al. Proceedings of the 53st ORS, 2007.

ACKNOWLEDGMENT

The present study was financially supported in port by the NEDO (060019404-0), the JST (06090026), and the "High-Tech Research Center" Project of the MEXT, Japan (SMBC, Kogakuin University).

EFFECTS OF 3-D CULTURE ON THE RESPONSE OF ACL-BONE INSERTION FIBROCHONDROCYTES AND ARTICULAR CHONDROCYTES

W.H. Sun, K.L. Moffat, Yoo-Na Kim, and H.H. Lu
Department of Biomedical Engineering, Columbia University, New York, NY

INTRODUCTION: The anterior cruciate ligament (ACL) inserts into subchondral bone via a fibrocartilagenous insertion site, which facilitates load transfer between soft and hard tissue [1-2]. Characterization of the insertion fibrochondrocytes will be essential for the regeneration of this critical interface. Previously, using a 2-D model, we characterized the phenotype of insertion fibrochondrocytes and compared their response to those of articular chondrocytes and meniscal fibrochondrocytes [3]. Insertion fibrochondrocyte proliferation and biosynthesis differed significantly from those of meniscal fibrochondrocytes but were similar to those of articular chondrocytes. Building on these results, **the objective of this study** is to compare the response of insertion fibrochondrocytes and articular chondrocytes on two types of 3-D scaffolds: a degradable polyglycolic acid (PGA) mesh and a hybrid scaffold of PGA mesh+hydrogel. It is **hypothesized** that scaffold geometry will have a significant effect on fibrochondrocyte as well as chondrocyte morphology, proliferation and biosynthesis.

MATERIALS AND METHODS: ACL insertion fibrochondrocytes (FC) and articular chondrocytes (AC) were isolated from neonatal bovine tibiofemoral joints via enzymatic digestion[3]. Cells were seeded on **1)** PGA mesh (5x5mm, $2.5x10^5$ cells/mesh) and **2)** biphasic PGA-Agarose scaffold (PGA-A, $3.0x10^5$ cells/scaffold) made by infusing 2% agarose-cell suspension into the PGA mesh. All cultures were grown at 37˚C in fully supplemented DMEM (10% FBS, 1% NEAA, 1% antibiotics and 0.1% amphotericin-ß). At days 1, 7, 14, and 21, cell proliferation (n=6, PicoGreen assay), glycosaminoglycan (GAG) production (n=6, dimethylmethylene-blue assay), and alkaline phosphatase (ALP, n=6, enzymatic assay) activity were evaluated. Cell viability and morphology were determined by Live/Dead assay and imaged by confocal microscopy. Two-way ANOVA followed by Tukey-Kramer HSD test was used for all pair-wise comparisons and significance was attained at $p<0.05$.

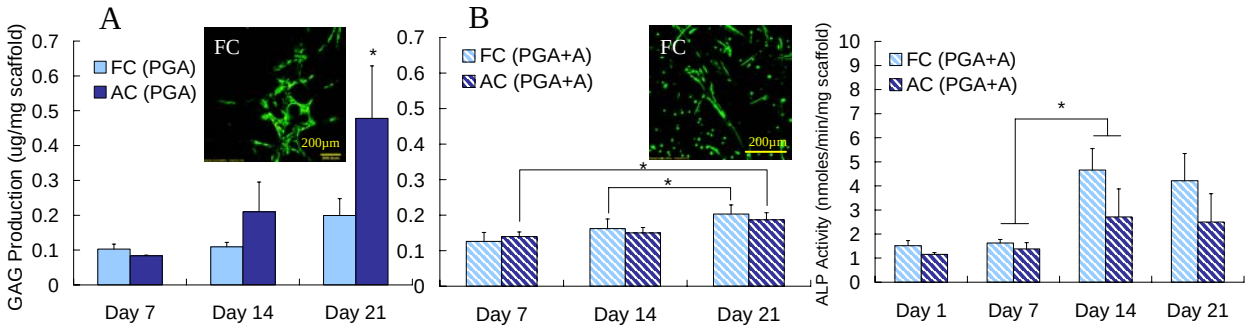

Fig.1: GAG production increased on A) PGA mesh and B) mesh+gel (PGA+A) scaffolds over time. Comparable GAG levels were found for chondrocytes (AC) and fibrochondrocytes (FC) in the PGA+A scaffolds. Both *spherical* and *elongated* cells were observed in the PGA+A scaffold.

Fig.2: ALP activity of FC and AC cultured on the PGA+A scaffolds peaked at day 7 (*: $p<0.05$).

RESULTS: *Cell Morphology and Growth*: As expected, cells grown in the PGA mesh (*Fig. 1A*) spread and assumed an elongated morphology, while both spherical and elongated cells were observed in the hybrid scaffold (*Fig. 1B*). Cells proliferated on both scaffold types, with a higher cell number on the PGA mesh at day 21 ($p<0.05$) (data not shown). *GAG Deposition*: GAG synthesis increased on both substrates over time, although AC produced significantly more GAG than FC at day 21 in the mesh group (*Fig. 1A*). In contrast, no difference in GAG production was found between the two cell types on the hybrid mesh+gel scaffold (*Fig. 1B*). *ALP Activity*: Cell ALP activity increased on both types of scaffolds. However for the mesh group, fibrochondrocytes exhibited a significantly higher ALP activity than chondrocytes (data not shown). In contrast, chondrocytes grown on the hybrid scaffold exhibit a similar ALP activity profile as that of insertion fibrochondrocytes (*Fig. 2*).

DISCUSSION: Our results demonstrate that both 3-D culture and scaffold geometry have profound effects on fibrochondrocyte response. When compared to results from the 2-D model[3], cell growth was slower on the 3-D scaffolds, while GAG production/cell was significantly higher. The ALP activity profile remained comparable between 2-D and 3-D cultures. Interestingly, the hybrid scaffold of PGA mesh+hydrogel promoted the phenotypic fibrochondrocyte morphology [4], and induced chondrocytes to exhibit similar GAG and ALP activity profiles as fibrochondrocytes. Future studies will explore chondrocyte-mediate interface regeneration on the hybrid scaffold.

REFERENCES: 1) Woo *et al*., 1983; 2) Benjamin and Ralphs, 2000; 3) Sun *et al*., 2007; 4) Wang *et al*., 2006.

ACKNOWLEDGEMENT: This study was supported by Wallace H. Coulter Foundation.

ATOMIC FORCE MICROSCOPIC ANALYSIS ON THE MICRO STRUCTURE OF A SYNOVIUM-DERIVED STEM CELLS-BASED SELF-ASSEMBLED TISSUE (SCSAT)

Suzuki T., Kumagai K., Ogawa A., and Fujie H.
Biomechanics Lab, Kogakuin University, 2665-1 Nakanomachi, Hachioji, Tokyo, 192-0015, Japan

INTRODUCTION

Ligaments and tendons usually have limited healing capacity and therefore feasibility of cell-based therapies has been widely investigated. For effective cell delivery, synthetic or animal-derived scaffolds are frequently used; however, the long-term safety and efficiency of such scaffolds still remain unclear. We have established a novel scaffold-free, stem cells-based self-assembled tissues (scSAT), composed of synovial-derived mesenchymal stem cells (MSCs) and their native extracellular matrix[1]. At the ISLT conference 2006, we reported that the mechanical property of the scSAT was improved during cell culture under the addition of 0.2 mM of ascorbic acid with the initial cell density of 4.0 x 10^5 cells/cm^2. In addition, we have been investigating the effects of static and dynamic loading on the property. In the present study, an atomic force microscopic analysis was performed on the scSAT to determine the micro structure of the scSAT.

METHODS

<Manufacture method of scSAT> Stem cells were obtained from the synovial membranes of porcine knee joints, and were cultured in DMEM in monolayer. When the cell density reached to 7.0 or 10.0 (x10^4 cells/cm^2) 0.2 mM of ascorbic acid 2-phosphate was injected to promote the synthesis of extracellular matrix in the subsequent cell culture for 21 or 28 days. The synthesized matrix including the stem cells was manually detached from the substratum. The matrix was then allowed to be self-assembled for 8 hours to develop 3-dimentional synthetic tissue.
<Atomic force microscopic analysis> First, the scSAT was air-dried on a stainless plate. The dried scSAT was fixed on a sample stage of an AFM (Nanoscope IIIa, Digital Instruments), and appropriate conditions were set for measurement. The contact mode in air was utilized for the determination of the surface structure of the scSAT with a silicon nitride pyramidal probe having the tip curvature of 5 nm of radius with a spring constant of 0.06 N/m.

RESULTS AND SUMMARY

Results revealed that the scSAT exhibited micro-convexoconcave surface and was covered by a plenty of indefinite materials with the height of approximately from about 1 µm to 3.5 µm. These structures were connected by collagen fibril-like material with the diameter of approximately from 1.5 µm to 3 µm. These collagen fibril-like materials were varied in diameter and network structure, depending on the cell density and cultured period. The diameter of the fibril-like material was approximately 1.5 µm in the scSATs with the initial cell density of 7 (x10^4 cells/cm^2). And scSAT with initial cell density of 10.0 (x10^4 cells/cm^2), the fibril-like material became larger and more densed with the diameter of approximately 3 µm.

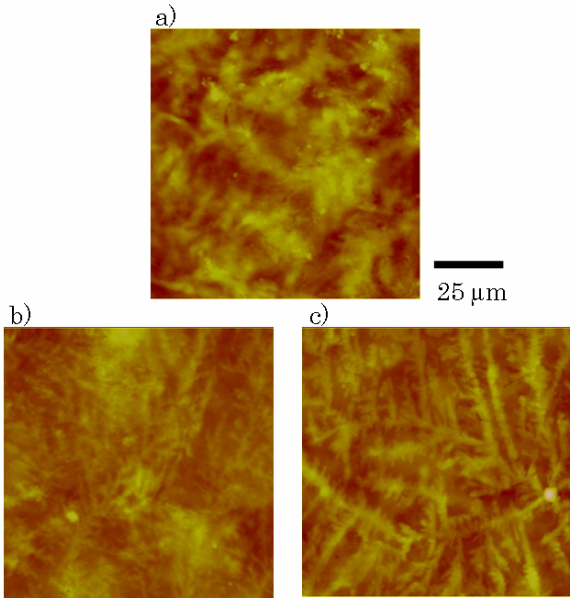

Fig.1 Atomic force microscopic observation of the surface of the scSATs cultured for 21 days (a) and 28 days (b) both with the initial cell density of 7.0 (x10^4 cells/cm^2), and for 21 days with the density of 10.0 (x10^4 cells/cm^2) (c).

References

[1] Nagai K., et al. ISLT-VI 2006.

EFFECT OF ANTERIOR TRANSLATION ON TOTAL KNEE FORCE IN A PORCINE MODEL

D.V. Boguszewski[1], J. T. Shearn[1], C. T. Wagner[2], D.L. Butler[1]
[1] Biomedical Engineering, University of Cincinnati, Cincinnati, OH and [2] LifeCell Corporation, Branchburg, NJ

INTRODUCTION

The three objectives of this study were to examine how anterior translation affected overall knee force, to determine if right-left differences exist, and to determine if the porcine knee is ACL dependent.

METHODS

Right and left hind limbs from four animals were dissected free of all tissue except the four major knee ligaments and joint capsule. The tibia was secured in a specially designed fixture and attached to a load cell on the end of a 6 DOF Robot (KR210; Kuka). All rotations and translations occurred about the joint center point (ACL insertion site between the tibial spines). Each test recorded the joint reaction loads for 10 cycles of a 6 DOF gait path determined from data collected by Tapper et al [1]. Each limb was tested at 0, 2, 4, 6, 8 and 10 mm of anterior translation of the tibia with the ACL intact and then repeated with the ACL transected. The 8th and 9th cycles were analyzed. A two-way repeated measures ANOVA was performed with anterior translation and limb as fixed factors. Post hoc comparisons were performed using the Bonferroni's correction. The significance level was $p < 0.05$.

RESULTS

Anterior translation had a significant effect on anterior knee force out to 4mm, there were no significant differences between right and left limbs, and the porcine knee is ACL dependent. From 0mm to 2mm and again from 2mm to 4mm anterior translation, the average force significantly increased ($p < 0.004$) between 35N-40N (Fig. 1). With increases beyond 6mm of anterior translation the average force was not significantly different than the previous increment. Comparing the four right knees and four left knees showed no significant difference in anterior knee force (Fig. 2). Comparing ACL-intact force data to ACL-deficient force data showed a loss ranging between 75% and 120% in anterior knee force depending on the flexion angle.

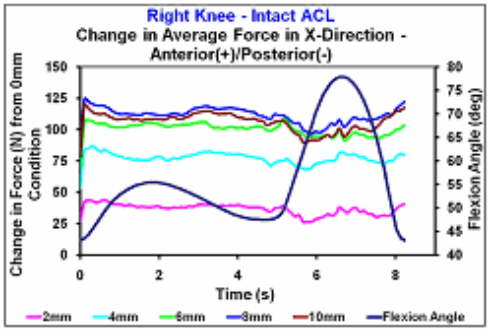

Fig. 1: Change in anterior knee force from 0mm of anterior translation (intact ACL)

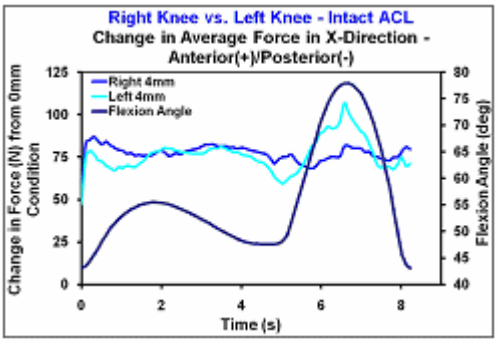

Fig 2: Change in anterior force from 0mm for right and left knees at 4mm of translation (ACL intact)

DISCUSSION

Anterior translation has a significant effect on anterior knee force up to 4mm of anterior translation. At this translation, the anterior knee force is over 75N. Beyond 4mm of anterior translation, the knee exhibits signs of possible joint damage as the resulting increase in anterior knee force with additional anterior translation decreases to 25N at 6mm, 10N at 8mm and -5N at 10mm. The porcine model lost 75%-120% of its anterior knee force when the ACL was transected, clearly indicating ACL dependence. Future studies will examine different ACL reconstructions to determine immediate repair efficacy. The findings from this study indicate that the porcine knee is an appropriate model for future ACL studies, and we have established a set of reproducible testing conditions that will challenge the ACL reconstructions in future studies.

REFERENCES AND ACKNOWLEDGEMENTS

1. Tapper et al, *J Orthop Res*, 24:782-792, 2006.
2. Supported by DOD-PRMRP W81XWH-06-1-0136 (CTW).

A NEW MODEL TO EXPLORE THE EFFECTS OF ACL GRAFT TENSION AND TWIST ON IN VIVO STIFLE BIOMECHANICS

J.E. Beveridge, B.J. Heard, S.P. Darcy, L. MacDonald, C.A Sutherland, N.G. Shrive, and C.B. Frank
McCaig Institute for Bone and Joint Health, University of Calgary, Calgary, Canada

INTRODUCTION

While the *in vitro* literature acknowledges that varying anterior cruciate ligament (ACL) graft tension alters knee kinematics [1], the effects of varied tension on *in vivo* kinematics remain unknown. Using the native ACL as the graft, the aim of this study was to determine if altering the graft tension and the ACL's natural twist alters *in vivo* stifle kinematics in an ovine model. We hypothesized that increasing graft tension and the natural ligament twist would increase internal tibial rotation and reduce anterior and inferior translation of the tibia.

METHODS

Two skeletally mature Suffolk-cross sheep underwent ACL 'reconstruction' using the native ACL as the graft material. For each animal, a bone trephine was used to core around the femoral origin of the ACL leaving it attached to a bone block that could then be manipulated while the tibial insertion remained intact. One of the animals served as a control whereby the bone block was left in its anatomical orientation and fixed using two heavy crossed Kirschner wires. For the experimental animal, the bone block was retracted 3mm and rotated 90º to increase tension and accentuate the natural twist of the ligament. The bone block was then fixed in the same way as the anatomical graft, resulting in a graft that was 'twisted tight'.

In vivo 3D kinematics of the hind right stifle were collected prior to, and again at 4 weeks (4w) post-'reconstruction' using the methods of Tapper *et al.* [2]. In this way, each animal served as its own control. The average stifle joint angles and translations were calculated from 100 strides, expressed in a joint coordinate system [3], and were normalized to 0-100% gait. Changes in stifle kinematics were assessed using a one-way repeated measures ANOVA with reconstruction as the between-measures factor, while changes in coupled motion were assessed using Pearson's correlations. The significance level for all tests was set at $P \leq 0.05$.

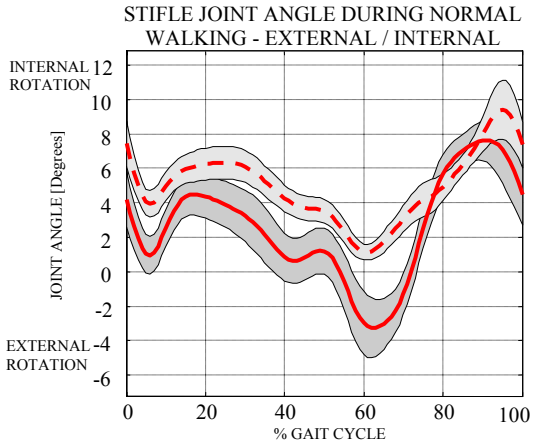

Figure 1. Stifle kinematics before (solid line) and 4 weeks post-twist-tight reconstruction (dashed line) +/- 1 standard deviation (shading).

RESULTS

In vivo kinematics before and 4w after the 'anatomical' reconstruction were not significantly different, however 'twist tight' kinematics were ($p<0.01$). Abduction-adduction (AA), internal-external tibial rotation (IE) (Figure 1), and medial-lateral tibial translation (ML) were most affected. Coupled motion was also affected by the 'twist tight' reconstruction. While still significantly correlated, the degree to which the tibia rotated externally as a function of joint flexion fell from a Pearson correlation coefficient of 0.82 to 0.61. Similarly, the degree to which the tibia translated laterally with joint flexion fell from a coefficient of 0.66 to 0.28. Conversely, the degree of flexion – abduction coupling was less affected: 0.98 vs. 0.96 post-reconstruction.

DISCUSSION

Twisting and tightening the native ACL graft had a significant effect on *in vivo* stifle biomechanics, partially supporting our hypothesis. While the 'twist tight' animal experienced an increase in internal tibial rotation, changes in anterior and inferior tibial translation were not as obvious. Changes in AA and IE rotation may represent more of a shift in the pattern of joint kinematics as a result of increased graft tension and twist, whereas changes in ML translation represent a restraint in lateral translation. Due to its more lateral insertion, we speculate that the posterior-lateral bundle of the ACL may have been the primary restraint to lateral translation and adduction of the tibia, while the anterior-medial bundle of the ACL contributed to increased internal tibial rotation. Leaving the native ACL in its anatomical orientation represents a best-case scenario for ligament reconstruction and has not affected stifle kinematics in this model. However, alterations in graft tension and twist to this otherwise 'perfect' graft results in altered *in vivo* joint mechanics. Future work using this model will centre around deciphering the interaction of mechanical and biological factors that influence secondary osteoarthritis and graft healing.

References: 1. Brady, MF, et al. Am J Sports Med, 2007. 2. Tapper, J, et al. J Biomech Eng, 2004. 3. Grood, ES et al. J Biomech Eng, 1983. **Acknowledgements:** Leslie Jacques, AHFMR, CIHR, CAN, NSERC, GEOIDE, TAS.

MAGNETIC RESONANCE MICROSCOPIC IMAGES OF REGENERATED SEMITENDINOSUS TENDON AFTER HARVESTING FOR ACL RECONSTRUCTION

Nomura Y[1], Kuramochi R[2], Tawara N[3], Hirano A[4] and Fukubayashi T[5]
1: Graduate School of Sports Science, Waseda University, Saitama, Japan
2: Faculty of Life Sciences, Teikyo Heisei University, Chiba, Japan
3: Japan Institute of Sports Sciences, Tokyo, Japan
4: Mito Kyodo General Hospital, Ibaraki, Japan
5: Faculty of Sports Science, Waseda University, Saitama, Japan

【INTRODUCTION】

Previous studies have suggested that hamstring tendons can regenerate following harvesting for anterior cruciate ligament reconstruction. However, there are still unanswered questions including the exact mechanism of the tendon regeneration and the end time of the maturation process[1]. Magnetic resonance (MR) microscopy appears exceptionally well suited to in vitro or ex vivo studies of heterogeneous tissue, due to its high spatial resolution[2]. The purpose of this study is to clarify the regeneration of the semitendinosus (ST) tendon with MR microscopic images.

【METHODS】

Four patients (3 males, 1 females, mean age ± SD: 30.7 ± 15.9 years) who had undergone ACL reconstruction with ST tendon participated in this study. Axial proton density-weighted images were taken at 1, 3, 6, and 9 months, postoperatively. First, conventional MRI scans of the whole knee joint were obtained using a knee coil. (thickness: 4mm slice, repetition time: 914 ms, echo time: 26 ms, field of view: 160 × 160 mm, and matrix size: 512 × 512 pixels). Then, MR microscopic image scans using a microscopy coil in the posteromedial aspect of the distal thigh were obtained at the level of the superior pole of the patella, targeting the ST tendon (thickness: 2mm slice, repetition time: 600 ms, echo time: 20 ms, field of view: 50 × 50mm, and matrix size: 256 × 256 pixels).

【RESULTS】

One month after ACL reconstruction, MR microscopic images showed white tissue and irregular structures. After three months, a ST tendon-like structure appeared as gray tissue surrounded with a high intensity membrane which appears to be the synovial tendon sheath. At six month, the high water content structure changed into nearly black, but the structure was not well organized (Fig.1-B). Conventional MRI could not show this change of regeneration clearly (Fig.1-A).

【DISCUSSION AND CONCLUSION】

In this research, high-resolution MRI was used to identify the gradual maturation of a ST tendon-like structure including high degrees of moisture and a synovial tendon-like surrounding structure which expanded proximal to distal of the regenerated ST tendon. A previous study has shown that regeneration occurs along "fascial planes" which lie in the medial aspect of the knee and connect with the muscle septum and the sheaths investing the ST[3]. This theory is in accordance with our findings. In addition, MR microscopic images give us more detailed information than conventional MRI; therefore continuous research including a histological study is needed.

Fig.1-A, B
This figure is a typical case of regeneration process. Longitudinal changes of the regenerated ST tendon (arrow) seen by conventional MRI (A), and MR microscopic imaging (B). Each image was taken at 1, 3, and 6 months after ACL reconstruction.

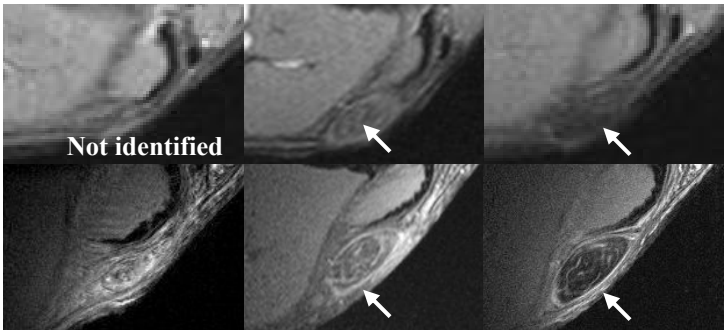

【REFERENCES】

1. Nikolaou, Efstathopoulos, Wredmark: Hamstring tendons regeneration after ACL reconstruction: An overview. Knee Surg, Sports Traumatol Arthrosc, 15:153-160, 2007.
2. Niitsu M, Ikeda K (2004) Magnetic resonance microscopic images with 50-mm field-of-view of the medial aspect of the knee. Acta Radiologica, 45: 760-768, 2004.
3. Simonian, Harrison, Cooley, et al.: Assessment of morbidity of semitendinosus and gracilis tendon harvest for ACL reconstruction. Am J Knee Surg., 10:54-59, 1997.

SECOND HARMONIC IMAGING AND FOURIER SPECTRAL ANALYSIS OF NORMAL AND DAMAGED TENDON MICROSTRUCTURE

D.T. Fung, J. Basta-Pljakic, J.B. Sereysky, D.M. Laudier, M.H. Tseng, M.B. Schaffler and E.L. Flatow
Leni and Peter W. May Department of Orthopaedics, Mount Sinai School of Medicine, New York, NY
evan.flatow@msnyuhealth.org

INTRODUCTION

Damage accumulation from overuse/fatigue contributes to degradation of mechanical properties in degenerated tendons.[1] Conventional histologic methods of studying tendon morphology are largely qualitative and limited to thin section cutting, which makes it difficult to reliably assess matrix level damage. In this study, we introduce a novel imaging method based on second harmonic generation (SHG) of fibrillar collagen[2] to characterize tendon microstructure in 3D, and to investigate the quantitative, spatial nature of damage formation in tendons.

METHODS

Patellar tendons of female S-D rats were fatigue loaded in vivo to *Low* or *High* levels of damage based on an IACUC-approved loading protocol.[3] Tendons were processed in a plastic embedding protocol[4] and thick sections (200-250 μm) were cut in the sagittal plane using a diamond wafering saw. SHG imaging was performed at 1 μm optical intervals through the entire section thickness under a multiphoton microscope with a Ti:Sapphire laser at 840 nm wavelength. No staining was used. *FT spectral gradient distribution*: A Matlab Fast FT algorithm was applied to generate a power spectrum expressed in polar coordinates for each image in the stack. Spectral intensity values were plotted as a function of spatial frequency, and a line was fitted using regression to compute the slope, or *gradient*, of spectral intensity. This computation is repeated in all directions to create a radial distribution of spectral gradients for the image stack. *Local fiber orientation mapping*: With each image discretized into windows, Fast FT spectrum of each window was generated. A line was fitted using regression to characterize alignment of thresholded, high intensities on the spectral plot, which is orthogonal to the principle orientation of the fibers within the window. A map was created by determining and displaying the principle orientation of fibers in all windows, representing the localized fiber orientations over the entire image.

RESULTS

Tendon microstructure defined by SHG signals from collagen fibers was clearly visualized through the entire section depth using multiphoton microscopy. Control tendons are characterized by undisrupted, longitudinally-aligned collagen fibers, while loaded tendons showed localized kinked fiber deformations in Low, and severe fiber angulation and discontinuities at High level damage (Figs. 1a-c). FT spectral gradient distributions among these tendons showed different profiles (Figs. 1d-f). Notably, spectral gradient values are lowest along directions transverse to the undisrupted, longitudinal fibers alignment (Fig. 1d), and increase with severity of damage, or number of deformation patterns (Figs. 1e-f). Fiber orientation mapping (Fig. 2) demonstrated faithful representation of local orientation of fibers in all images of both control and damaged tendons.

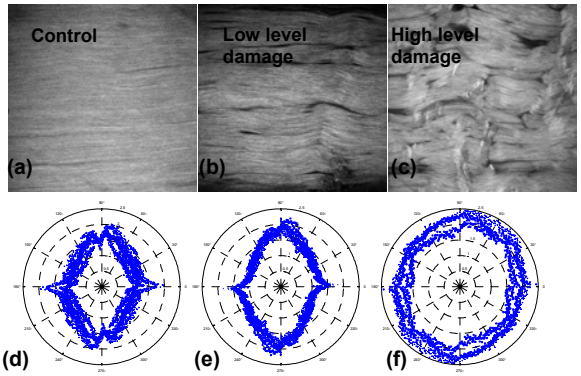

Fig. 1. Representative multiphoton micrographs (a-c) and composite FT spectral gradient distributions (d-f) of tendons at increasing levels of fatigue damage.

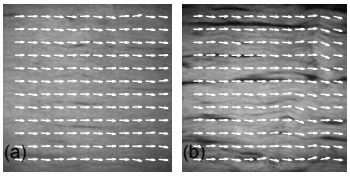

Fig. 2. Fiber orientation mapping of (a) control and (b) damaged tendons.

DISCUSSION

SHG is an inherent, nonlinear optical property of collagen, attributed to its molecular composition and fibrillar formation.[2] SHG signals are generated by illuminating the tissue using a phase-locked, high power laser, which is capable of probing collagen property, into the depth of the tissue. Alterations to the microstructure of collagen fibers (as a result of loading or pathologic processes) would be reflected by changes in the nature of the SHG signals.[5] Indeed, the current study presented two analytical methods by which changes in the tendon microstructure at Low level fatigue damage could be detected and evaluated. As such, SHG imaging is a powerful tool in studying tendon morphology, providing the ability to characterize normal and damaged tissue microstructure in 3D without the use of stains, and sensitivity to detect to small matrix level changes.

REFERENCES: [1]Leadbetter (1992) *Clin Sports Med* 22:761-76. [2]Gauderon (2002). *Micron* 32:691-700. [3]Lee (2007) *Trans ORS* 31:1058. [4]Laudier (2007) *J Ortho Res* 25 :390-5. [5]Kim (2000). *Laser Surg Med* 27:329-35.

CELL ORIENTATION AND LOCAL STRAIN DISTRIBUTION IN AN *IN VITRO* ACHILLES TENDON TISSUE ENGINEERING MODEL

R.D. Sumanasinghe[1], J. Qi[1,2], J. Wang[1], M. Tsuzaki[1], M. Wall[1], W. Pfeiler[2], E. Loboa[2], D.A. Hart[3], A.J. Banes[1,2].
[1]Flexcell International Corp., Hillsborough, NC, USA, [2] Joint Department of Biomedical Engineering, NCSU/UNC, Raleigh and Chapel Hill, NC, USA, [3]Faculty of Medicine, University of Calgary, Calgary, Canada.

INTRODUCTION

The causes for Achilles tendon rerupture after reconstruction in patients under 30 years is still unknown. [Rettig et al, Am J Sports Med 2005]. While gap junctions regulate response of tendon cells to mechanical loading [Banes et al, Clin Orthop Relat Res 1999], different regions of rat Achilles tendon show differential cell morphology and gap junction protein expression [Ralphs et al, J An 1998]. The purpose of this study is to determine contraction, cell morphology, and local tensile strains in a 3D tissue engineering murine size model created in the shape of an Achilles tendon *in vitro* and to compare this with the existing 3D linear model [Garvin et al, Tissue Eng. 2003].

MATERIALS AND METHODS

Cell-seeded collagen matrix fabrication: Both linear and trapezoidal mouse Achilles tendon cell-seeded (p6, 2 × 10^6 cells/mL) 3D Type 1 collagen constructs were created using linear (not shown) and trapezoidal trough loaders (Figure 1A) respectively. **Construct contraction:** Constructs were imaged every 24 hours for 7 days using Scanflex software (Flexcell) and areas of the constructs were measured using MicroSuite software. **Cell orientation:** After 7 days, DAPI (cell nuclei) and Phalloidin (actin filaments) stained constructs were imaged at different locations along the length of the construct. **Modeling:** Local tensile strains in one-half of cell-seeded constructs after 0 and 7 days in culture and under 10% uniaxial tensile strain were analyzed using linear finite element models in ABAQUS 6.4-3.

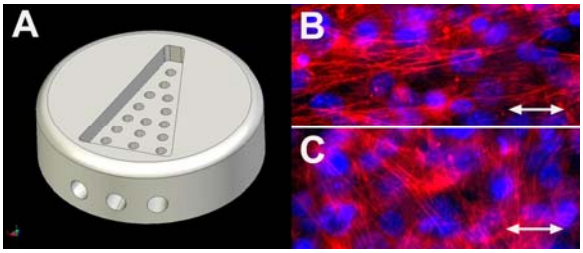

Figure 1. A) Trapezoidal trough loader that simulates shape of an Achilles tendon. Actin filament orientation in DAPI/Phalloidin stained mouse Achilles tendon cell-seeded trapezoidal collagen constructs in the center area B) at the mid point and C) near wide end. Arrows show the longitudinal direction of constructs.

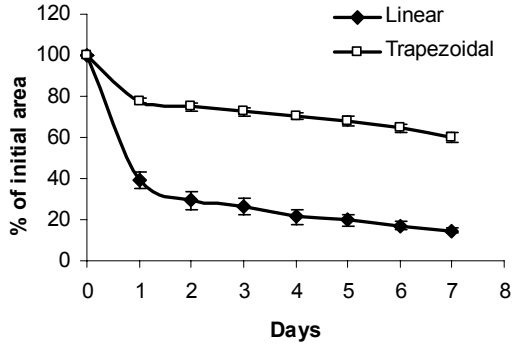

Figure 2. Compaction of mouse Achilles tendon cell-seeded linear and trapezoidal collagen constructs expressed as a percent of initial area. Bars represent ± SD.

RESULTS

Actin filaments in cells were oriented parallel to the axial direction in most areas of the trapezoidal shaped gel-cell constructs (Figure 1B). However, at the center near the wide anchor actin filaments were oriented in the transverse direction (Figure 1C). Achilles tendon cells in trapezoidal forms contracted at a rate that was 45% less than that of linear constructs after 7 days (Figure 2). Culture duration or compaction did not affect the maximum local strains in the constructs. Constructs cultured for 7 days showed reduced lateral displacement during loading (not shown).

DISCUSSION

Reduced construct compaction under unloaded conditions indicated the suitability of these constructs for longer studies. Varying local strains within the loaded construct shown by finite element analysis (not shown) may cause differential cell responses in the construct. These results indicate that the new 3D cell-seeded trapezoidal collagen constructs can be effectively used for further studies on tissue engineering of Achilles tendon *in vitro*.

CONCLUSION

One of the problems with compacting cell-hydrogel constructs is the reduced nutrient diffusion to cells. A key observation in the current study is that the trapezoidally shaped Achilles tendon simulate had less gel compaction than did a linear construct.

ACKNOWLEDGEMENTS

The authors thank Robert Lee for his help on compaction measurements. Funded by Flexcell Int. Corporation.

DIFFUSION TENSOR IMAGING OF KNEE LIGAMENTS: A PRELIMINARY IN VIVO STUDY

VM Wang[1], BR Bach[1], DA Turner[2], GT Stebbins[3]
Departments of Orthopedic Surgery[1], Radiology[2], and Neurology[3]; Rush University Medical Center, Chicago, IL

INTRODUCTION

Diffusion tensor imaging (DTI) is a MRI approach to assessing tissue microstructure by quantifying 3D diffusion of water molecules within tissues. DTI has been widely used to quantify the orientation of white matter tracts in the brain [1,2]. Few studies, however, have utilized DTI to characterize musculoskeletal connective tissues [3-5]. The highly-organized collagenous architecture of ligaments and tendons may be well suited for DTI since this imaging technique is a reliable means of quantifying anisotropic diffusion in tissues. The objective of the present study was to assess the applicability of DTI for *in vivo* analyses of the human anterior cruciate ligament (ACL) and patellar tendon (PT).

MATERIALS AND METHODS

Subjects: Five healthy, asymptomatic volunteers (mean age 25±5 y.o.) participated in this IRB-approved study. All knees were positioned in full extension for scanning and each subject received one imaging protocol.

Scanning Protocols: All MR images were acquired on a 1.5 Tesla General Electric Signa scanner (GE Medical Systems, Milwaukee, WI, USA) equipped with high speed gradients (LX Horizon, Rev 10.4). The structural protocol featured a fast spin echo (FSE) proton density (PD) weighted pulse sequence (60 contiguous sagittal plane images, 1.6 mm sections, matrix = 256x256, repetition time (TR)/echo time (TE) = 2000/15 ms, echo train length = 4). The DTI protocol consisted of diffusion weighted single shot spin echo, echo planar images acquired in the sagittal plane, TR/TE = 12100/97 ms, FOV = 16 cm, matrix =128x128, 30 3 mm gapless slices, 6 repetitions, and application of high-order shimming. In all DTI parameters, two diffusion weights were used: b = 0 and 800 s/mm^2. An additional set of inversion recovery images was acquired and used to un-warp the eddy current effect of the diffusion gradients [6].

DTI Processing: The six coefficients defining the elements of the diffusion tensor were calculated [1] from eddy current-corrected, averaged images. Eigenvectors, defining the three principal directions of diffusion for each voxel, were derived from the diffusion tensor. Two values were constructed for each voxel: *Fractional anisotropy* (FA, a scalar metric ranging from 0-1 that describes directionality of the diffusion tensor) and *mean diffusivity* (MD, a non-directional measure of free translational diffusion) [2,7].

Image Processing: First, the structural scan was co-registered with the DTI scan using a rigid-body transformation between the DTI b=0 (T2) scan and the structural scan. The resultant deformation matrix was stored for later processing. ROIs for the ACL and PT were drawn on the structural scan using Analyze Software (Mayo Clinic, Rochester, MN, USA). The sagittal plane was used for tracing with confirmation in the axial and coronal planes. The coregistration deformation matrix was applied to the ROIs to ensure accurate matching between the structural and DTI scans.

RESULTS

Coregistration between structural and DTI scans was acceptable with no loss of transfer of ROI from structural to DTI locations. FA and MD results are presented in the accompanying table.

ROI	Subject #	FA	MD (x 10^{-6} mm^2/s)
PT	1	0.645 ± 0.378	576.3 ± 667.0
	2	0.589 ± 0.405	466.1± 135.2
ACL	1	0.487 ± 0.296	359.5 ± 251.7
	2	0.455 ± 0.345	469.3 ± 191.0

DISCUSSION

The results of this pilot study of normal, asymptomatic volunteers demonstrate the feasibility of investigating FA and MD of the ACL and PT, *in vivo*, using diffusion tensor imaging with 1.5T MRI. Despite their relatively high variability, our preliminary results for FA and MD are, respectively, higher and lower than those reported for articular cartilage, intervertebral disc, and skeletal muscle [3-5]. The aforementioned comparisons are consistent with the microstructural organization of the fibrous matrix of the respective tissues. Additional modifications to the DTI parameters may improve the sensitivity of the scan, including adding more repetitions to the scan and using a higher diffusion weighting. Increasing the diffusion weighting may provide better resolution of the slow diffusion components associated with tendons and ligaments.

REFERENCES: [1] Basser PJ et al, Biophys J 1994;66:259-67. [2] Basser PJ, Pierpaoli C. J Magn Reson B 1996;111:209-19. [3] Hsu EW, Setton LA. Magn Reson Med 1999;41:992-9. [4] Zaraiskaya T et al, J MRI 2006;24:402-8. [5] Deng X et al, Magn Reson Imaging 2007;25:168-71. [6] de Crespigny A et al, J Cereb Blood Flow Metab 1998;18:1008-17. [7] Basser PJ. NMR Biomed 1995;8:333-44.

THE EFFECT OF IN VIVO SENSOR IMPLANTATION IN THE SHEEP KNEE

ST Herfat[1], JT Shearn[1], D Bailey[1], ME Mehl[1], N Perry[1], MT Galloway[2], M Greiwe[3], C Gooch[1], DL Butler[1]
[1]Department of Biomedical Engineering, University of Cincinnati, Cincinnati, OH;
[2]Cincinnati Sports Medicine, Cincinnati, OH; [3]Department of Orthopaedic Surgery, University of Cincinnati, OH

INTRODUCTION. Establishing functional tissue engineering parameters (FTEPs) for orthopaedic tissues will provide design criteria and evaluation benchmarks for tissue engineered repairs [1]. Among FTEPs common to all soft tissue are in vivo forces and displacements. As these measures have proven difficult to simultaneously record due to the invasive nature of the sensor implantation, it becomes important to determine how sensor implantation affects in vivo outcome measures. Therefore, this study was designed to determine the effect of implanting motion tracking sensors and force transducers on vertical ground reaction forces (VGRF) in the ovine model. We hypothesized that surgery to implant these devices would not significantly alter VGRF magnitudes or patterns.

MATERIALS AND METHODS. Eight skeletally mature, female sheep (3–4 yrs old; 100-150 lbs) were used to test our hypothesis. Each animal was walked on an instrumented treadmill (Gaitway Instrumented Treadmill, Kistler Instrumente AG) for at least 10 min/day for a minimum of 5 days before surgery. The treadmill is equipped with front and rear force plates to record fore- and hind limb VGRFs. Motion sensors were then surgically implanted onto the medial proximal tibia and distal femoral condyle on each left hind limb. A force transducer was also inserted transversely into a small pocket in the distal, anterior ACL. Each sheep was then subjected to four combinations of speeds (1.0 m/s and 1.3 m/s) and inclinations (0º and 6º) each day with the order being altered from day to day to minimize fatigue effects. Two sheep were removed from analysis because the rear force plate could not distinguish individual hind limb strikes. Gait patterns were determined from the last day of testing before surgery and the day before sacrifice. Prior to analysis, VGRFs were normalized to body weight and gait cycles were normalized between 0 and 1.

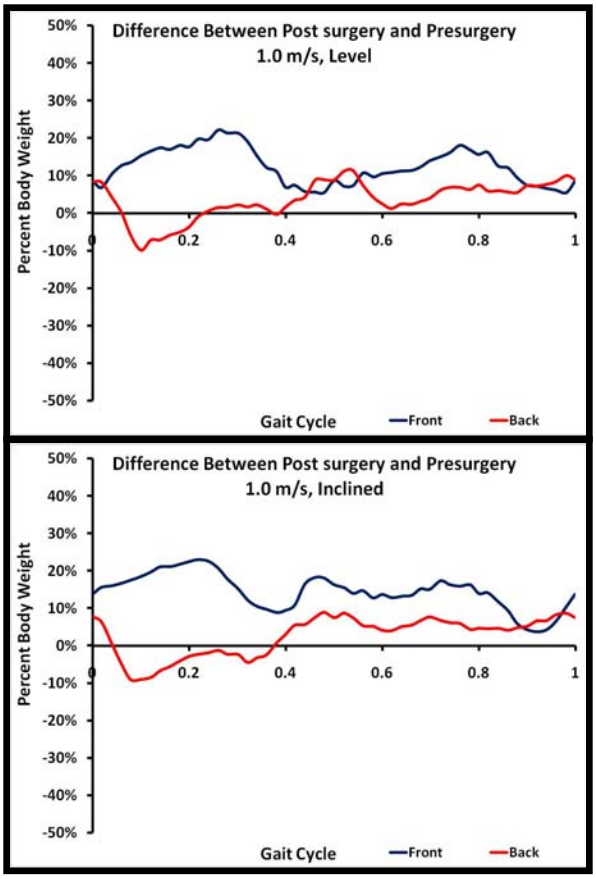

Fig 1. Surgery did not significantly affect hind limb VGRF magnitudes or patterns for level (top) or inclined gait (bottom).

RESULTS. Although surgery did not affect peak VGRF in the operated left hind limb ($p>0.05$), it did: a) significantly increase contact time for the right hind limb and b) shift peak right fore limb VGRFs 20% later in the gait cycle. ***1 m/s, level (Fig. 1):*** After surgery, maximum VGRF in the left hind limb decreased 9.9 ± 11.7 % ($p>0.05$). However, the time period of contact between the right limb and the treadmill increased 14.6 ± 3.2 % after surgery ($p<0.003$). By contrast, left hind limb contact time decreased 5.6 ± 2.0 % after surgery ($p>0.05$). ***1 m/s, inclined (Fig. 1):*** After surgery, maximum VGRF in the left hind limb decreased 9.1 ± 13.9 % ($p>0.05$). However, the time period of contact between the right limb and the treadmill increased 15.4 ± 5.1 % after surgery ($p>0.007$). By contrast, left hind limb decreased 6.5 ± 1.0 % ($p>0.05$). ***Similar results were found at the higher gait speed.***

DISCUSSION. One would expect VGRFs in the operated limb to decrease after surgery. However, we were surprised to find that these forces decreased less than the 10%, within 80% of our pre-surgery acceptance criterion. Hind limb contact time did vary with activity level. Specifically, contact time increased most in the non-operated hind limb for inclined walking at 1 m/s (15.4 ± 5.1 %) and decreased most in the operated hind limb for level walking at 1 m/sec (9.9 ± 11.7 %). Our studies did not extend beyond 8 days post surgery due to the declining health of the animal. Now that surgery to implant these devices has been found to not significantly alter VGRF in the operated limb, in vivo forces and motions can represent normal values. **REFERENCES.** [1] Butler et al. CORR, 2004. **ACKNOWLEDGMENTS.** Partial support from NIH grants EB004859-01 and AR46574-06.

BIOMECHANICAL EVALUATION OF SUPERIOR CAPSULAR RECONSTRUCTION FOR TREATMENT OF IRREPARABLE MASSIVE ROTATOR CUFF TEAR

Teruhisa Mihata[1,2], Michelle H. McGarry[1], Joseph M. Pirolo[1], Mitsuo Kinoshita[2], Thay Q. Lee[1]
[1]Orthopedic Biomechanics Laboratory, VA Long Beach Healthcare System and UC Irvine, California, USA
[2]Department of Orthopedic Surgery, Shoulder & Elbow Biomechanics Laboratory, Osaka Medical College, Japan

INTRODUCTION

Despite the use of both biologic and prosthetic grafts to treat irreparable massive rotator cuff tears, high rates of graft retear have been reported. Abrasion of the undersurface of the acromion after superior migration of the humeral head and subsequent subacromial impingement may contribute to retear. The superior shoulder capsule, which stabilizes the glenohumeral joint, often is destroyed during massive rotator cuff tear. Reconstruction of the capsule might prevent superior migration of the humeral head. Here we investigated the biomechanical effect of superior capsular reconstruction for treatment of irreparable rotator cuff tears.

METHODS

Eight cadaveric shoulders were tested in a custom shoulder testing system. Shoulders were dissected free of skin and subcutaneous tissue, and rotator cuff insertions were preserved. Superior translation of the humerus (Microscribe 3DLX), subacromial contact pressure (Tekscan), glenohumeral joint force (6 degrees-of-freedom load cell), and rotational range of motion (goniometer) were measured at 0º (0º and 30º external rotation), 45º (30º and 60º external rotation), and 90º (30º and 60º external rotation) of shoulder abduction. Each parameter was measured as a change from a balanced load condition with supraspinatus, 10 N; infraspinatus/teres minor, 10 N; subscapularis, 10 N; deltoid, 40 N; pectoralis major, 20 N; and latissimus dorsi, 20 N and after increasing the superior force by loading the deltoid to 80 N, and unloading the pectoralis major and latissimus dorsi. Measurements were obtained when the rotator cuff was intact, after cutting the supraspinatus, after patch graft of the supraspinatus tendon, after patch graft of the superior capsule (superior capsular reconstruction), and after patch graft of both the supraspinatus tendon and superior capsule (double-layer patch graft). Fascia latae was used for all patch grafts. Data were analyzed using repeated measures ANOVA with a Tukey's post hoc test ($P < 0.05$).

RESULTS

Compared with values for intact rotator cuffs, cutting the supraspinatus increased superior translation ($P < 0.05$), increased subacromial contact pressure ($P < 0.05$), and decreased glenohumeral compression force and superior force ($P < 0.05$). Superior translation was partially restored after placement of the supraspinatus tendon patch graft and fully restored after superior capsular reconstruction. Mean superior translation after double-layer patch graft was less than that after superior capsular reconstruction, albeit not significantly. Placement of either graft restored subacromial contact pressure ($P < 0.05$) and did not alter glenohumeral joint force. Superior capsular reconstruction decreased total rotational range of motion by 15º ($P < 0.05$).

DISCUSSION

Lack of superior stability may contribute to the high rates of retear after patch grafting of the supraspinatus tendon. Reconstruction of the superior capsule completely restored superior stability of a simulated irreparable cuff tear, perhaps preventing abrasion of the graft. Therefore, superior capsular reconstruction may be a beneficial additional surgery during the repair of an irreparable rotator cuff tear. Patch grafting either the supraspinatus tendon or the superior capsule can decrease subacromial contact pressure. For severe irreparable cuff tears, double-layer patch grafting may be more useful. Mild shoulder contracture may occur after superior capsular reconstruction.

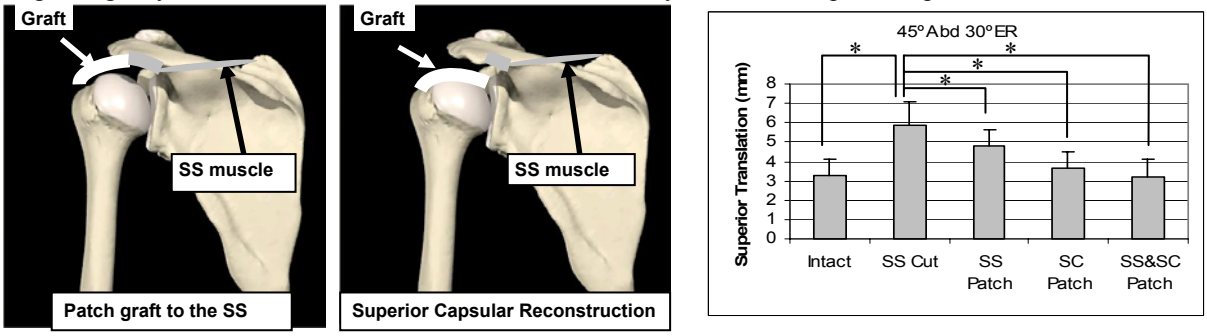

Left: Patch graft to the supraspinatus tendon. Middle: Superior capsular reconstruction. Right: Superior translation. SS, supraspinatus tendon; SC, superior capsule; *, $P < 0.05$

ARE THE MECHANICAL PROPERTIES OF THE ANTERIOR BAND OF THE INFERIOR GLENOHUMERAL LIGAMENT AND THE AXILLARY POUCH SIMILAR?

C.A. Voycheck, A.J. Brown, P.J. McMahon, R.E. Debski
Musculoskeletal Research Center, Department of Bioengineering
University of Pittsburgh, Pittsburgh, PA, USA

INTRODUCTION

The anteroinferior glenohumeral capsule stabilizes the joint during positions most commonly associated with dislocation. Prior anatomic study found the anteroinferior capsule had two discrete portions: the band-like anterior band of the inferior glenohumeral ligament (AB-IGHL) and the sheet-like axillary pouch. However, recent studies of function have shown that the capsule should be treated as a continuous sheet of tissue, and that the collagen fibers are randomly aligned in both regions. [1,2,3,4] Whether the AB-IGHL has properties similar to other band-like ligaments or instead to a continuous sheet of tissue has profound implications for its function. The objective of this work was to compare the mechanical properties of the AB-IGHL and axillary pouch during a non-destructive tensile elongation. We hypothesize that the band-like portion, the AB-IGHL and sheet-like portion, the axillary pouch have similar mechanical properties.

METHODS

Six cadaveric shoulders (53±9 yrs) were dissected down to the humerus, scapula, and glenohumeral capsule. The AB-IGHL (10x15 mm) and axillary pouch (25x25 mm) were excised and preloaded to a tensile load of 0.5 N in the medial/lateral axis, followed by width and thickness measurements. Each tissue sample then underwent 10 cycles of preconditioning (0-1.5 mm, 10 mm/min) and was elongated to 2.25 mm. Boundary conditions from the experimental test were used to create finite element models of each tissue sample, with a hyperelastic isotropic strain energy function used to describe the response of the tissue. [5,6] The two material coefficients of the model, C_1 and C_2, were determined using an inverse finite element optimization routine. The optimized material coefficients of the AB-IGHL and axillary pouch were compared using a Wilcoxon rank sum test ($p < 0.05$). These coefficients were then used to generate Cauchy stress-stretch curves to represent the mechanical response of each tissue sample to uniaxial extension. This calculation is based on the deformation gradient for uniaxial extension and the constitutive model. The stress-stretch curves were discretized into 11 points and averaged across all tissue samples to generate one average stress-stretch curve for each region. To determine if differences existed between regions, the stress values at each of the 11 points were compared using a Friedman test. Post-hoc analyses were preformed using Wilcoxon rank sum tests. The average stress-stretch curves were then fit to the constitutive relationship to generate an average set of material coefficients for each region.

RESULTS

The values of C_1 and C_2 for the AB-IGHL were 0.33 ± 0.18 MPa and 5.0 ± 2.5, respectively. For the axillary pouch, the material coefficients were 0.23 ± 0.11 MPa (C_1) and 7.6 ± 3.6 (C_2). No statistical differences were found between the material coefficients of the AB-IGHL and axillary pouch ($p = 0.25$ for C_1 and $p = 0.12$ for C_2). Further, no statistical differences were found when comparing the stress values at each of the 11 discretized points on the average stress-stretch curves ($p > 0.05$). The average material coefficients generated for the AB-IGHL were 0.25 MPa and 5.7 for C_1 and C_2, respectively. For the axillary pouch, the generated values of C_1 and C_2 were 0.18 MPa and 8.9, respectively. Based on preliminary analyses to determine the sensitivity of the stress-stretch curves to the material coefficients, a difference of greater than 0.3 for C_1 or greater than 3.0 for C_2 was considered significant. Therefore, a significant difference was found between the regions for C_2, but not for C_1.

DISCUSSION

Comparison of the band-like and sheet-like portions of the IGHL, and their respective Cauchy stress-stretch curves generated using the material coefficients of a hyperelastic isotropic constitutive model, revealed no differences between the two regions. An exception was the value of C_2 representing the average stress-stretch curves. This difference may be due to the small sample size. These findings are supported by the similarities in Young's moduli of both regions reported previously during uniaxial tensile testing. [7] Our results further validate that the glenohumeral capsule is a continuous sheet of tissue despite the study of anatomy that has found otherwise. This function needs to be considered during diagnosis and techniques for optimal capsular repair. In the future, these material coefficients may be utilized to construct finite element models of the glenohumeral capsule.

REFERENCES

(1) Malicky, DM *et al.* JBME, 2001. (2) Malicky, DM *et al.* JSES, 2000. (3) Moore, SM. Thesis Doc. Univ. Of Pittsburgh, 2006. (4) Debski, RE, *et al.*, 2003. (5) Weiss, JA, *et al.*, JBM, 2002. (6) Weiss, JA, *et al.*, Comput. Meth. Appl. Mech. Engr. 1996. (7) Matsen, FA, *et al.*, 1993, The Shoulder: A Balance of Mobility and Stability. 46-53.

The effects of various temperatures (-5°C, -25°C and –80°C) on biomechanical properties of tendon allografts.

A Guney, M Oner, M Halici, S Karaoglu
Department of Orthopaedics and Traumatology, Erciyes University, Kayseri, Turkey

Introduction: Fresh frozen allografts, in need of use of allograft, are preferably chosen by surgeons for variety of reconstructive interventions in orthopedic surgery due to the presence of their initial structural properties. Between minus 70 and 80 °C are usually chosen for fresh frozen allografts. At cellular level, freezing the tendons at – 70 or lower causes swelling in different severity while it is known that, more or less, they keep biomechanical properties. For several studies in the literature, tendons have been kept at -25 °C as well.

Aim: This study has been researched biomechanical features of prolonged freezing degrees of sheep flexor tendons under different degrees below zero; – 5 °C, – 25 °C, and – 80 °C.

Materials and Methods: In this study 30 forearm of 15 sheep's flexor digitorum profundus tendons have been used. Randomly selected three groups were formed and each of them included 20 fresh tendons. Groups were determined; group A: – 5 °C, group B: – 25 °C, and group C: – 80 °C, respectively. All the samples were wrapped up with saline soaked sponges and placed into the freezer. They were kept in the freezer for 4 months.

Then the transports of the samples were done appropriately according to the cold chain by using thermal break foam boxes and brought to Middle East Technical University Laboratory of Biomechanics. Before the tests samples dissolved with saline solution in the room temperature and during the experiment clammy environment were provided. The tendons were then fixed to soft tissue clamps and tested on a Lloyd LS500 Tensometer. The load to failure test was performed using an elongation rate of 20 mm/min. Traction was continued until the rupture of the tendon. Data taken from the device recorded with 0,625 second intervals. The load-elongation curve and failure mode were recorded. The structural properties were represented by stiffness (N/mm), and ultimate load (N), and obtained from the resulting load-elongation curve. The greatest slope in the linear region of the load-elongation curve was used to calculate stiffness. For the stiffness and ultimate load values, the distribution of each data set was assessed by using the Kolmogorov-Smirnov test. Intragroup multiple comparisons were then performed by using one-way analysis of variance (ANOVA). The post hoc Sheffe test was performed to identify significantly different group means when the ANOVA test was significant. *P* values < 0.05 were considered to be statistically significant.

Results: Groups A, B and C had maximum failure loads of (mean±SD), 614.8 ± 63.4, 514.4 ± 95.5 and 591.0 ± 70.5 N, had stiffness values of 35.4 ± 5.5, 34.2 ± 6.8 and 35.1 ± 6.0 N/mm, and had energy absorbed values of 4.89 ± 1.03, 3.79 ± 1.14 and 4.74 ± 1.10 J, respectively. While there was no statistically significant difference among the stiffness values, there were statistically significant differences with maximum failure loads and energy absorbed values. Further analysis shown that there were no differences between gropus A and C while group B was significantly lower than the other two **(Table I)**.

Discussion: Keeping and transporting procedures are very important for frozen allografts. Sometimes to keep and to transport the allografts at -80°C may be troublesome.
To maintain their biomechanical properties is another issue for this field. From this point of view and with the light of the data from our study, -5°C might be an alternative way to store the tendon allografts. Further studies should be done on the other properties of the allografts kept at -5°C such as immunologic characteristics.

References

1. Ralis ZA. JBJS-Br. 1989 71:55-7.
2. Clavert P, Kempf JF, et al. Surg Radiol Anat. 2001;23:259-62.
3. Pearsall AW 4th, Hollis JM, et al. Arthroscopy. 2003 19:1091-6.
4. Lambertz D, Perot C, et al. J Appl Physiol. 2001; 90:179-88.
5. Granzier HL, Wang K, et al. Biophys J. 1993;65:2141-59.
6. Moon DK, Woo SL, et al. J Biomech. 2006;39:1153-7.

GROUPS	Max Failure Load (N)	Energy Absorbed (J)	Stiffness (N/mm)
A	614,8 ± 63,4[b]	4,89 ± 1,03[b]	35,4 ± 5,5
B	514,4 ± 95,5[a,c]	3,79 ± 1,14[a,c]	34,2 ± 6,8
C	591,0 ± 70,5[b]	4,74 ± 1,10[b]	35,1 ± 6,0
P	0,000	0,006	0,807

Table I. Test results for the groups in X±SD

Substance P injections enhance tendon healing. A study in the rat.

Carlsson O, J Dahl, +PW Ackermann
Section of Orthopedics and Sports Medicine, Department of Molecular Medicine and Surgery, Karolinska Institutet, Stockholm, Sweden,
+Paul.Ackermann@ki.se

INTRODUCTION

In Achilles tendon healing a drastic nerve in-growth has been shown, supplying neuropeptides, predominantly substance P (SP). SP is hypothesized to orchestrate the healing process [1], mainly by stimulation of angiogenesis and fibroblast proliferation [2]. In this study, SP was supplemented to the healing Achilles tendon and its effects on the repair process were assessed by histological-, immunohistochemical- and polarization light analyses.

METHODS

54 male Sprauge Dawley rats (200 g) were subjected to blunt rupture of the right Achilles tendon. Starting the second day post-surgery rats were injected intra-tendinously once daily for 6 days. Three groups: 0.05 ml, 10-6 mol/kg BW endopeptidase inhibitor captopril/thiorphan (CT) was injected in the CT- and SP-groups and 0.05 ml NaCl in the control group. 30 min later the SP-group was injected with 0.05 ml 10-6 µmol/kg BW SP-solution. The animals were euthanized at 1, 3 and 6 weeks. *Histology:* H&E staining was analysed with regard to fibroblast density and collagen fiber amount, orientation and maturation. *Immunohistochemistry:* SP antibody (Bachem) was visualized by Cy2-fluorescence to evaluate SP-positive nerves. *Polarization microscopy:* Picro-sirius red staining was visualised with plane polarized light to assess collagen III-like structures. An epifluorscence microscope (Nikon, Eclipse E800; Japan) equipped with plane-polarizing analysis filters was used for analyses. *Computerized analysis:* In conjuction with all above analyses objective measurements were made using the software Easy Image 2000©. Histological healing was assessed, measuring the smallest diameter of organized, parallel collagen, found at the rupture site. Semi-quantitative image analysis assessed the area occupied by SP-positive nerves and by collagen III-like structures. *Statistical analysis:* Kruskal-Wallis ANOVA and Mann-Whitney U-test. Significance at $P < 0.05$.

RESULTS

Histology: At 1 week the SP group was found to be significantly higher than control with respect to collagen organisation ($p=0.04$) lending support to the subjective assessment. At 3 weeks both subjective and objective assessments demonstrated that the SP- and the CT-groups exhibited increased collagen fiber organisation ($p=0.02$, $p=0.002$). The SP-group also showed higher fibroblast prevalence ($p=0.002$). At 6 weeks, these differences were still observed subjectively. *Immunohistochemistry:* At 1 week, subjective analysis indicated a decreased SP-positive nerve fiber occurrence in the SP- and CT-groups as compared to control. At 3 weeks subjective and semi-quantitative analysis verified decreased SP-nerve fiber occurrence in the SP-group compared to control ($p=0.02$). At 6 weeks there were no differences between the groups. *Polarization microscopy*: At 1 week, subjective and semi-quantitative analysis showed the SP-group to exhibit elevated occurrence of collagen III-like structures (collagen III-L) compared to control ($p=0.03$). This trend persisted throughout the 3- and 6-week time points, though non-significantly.

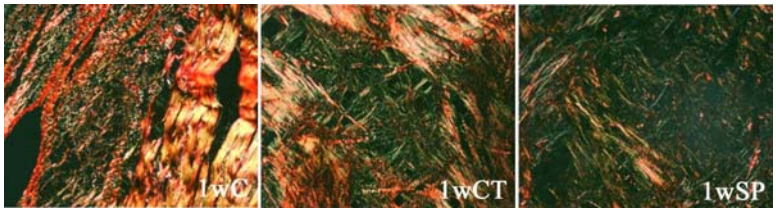

Figure: At 1 week, the SP-group (1wSP) exhibits higher amount of collagen III-L fibers (green) vs. controls (1wC)($p=0.03$) in polarized light.

DISCUSSION

This study shows that SP injections enhanced both fibroblast prevalence and tissue organization during tendon repair. The finding at 1 week post-rupture of higher amount of collagen III-L as assessed by plane-polarized light analysis may reflect increased scar-formation, which is a characteristic of increased tissue regeneration. In addition, at 3 weeks, the fibroblast count showed an increased number of fibroblasts after SP injections, which may suggest a process of increased collagen formation. This fact was supported by the finding at 3 weeks of enhanced amount and organization of collagen fibers in the SP-group as assessed both subjectively and semi-quantitatively. Notably, at 3 weeks post-rupture, SP-positive nerve fiber occurrence was significantly lower in the SP-group, which may reflect regulatory feedback. Taken altogether, the results of this study indicate that exogenous neuropeptide supplementation may be used as an adjunct to growth factors and tissue engineering in the pursuit of enhanced tendon repair.

REFERENCES

1. Ackermann, PW et al, Neuronal plasticity in relation to … J Orthop Res. 2003 May;21(3):432-41.
2. Nilsson J et al., Stimulation of connective tissue cell growth by substance P.. Nature 2-8;315:61-3. 1985.

SUBSTANCE P EXPRESSION WAS ASSOCIATED WITH TENDON PAIN IN A RAT MODEL OF COLLAGENASE-INDUCED TENDON INJURIES

Chan LS, Fu SC, Fong DTP, Chan KM
1. Department of Orthopaedics and Traumatology, Faculty of Medicine, The Chinese University of Hong Kong, Hong Kong SAR, China
2. The Hong Kong Jockey Club Sports Medicine and Health Sciences Centre, Faculty of Medicine,
The Chinese University of Hong Kong, Hong Kong SAR, China
kaimingchan@cuhk.edu.hk

INTRODUCTION:

Chronic tendinopathy is characterized with longstanding tendon pain, but the origins of pain remains unclear. As increased substance P (SP) positive nerve fibres were found in tendon sample from chronic tendinopathy (1), it is possible that SP in tendon degeneration contributed to increased nociception. In previous experimental studies, collagenase-induced degenerative tendon injuries showed similar histopathological features of tendinopathy, but it is not known if increased nociception was associated with these histopathological features. Since knee pain in rats could be measured as increased double stance duration (2), we propose to characterize nociceptive responses by gait analysis in a rat model of collagenase-induced injuries, and determine if SP expression in the degenerative tendons was associated with increased nociception.

METHODS:

A total of 36 male Sprague Dawley rats (6-8 weeks old) were used in the present study. A 20 µl aliquot of 0.015 mg/ul collagenase was injected intratendinously into the left patellar tendon of 30 rats. Equal volume of saline was injected in the remaining 6 rats as control. Video capturing for gait analysis was performed in the control group as well as the collagenase injection groups at 2 weeks, 4 weeks, 8 weeks, 12 weeks and 16 weeks post injury (n= 6). During video capturing, the rats were forced to run on a transparent track. Black ink joint markers were labeled on shaven skin of the hind limbs at the major joints. A high-speed video camera (JVC 9600, Japan) was used to record the movement of hind limbs at 100 Hz. The video data were captured and analyzed by a motion analysis system (Ariel Performance Analysis System, USA). Trials with propagation speeds not less than 0.02m/s were obtained to measure the double stance duration. After video capturing, the rats were eunthanized and the left patellar tendons were harvested for histological processing and SP immunohistochemistry.

RESULTS:

As compare to the saline control, the double stance duration of the rat gait was increased (p=0.048, One-way ANOVA), indicating knee pain according to the study by Coulthard(2). However, the double stance duration restored to normal level at 8 weeks and increased again at 16 weeks post injury (Fig 1B). A similar biphasic pattern was noticed in the change of immunopositivity of SP (p<0.005, Kruskal-Wallis Test) in the injured tendons (Fig 1A). Correlation analysis by Spearman's rho test revealed significant association between double stance duration and immunoreactivity of SP (r=0.607 and p<0.005).

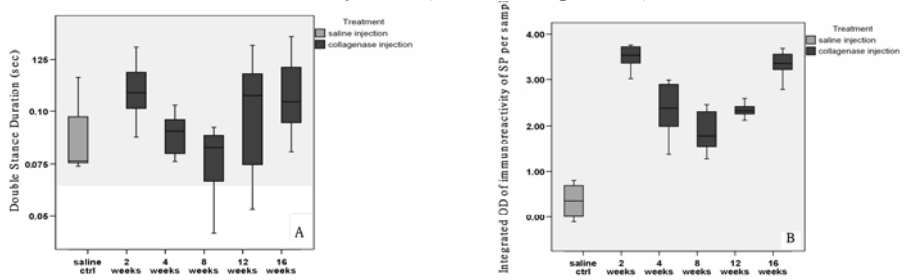

Figure 1 A&B. (A) The double stance duration (p=0.048, One-way ANOVA), and (B) the immunoreactvity of SP on the tendon section (p<0.005, Kruskal-Wallis Test) at different time point.

DISCUSSIONS:

This was the first attempt to measure tendon pain in a collagenase-induced degenerative tendon injury model which mimicked the histopathology of chronic tendinopathy. The painful response was monitored by increased double stance duration which may reduce nociceptive stimuli associated with loading of hindlimbs. We found that the degenerative injuries were not healed up to 16 weeks post injury, and increased double stance duration indicated persistent knee pain. It indicated that the rat model of collagenase-induced injury exhibited crucial characteristics of chronic tendinopathy, namely pain and failed healing. Since the expression of SP in the injured tendons was correlated to the pain level, it is possible that SP may play a role in development of chronic pain in tendinopathy. However, a causal relationship was not implied even though SP is a well-known nociceptive substance. Further investigation is necessary for the exploration of the roles of SP in chronic tendinopathy.

REFERENCES:

1. Schubert TE et al. Ann Rheum Dis. 64(7):1083-6. 2005
2. Coulthard P et al. J Neurosci Methods. 116(2):197-213. 2002

Circulating substance P levels and shoulder joint contracture after arthroscopic repair of the rotator cuff.

Francesco Franceschi *, Umile Giuseppe Longo*, Laura Ruzzini *,

Fabrizio Battistoni **, Giordano Dicuonzo, Nicola Maffulli [+],**

Vincenzo Denaro*

*** Department of Orthopaedic and Trauma Surgery, Campus Biomedico University, Via Longoni, 83, 00155 Rome, Italy**

****Department of Laboratory Medicine and Microbiology, Campus Biomedico University, Via Longoni, 83, 00155 Rome, Italy**

[+] Department of Trauma and Orthopaedic Surgery, University Hospital of North Staffordshire, Keele University School of Medicine, Stoke on Trent, ST4 7LN United Kingdom.

Abstract

Objective: To determine the plasma levels of substance P (SP) in patients with postoperative stiffness after arthroscopic rotator cuff repair.

Design: Plasma samples were obtained at 15 months from surgery from 2 groups of patients who underwent arthroscopic repair of a rotator cuff tear. In Group 1, 30 subjects (14 men and 16 women, mean age: 64.6 years, range 47 to 78) with shoulder stiffness 15 months after arthroscopic rotator cuff repair were recruited. In Group 2, 30 patients (11 men and 19 women, mean age: 57.8 years, range 45 to 77) were evaluated 15 months after successful arthroscopic rotator cuff repair. Immunoassays were performed with commercially available assay kits to detect the plasma levels of SP.

Results: The mean plasma levels of SP in patients with postoperative stiffness were significantly greater than those in the control group (81.06 ± 27.76 versus 23.49 ± 5.64, $P < 0.05$).

Conclusions: The plasma concentrations of substance P in patients with shoulder stiffness after arthroscopic rotator cuff repair are higher compared to plasma levels of SP in patients with a good postoperative outcome. The neuronal up-regulation of SP shown in the plasma of patients with post operative shoulder stiffness may underlay not only the symptoms of adhesive capsulitis, but also its development.

Notes

Notes

Notes

International Symposium on Ligaments & Tendons - VIII

March 1, 2008

Stanford, CA

7:30 am - 8:00 am	Registration & Check-In
8:00 am - 8:20 am	Opening Ceremony, Welcome & Announcements Dr. Savio L-Y. Woo & Dr. Braden C. Fleming
8:20 am - 9:35 am	Podium Session 1: ACL Reconstruction & Development of OA Moderators: Dr. Bruce Beynnon & Dr. Maury Hull
9:35 am - 10:15 am	Podium Session 2: Knee Kinematics & Mechanics Moderators: Dr. Toru Fukubayashi & Dr. Michael Torry
10:15 am - 10:45 am	Break and Poster Session 1
10:45 am - 11:50 am	Podium Session 3: Mechanobiology & Biochemistry Moderators: Dr. Albert Banes & Dr. Roger Smith
11:50 am - 12:20 pm	Podium Session 4: Tissue Healing & Mechanics Moderators: Dr. Louis Soslowsky & Dr. Christos Papageorgiou
12:20 pm - 1:30 pm	Lunch and Poster Viewing
1:30 pm - 2:30 pm	Podium Session 5, Part I: Functional Tissue Engineering - Bioscaffolds Moderators: Dr. Steven Arnoczky & Dr. Helen Lu
2:30 pm - 3:10 pm	Podium Session 5, Part II: Functional Tissue Engineering - Bioscaffolds Moderators: Dr. Chih-Hwa Chen & Dr. Stavros Thomopoulos
3:10 pm - 3:40 pm	Break and Poster Session 2
3:40 pm - 4:15 pm	Podium Session 6: Techniques Moderators: Dr. Hiromichi Fujie & Dr. Guoan Li
4:15 pm - 4:45 pm	Podium Session 7: Shoulder & Upper Extremity Moderators: Dr. Evan Flatow & Dr. Thay Lee
4:45 pm - 5:30 pm	Podium Session 8: Symposium on Substance P Moderators: Dr. Sinan Karaoglu & Dr. Jennifer Wayne
5:30 pm - 5:40 pm	Closing Remarks: Dr. Savio L-Y. Woo
5:45 pm	Tour of BioMotion Laboratory, Durand Building, Stanford University
5:45 pm - 7:00 pm	Reception and Cocktail Hour
7:00 pm	Dinner and Award Ceremony